

**THE EFFECT OF ADENOSINE A_{2A} RECEPTOR ACTIVATION ON
LEUKOCYTE ADHESIVENESS**

A Thesis

**Presented to the Faculty of
The School of Engineering and Applied Sciences
University of Virginia**

**In Partial Fulfillment
Of the Requirements for the Degree of
Masters of Science in Biomedical Engineering**

By

Annika Katrin Shuali

May 2012

Approval Sheet

This Thesis is submitted in partial fulfillment of the requirements for the degree of
Masters of Science in Biomedical Engineering

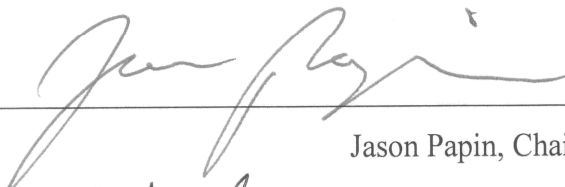


Annika K. Shuali, Author

This thesis has been read and approved by the examining committee:



Michael Lawrence, Advisor



Jason Papin, Chair

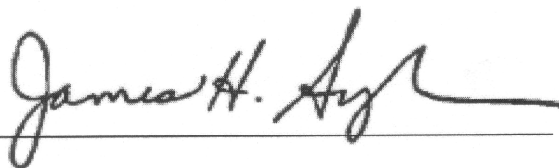


Jeffrey Saucerman



Alison Criss

Accepted for the School of Engineering and Applied Science:



Dean, School of Engineering and Applied Science

May 2012

ACKNOWLEDGEMENTS

This thesis could not have been completed without the assistance and guidance of many people. I would like to take a moment to thank a few of them for their continuing support.

First I would like to thank my loving husband, Vincent Shuali for his love, support and unwavering faith in me. I would also like to thank my mother, Debbie Hedin along with Daniel, Nicki, Derek, Justin, and Joe.

I would like to thank my advisor Dr. Michael Lawrence for his remarkable insight and guidance. Thank you for challenging me and being patient with me. I would also like to thank faculty members of the University of Virginia for helping contribute to my research progress: Dr. Jason Papin, Dr. Joel Linden, Dr. Jeffrey Saucerman, Dr. Alison Criss, and Dr. Alexander Klibanov. I would also like to thank members of the Biotechnology Training program including Gordon Laurie.

Thank you Lawrence lab members, current and former: Jeffrey DiVietro, Tony Ham, Chris Paschall, Brian Schmidt, Bryan Smith, José Tlaxca, Kyou-nam Cho, Yuhling Wang, Caroline Whitaker, and Nicole Brackett. I also need to thank Arvind Chavali, Elisa Ferrante and Sunil Unnikrishnan. Thank you all for your feedback, friendship and encouragement.

I would like to also give a special thanks to my ‘healthy consenting adults’ who volunteered to be a part of my study and shall remain anonymous—without you there would be no data!

TABLE OF CONTENTS

Abstract	vi
List of Tables and Figures	viii
List of Abbreviations	x
Chapter 1: Introduction	1
1.1 Overview of Inflammation.....	1
1.1.1 The Leukocyte Adhesion Cascade.....	2
1.1.1.1 Selectins.....	4
1.1.1.2 Integrins.....	5
1.1.1.3 Cytoskeletal Reorganization.....	17
1.1.2 Neutrophil Activation.....	19
1.1.3 Adenosine Receptor Signaling.....	26
1.2 Specific Aims.....	30
1.2.1 Specific Aim 1 (Chapter 2) To examine the effects of adenosine A _{2A} receptor agonist stimulation on PKC-activated human neutrophils.....	31
1.2.2 Specific Aim 2 (Chapter 3) To describe the effects of adenosine A _{2A} receptor agonist stimulation on the firm adhesion and spreading of neutrophils to ICAM-1.....	33
Chapter 2: The Effect of ATL313 Stimulation on Neutrophil Activation Markers	36
2.1 Introduction.....	36
2.2 Materials and Methods.....	37
2.2.1 Antibodies.....	37
2.2.2 Small Molecules.....	37
2.2.3 Neutrophil Isolation.....	37
2.2.4 Flow Cytometry.....	39
2.3 Results.....	40
2.3.1 ATL313 Stimulation Does Not Alter the Surface Expression of Mac-1 (CD11b) on Neutrophils.....	40
2.3.2 ATL313 Stimulation Does Not Alter L-selectin Shedding in Neutrophils.....	43
2.3.3 ATL313 Stimulation Does Not Alter the Concentration of Filamentous Actin in Neutrophils.....	45
2.4 Discussion.....	47
Chapter 3: ATL313 Stimulation Decreases β_2-Dependent Adhesion of Neutrophils to ICAM-1	50
3.1 Introduction.....	50
3.2 Materials and Methods.....	51
3.2.1 Cell Lines.....	51
3.2.2 Anti-human ICAM-1 mAb R6.5.....	51
3.2.3 ICAM-1.....	52
3.2.4 Preparation of Adhesion Substrates.....	55
3.2.5 Flow Chamber Set-up.....	55
3.2.6 Shear Stress Detachment after Static Adhesion Assay.....	56
3.2.7 Static Adhesion Assay to Assess Cell Spreading.....	57
3.3 Results.....	57

3.3.1 ATL313 Stimulation Decreases Neutrophil Firm Adhesion on ICAM-1 During a Shear Detachment Assay After Static Adhesion.....	57
3.3.2 ATL313 Decreases Neutrophil Spreading on ICAM-1 during Static Adhesion Assays	58
3.4 Discussion.....	60
Chapter 4: Conclusions	63
4.1 Concluding Remarks.....	63
4.2 Future Directions	65
Appendix	70
Appendix A. Silver Staining of R6.5 Elution Fractions	70
Appendix B. Confirmation of the isolation of functional mAb R6.5 using Flow Cytometry	73
Appendix C. Silver Staining of ICAM-1 Elution Fractions	75
Bibliography	81

Abstract

Neutrophils infiltrate inflamed tissues and become activated in response to a variety of inflammatory stimuli. Once activated neutrophils release cytokines, migrate towards chemoattractants, increase their expression of integrins (e.g. CD11b), shed L-selectin and undergo processes that aid in the destruction of pathogens. The migration of leukocytes to inflamed tissues is a multi-step process that involves specific ligand-receptor interactions between adhesion molecules expressed on the surface of both endothelial cells and the leukocytes. Adenosine A_{2A} receptors have been shown to exert anti-inflammatory effects in animal models of inflammation, however their effect on neutrophils is unknown.

The aim of the present work is to investigate the effects of Adenosine A_{2A} receptor stimulation on the expression of neutrophil activation markers and LFA-1 integrin-mediated adhesion to the ligand ICAM-1 using the agonist ATL313.

Flow cytometry was used to assess the expression of neutrophil activation markers (CD11b, L-selectin, F-actin) in cells stimulated with Phorbol 12-myristate 13-acetate (PMA) with and without 1 μ M ATL313 stimulation. PMA-stimulation led to a 2.26-fold increase in neutrophil CD11b expression, a 5.25-fold decrease in L-selectin expression, and a 1.49-fold decrease in F-actin polymerization that was statistically significant compared to unstimulated cells. ATL313 incubation with and without PMA stimulation was not statistically different from untreated cells or cells treated with PMA alone, respectively.

PMA-stimulated neutrophil adhesion to ICAM-1 was examined using a flow chamber with and without ATL313 incubation. PMA stimulation increased cell

spreading on ICAM-1 16.7-fold in comparison to unstimulated cells. Stimulation with both ATL313 and PMA led to a 10.6-fold decrease in cell spreading on ICAM-1 compared to PMA-stimulated neutrophils. Furthermore, incubation with ATL313 resulted in a 60 to 90% decrease in the average percent of cells that remained firmly adhered to ICAM-1 after 30 seconds of shear stress at 1 dyne/cm².

In conclusion this study demonstrated that ATL313 stimulation is unable to abolish Protein Kinase-C (PKC)-mediated changes in the expression of neutrophil activation markers but can robustly alter the adhesion of neutrophils to ICAM-1. Occupancy of A_{2A} receptors with drugs such as ATL313 may exert their anti-inflammatory effects on neutrophils through inhibition of LFA-1-mediated adhesion and migration.

List of Tables and Figures

Tables

Table 1.1 Ligand and Tissue Distribution of a few Key Integrins.....	7
Table 1.2 Chemokines that target Neutrophils and their Function	21
Table 1.3 Binding Affinities of Adenosine and ATL313 for each of the Human Adenosine Receptor Subtypes	30

Figures

Figure 1.1 Production of blood cells from pluripotent stems cells in the bone marrow and their function.....	2
Figure 1.2 The Leukocyte Adhesion Cascade	3
Figure 1.3 Schematic of L-selectin, P-selectin and E-selectin Structure.....	5
Figure 1.4 The Integrin Receptor family	6
Figure 1.5 Schematic of Integrin Structure showing a Conformational Change as a Result of Activation.	9
Figure 1.6 Schematic of Integrin Inside-out Signaling.....	11
Figure 1.7 Modes of cellular integrin reorganization associated with valency regulation	13
Figure 1.8 Schematic of Focal Adhesion proteins involved in the signaling between integrins and the actin cytoskeleton.....	14
Figure 1.9 Intracellular Signaling Cascade Initiated by Integrin Activation	16
Figure 1.10 Diagram of the interaction of the integrin and chemoattractant GPCR signaling pathways.....	18
Figure 1.11 Effectors of Outside-in signaling to integrins in Neutrophils.	23
Figure 1.12 Schematic of the Neutrophil Phagosome	25
Figure 1.13 Adenosine subtype mRNA expression in LPS-stimulated human Neutrophils	27
Figure 1.14 Adenosine A _{2A} Receptor Signaling Pathway	28
Figure 2.1 Ficoll-Paque Gradient Separation of Whole Blood.....	39
Figure 2.2 Histogram of APC-Cy7-labeled CD11b Fluorescent Intensity for Neutrophils stimulated with PMA for various time periods.....	41
Figure 2.3 Histogram of APC-Cy7-labeled CD11b Fluorescent Intensity for Stimulated cells.	42
Figure 2.4 Fold Change in median Mac-1 Fluorescent Intensity in Neutrophils.....	42
Figure 2.5 Histogram of FITC-labeled CD62L Fluorescent Intensity for Stimulated Cells	44
Figure 2.6 Fold Change in median L-selectin Fluorescent Intensity in Neutrophils	44
Figure 2.7 Histogram of FITC-labeled F-actin Fluorescent Intensity for Stimulated Cells.	46
Figure 2.8 Fold Change in Median F-actin Fluorescent Intensity in Neutrophils.	46
Figure 3.1 Flow chamber Set-up.....	56
Figure 3.2 Effect of PMA and ATL313 Stimulation on the Static Adhesion of Neutrophils to ICAM-1.....	58

Figure 3.3 Neutrophils Spreading on Plates coated with ICAM-1	59
Figure 3.4 Stimulation with 1 μ M ATL313 (alone or with 50 ng/mL PMA) decreases the percent of neutrophils per field of view that spread on ICAM-1	60
Figure 4.1 Schematic of the Signaling Cascades involved in A2A Receptor and Integrin Activation.....	69
Figure A.1 Images of elution fractions used in SDS-PAGE Gels	72
Figure A.2 ICAM-1 Staining using the R6.5 mAb isolated from the HB9580 Cell Line.	74
Figure A.3 Silver Staining of a gel run with ICAM-1 elution fractions.	75
Figure A.4 Orientation of Fluid Flow Inside the Flow Chamber.	77

List of Abbreviations

AC	Adenyl Cyclase
ADP	Adenosine diphosphate
AMP	Adenosine monophosphate
APC-Cy7	Fluorescein Isothiocyanate
APS	Ammonium Persulfate
AR	Adenosine Receptor
Arp	Actin Related Protein
ATL313	(4- {3-(6-amino-9-(5-cyclopropylcarbamoyl-3,4-dihydroxytetrahydrofuran-2-yl)-9H-purin-2-yl)prop-2-ynyl}piperidine-1-carboxylic acid methyl ester), Adenosine A _{2A} receptor agonist
ATP	Adenosine triphosphate
b	Gasket window width
BSA	Bovine Serum Albumin
cAMP	Cyclic Adenosine Monophosphate
CBP	CREB binding protein
CD	Cluster of Differentiation
Cdc42	Cell Division Control protein 42 homolog
CGS21680	3-[4-[2-[[6-amino-9-[(2R,3R,4S,5S)-5-(ethylcarbamoyl)-3,4-dihydroxy-oxolan-2-yl]purin-2-yl]amino]ethyl]phenyl]propanoic acid, Adenosine A _{2A} Receptor Agonist
CNBr	Cyanogen Bromide
CREB	cAMP response element binding
CR3	Complement Receptor 3
CTAPIII	Connective Tissue activating peptide III
C5a	Proteolytic fragment of the fifth component of complement
DNA	Deoxyribonucleic acid
DPBS	Dulbeco's Phosphate Buffered Saline
DTT	Dithiothreitol
DW	Distilled Water
EC	Endothelial Cell
ECM	Extracellular Matrix
ED	Extracellular Domain
EGF	Epidermal Growth Factor-like
EM	Electron Microscopy
ENA-78	Epithelial cell-derived neutrophil activating peptide 78
EPAC	Exchange Protein directly Activated by cAMP
ERK	Extracellular signal regulated Kinase
F	Force required to aspirate cell into micropipette
F-actin	Filamentous actin
FAK	Focal Adhesion Kinase
FITC	Fluorescein Isothiocyanate
fMLP	N-formyl-methionine-leucine-phenylalanine
FOV	Field of View

FRET	Fluorescence Resonance Energy Transfer
G	Gravity
G-actin	Globular actin
GAP	GTPase Activating Protein
GCP-2	Granulocyte chemotactic peptide-2
GDP	Guanine diphosphate
GEF	Guanine Nucleotide Exchange Factor
GPCR	G-protein Coupled Receptor
GRO	Growth related oncogenes
GTP	Guanosine triphosphate
H	Gasket thickness
HBSS	Hank's Balanced Saline Solution
HEPES	4-(2-hydroxyethyl)-1-piperazineethanesulfonic acid
HAS	Human Serum Albumin
H ₂ O ₂	Hydrogen Peroxide
I domain	Inserted domain
ICAM-1	Intercellular Adhesion Molecule-1
IFN	Interferon
IgG	Immunoglobulin
ILK	Integrin Linked Kinase
IL	Interleukin
JNK	c-Jun N-terminal Kinase
kD	Kilodaltons
L	Length of gasket window
LAD	Leukocyte adhesion deficiency
LFA-1	Lymphocyte function associated antigen-1 (CD11a/CD18)
LIMK	LIM domain Kinase
LPS	Lipopolysaccharides
LTB ₄	Leukotriene B ₄
mAb	Monoclonal Antibody
Mac-1	Macrophage-1 antigen, (CD11b/CD18)
MAdCAM-1	Mucosal vascular addressin cell adhesion molecule-1
MAPK	Mitogen-activated protein Kinase
MAP2K	Mitogen-activated protein Kinase Kinase
MAP3K	Mitogen-activated protein Kinase Kinase Kinase
MARCKS	myristoylated alanine-rich C Kinase substrate
mDia1	Diaphanous-related forming 1
MGSA	Melanoma growth stimulating activity
MIDAS	Metal-ion dependent adhesion site
MIP	Macrophage inflammatory protein
mRNA	messenger Ribonucleic acid
NADPH	Nicotinamide adenine dinucleotide phosphate
NAP-2	Neutrophil-activating peptide-2
NK	Natural Killer
NMR	Nuclear Magnetic Resonance
NP-40	Nonyl Phenoxypolyethoxyethanol

O ₂ ⁻	Superoxide
OH*	Hydroxyl Radical
P	Pressure
PAF	Platelet-activating Factor
PAK	p21 activated kinase
PBP	Platelet Basic Protein
PBS	Phosphate Buffered Saline
PF4	Platelet Factor 4
PIP2	Phosphatidylinositol 4,5-bisphosphate
PIP3	Phosphatidylinositol (3,4,5)-trisphosphate
PI3K	Phosphatidylinositol-3 kinase
PKA	Protein Kinase A
PKB	Protein Kinase B (Akt)
PKC	Protein Kinase C
PLC	Phospholipase C
PMA	Phorbol 12-Myristate 13-acetate
PMSF	Phenylmethylsulfonyl fluoride
PSGL-1	P-selectin Glycoprotein Ligand-1
PSI	plexin-semaphorin-integrin
Q	Volumetric Flow Rate
Rac1	Ras-related C3 botulinum toxin substrate 1
RANTES	Regulated upon Activation, Normal T-cell Expressed, and Secreted, CCL5
RAPL	Regulator for cell adhesion and polarization enriched in lymphoid tissues
RGD	Arginine-Glycine-Aspartic Acid
RhoA	Ras homolog gene family, member A
ROS	Reactive Oxygen Species
R _p	Radius of micropipette
R _s	Radius of transducer
RT	Room Temperature
RT-PCR	Reverse transcription polymerase chain reaction
SCR	Short Consensus Repeats
SDS	Sodium dodecyl sulfate
Ser	Serine
SFK	Src Family Kinase
SOCS	Suppressor of Cytokine Signaling
Sos	Sons of Sevenless
STAT	Signal transducers and activators of transcription
t	Time
TACE	Tumor Necrosis Factor- α converting enzyme
TCR	T cell Receptor
TD	Integrin Tail Domain
TEMED	Tetramethylethylenediamine
TNF- α	Tumor Necrosis Factor- α
Tris	Tris(hydroxymethyl)aminomethane

TSA solution	0.01 M Tris-Cl (pH 8.0), 0.14 M NaCl, and 0.025% sodium azide
TTS buffer	50 mM Tris-Cl, 0.1% Triton-X-100, 0.5 M NaCl buffer
U	Mean Fluid Velocity in the Flow Chamber
U_f	Velocity of force transducer moving freely during pressure Δp
U_t	Velocity of force transducer during adhesion
\bar{v}	Fluid Velocity
v_x	Fluid Velocity in the x-direction
VCAM	Vascular cell adhesion molecule
Vinc	Vinculin
VLA	Very Late Activation Antigen
WASP	Wiskott-Aldrich syndrome protein
μ	Fluid Viscosity
ρ	Fluid Density
Δp	Suction pressure at manometer
τ_{xz}	Wall Shear Stress

Chapter 1: Introduction

1.1 Overview of Inflammation

Inflammation functions as part of normal host surveillance mechanisms to destroy or quarantine both harmful agents and damaged tissue¹. The immune system's response to inflammation is mediated primarily through leukocytes derived from pluripotent stem cells in the bone marrow during postnatal life including neutrophils, eosinophils, basophils, monocytes and macrophages, natural killer (NK) cells, and T and B lymphocytes².

Leukocytes are derived from a myeloid or lymphoid lineage and provide either innate or adaptive immunity, respectively as shown in **Figure 1.1**. Myeloid cells include highly phagocytic and motile neutrophils, monocytes, and macrophages that provide a first line of defense against most pathogens. The other myeloid cells, including eosinophils, basophils, and their tissue counterparts, mast cells, are involved in defense against parasites and in the production of allergic reactions². In contrast, lymphoid cells are responsible for long-lasting, acquired immunity against microbes and are differentiated into three separate lines: NK cells, T lymphocytes (T cells) and B lymphocytes (B cells). T lymphocytes are thymic-dependent cells that recognize antigens via their T cell receptors (TCR). B lymphocytes are thymic-independent and are able to secrete antibodies and present antigens to bind to TCRs located on T cells.

Leukocytes circulate in the blood and intercommunicate via specific ligand-receptor interactions between cells and via secreted molecules called cytokines. Cytokines such as Tumor Necrosis Factor- α (TNF- α) and Interleukin-1 (IL-1), in turn, act

as secondary messengers to induce the expression of adhesion molecules on the surface of endothelial cells (ECs) and leukocytes.

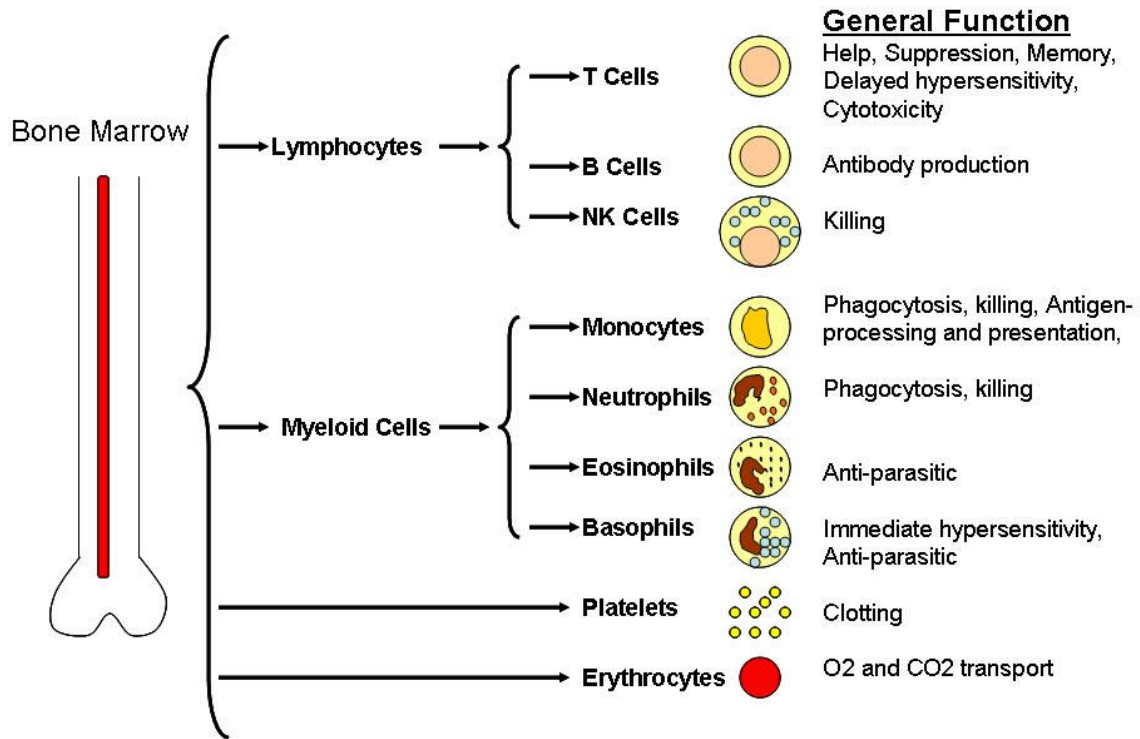


Figure 1.1 Production of blood cells from pluripotent stem cells in the bone marrow and their function

Lymphoid derived cells (T, B and NK cells) are responsible for adaptive immunity in the host while myeloid derived cells (monocytes, neutrophils, eosinophils and basophils) offer immunity through innate responses.

1.1.1 The Leukocyte Adhesion Cascade

Leukocytes migrate from the blood vessels to the inflamed tissue through a multi-step process that depends on specific ligand-receptor interactions which mediate different steps involved in the adhesion cascade as shown in **Figure 1.2**. The cascade involves the initial capture of the leukocytes from flow by the endothelium and subsequent rolling followed by arrest and finally transmigration through the endothelium and migration to the site of inflammation.

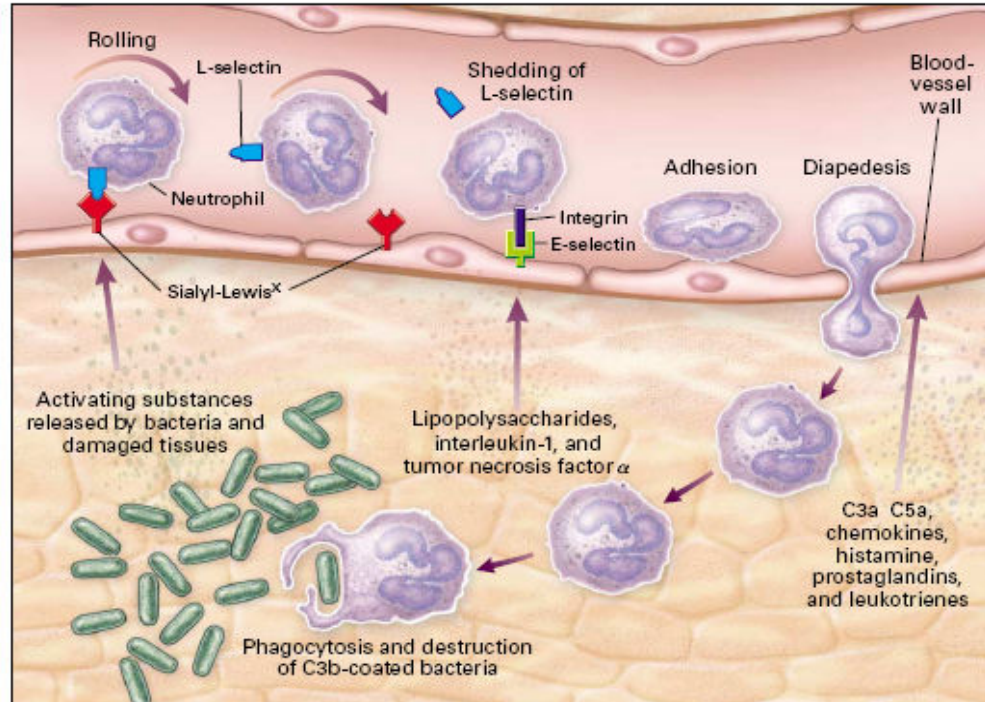


Figure 1.2 The Leukocyte Adhesion Cascade

During inflammation bacteria and damaged tissues release chemoattractants and cytokines that cause and increase in the expression of chemokines and adhesion molecules on the surface of the endothelium. Leukocytes circulating in the blood interact with these molecules in a multistep process known as the adhesion cascade. The first step of the cascade involves the initial capture and transient rolling interactions that are mediated by selectins and their ligand PSGL-1. The leukocytes then shed their L-selectin after cleavage by metalloproteases, while simultaneously increasing their surface expression of integrins. Integrin ligands such as ICAM-1 are IgG proteins that mediate the arrest and firm adhesion and ultimate transmigration of the cells to sites of inflammation. Once through the endothelial layer neutrophils attack pathogens through three processes: phagocytosis, the generation of ROS and degranulation. Reprinted from New Eng. J. of Medicine, Vol. 343, issue 1, Delves P.J. and Roitt I.M., *The Immune System: first of two parts*, 37-49, ©2000, with permission from the Massachusetts Medical Society.

The capture and transient rolling steps are generally mediated by selectins and their carbohydrate ligands. Once captured, leukocytes are exposed to chemokines on the surface of the endothelium. These chemokines activate G-protein coupled receptors (GPCR) on the surface of the leukocytes which initiate signaling cascades within the leukocytes and result in an increase in the adhesiveness of the integrins for their immunoglobulin (Ig) superfamily ligands expressed by the vascular endothelium³. The activated integrins decrease leukocyte rolling velocities and mediate the firm adhesion

and ultimate transmigration of the leukocytes through the vascular endothelial monolayer.

1.1.1.1 Selectins

Selectins are single chain transmembrane glycoproteins responsible for the initial capture of leukocytes from blood flow to the vascular endothelium. Three different members of the selectin family have been identified: L-selectin (CD62L), E-selectin (CD62E), and P-selectin (CD62P). All three selectins have similar structures featuring an N-terminal calcium dependent lectin domain, an epidermal growth factor-like (EGF) domain, a variable number of short consensus repeat (SCR) domains, a transmembrane domain, and a cytoplasmic tail domain⁴. **Figure 1.3** depicts a schematic of the structure for each of the selectins which has been determined experimentally in studies using X-ray Crystallography⁵ and nuclear magnetic resonance (NMR)⁶. Each selectin is also capable of binding to the sialyl Lewis X residue of P-selectin Glycoprotein ligand-1 (PSGL-1) and to a lesser extent its positional isomer sialyl Lewis A⁷.

Although similar in structure, members of the selectin family differ in their tissue distribution and binding kinetics. L-selectin is found only on leukocytes and is responsible for leukocyte-EC interactions and acts as a homing receptor for leukocytes to enter lymphoid tissues via high endothelial venules. P-selectin is expressed on platelets and ECs, while E-selectin is expressed only on ECs. In ECs stimuli such as cytokines (described in section 1.1.2), thrombin and histamine have been shown to stimulate the mobilization of P-selectin from stores inside cell to the cell surface⁸.

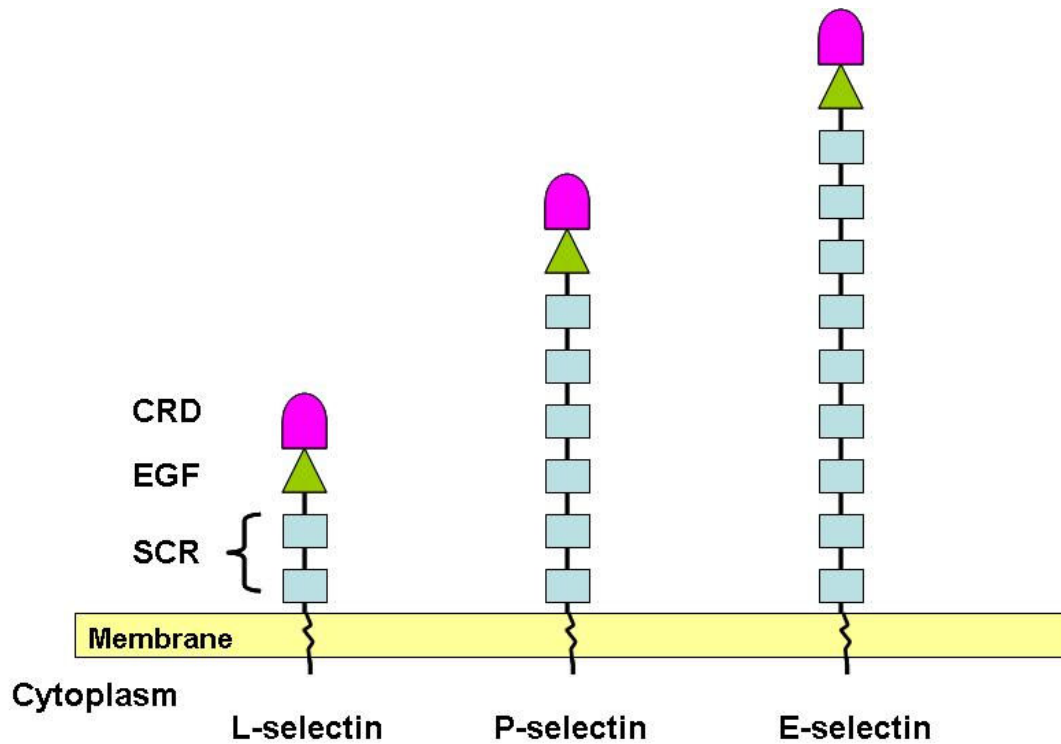


Figure 1.3 Schematic of L-selectin, P-selectin and E-selectin Structure.

Each selectin contains an N-terminal calcium dependent carbohydrate (lectin)-recognition domain (CRD), an epidermal growth factor-like (EGF) domain, a variable number of short consensus repeat (SCR) domains, a transmembrane domain, and a cytoplasmic tail domain.

1.1.1.2 Integrins

Integrins are heterodimers formed by the combination of one of eighteen different α subunits and one of eight different β subunits. In humans there are at least twenty-four known integrins as shown in **Figure 1.4**. Both the larger α (120 to 180 kiloDaltons (kD)) and smaller β (90 to 110 kD) subunits each contain two tails that span the plasma membrane and exhibit small cytoplasmic domains^{9 10}.

Integrins vary in their ligand specificity and tissue distribution as shown in **Table 1.1**. Several integrins are capable of binding to extracellular matrix proteins including collagen, laminin and proteins with the integrin binding motif Arginine-Glycine-Aspartic acid (“RGD”). Integrins with β_2 and β_7 subunits, including leukocyte function associated antigen-1 (LFA-1, $\alpha_L\beta_2$) and macrophage-1 antigen (Mac-1, $\alpha_M\beta_2$), are expressed

exclusively on leukocytes and involved in the localization of circulating cells to sites of tissue injury and host defense against bacterial infection. Studies have shown that humans with leukocyte adhesion deficiency (LAD), a mutation affecting human β_2 integrins, exhibit impaired neutrophilic responses and usually succumb to recurrent bacterial infections^{11,12}.

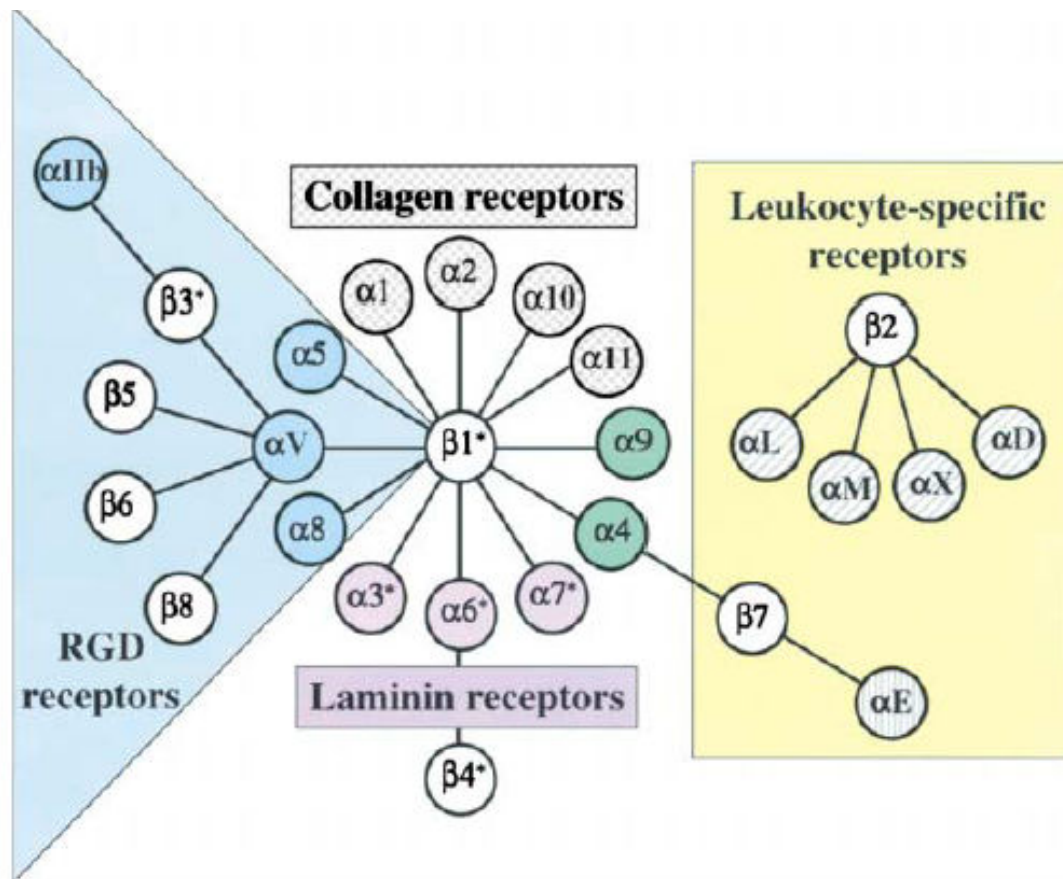


Figure 1.4 The Integrin Receptor family

The 24 known mammalian integrins are composed of combinations of one of 18 different α chains and 8 different β chains. Integrins can be further divided into subfamilies based on tissue distribution, ligand specificity and evolutionary relationships. α subunits with gray hatching or stripling have inserted I/A domains. α subunits with specificity for laminins (purple) or RGD (blue) are found throughout the metazoan. Integrins with β_2 and β_7 subunits (shown in the yellow box) are expressed exclusively on leukocytes¹¹. Reprinted from Cell, Vol 110, Hynes RO., Integrins: Bidirectional, Allosteric Signaling Machines, 673-87, Copyright (2002), with permission from Elsevier.

α chain	β chain	CD	Synonym	Ligands	Distribution
α_1	β_1	CD49a/CD29	VLA-1 (Very Late Activation Antigen-1)	Collagens, laminins	Many
α_2		CD49b/CD29	VLA-2	Collagens, laminins	Many
α_3		CD49c/CD29	VLA-3	Collagens, laminins, fibronectin	Lymphocytes
α_4		CD49d/CD29	VLA-4	Vascular cell adhesion molecule-1 (VCAM-1), Mucosal vascular addressin cell adhesion molecule-1 (MadCAM-1), pro-von willebrand factor, fibrinogen, fibronectin, thrombospondin,	Hematopoietic cells
α_5		CD49e/CD29	VLA-5	Fibronectin, proteinases	Widespread
α_6		CD49f/CD29	VLA-6	Laminins, matrix macromolecules	Widespread
α_L	β_2	CD11a/CD18	LFA-1	ICAM-1-5, Type I collagen	T cells, B cells, monocyte/macrophages, NK cell, neutrophils, eosinophils
α_M		CD11b/CD18	Mac-1, CR3 (Complement Receptor 3)	ICAM-1-2, ICAM-4, laminin, complement C3 fragment iC3b, collagen, heparin, fibrinogen, serum proteins	Neutrophils and monocytes/macrophages, eosinophils, basophils, NK cells
α_x		CD11c/CD18	p150, 95	Fibrinogen, collagen, heparin	Monocytes/macrophages, neutrophils, NK cells
α_D		CD11d/CD18		ICAM-3, VCAM-1	Macrophage, Lymphocytes, NK cells, eosinophils
α_4	β_7	CD49d/ β_7		MAdCAM-1	Lymphocytes (mucosal lymphoid nodules)

Table 1.1 Ligand and Tissue Distribution of a few Key Integrins

Integrins are a class of adhesion molecules responsible for both cell-cell and cell-ECM adhesion¹³⁻¹⁸. These adhesion molecules vary in distribution with the exception of β_2 and β_7 integrins that are expressed exclusively on leukocytes.

Both of the β_2 integrins LFA-1 and Mac-1 are capable of binding to the ligand intracellular adhesion molecule-1 (ICAM-1), however their ligation occurs at different sites¹³. ICAM-1 (90-120 kD) is a member of the immunoglobulin (IgG) superfamily of proteins whose structure is characterized by heavy glycosylation. The protein's structure features a cytoplasmic domain, a single transmembrane domain and an NH₂-terminal extracellular domain composed of multiple loops created by disulfide bridges. ICAM-1 is expressed on a variety of cells including endothelial cells (EC) and its expression can be upregulated in response to cytokines (see section 1.1.2) such as IFN- γ , IL-1, and TNF- α . Mutation studies have shown that LFA-1 binding requires the domain 1 (D1) (N-terminal), whereas Mac-1 binds to the third immunoglobulin-like domain (D3)¹³⁻¹⁴. This study will examine expression levels of Mac-1 and the binding of LFA-1 to ICAM-1.

The determination of the structure and conformation of integrins has required years of effort and has recently been determined through NMR, electron microscopy (EM) and crystallography¹⁹⁻²³. Both the α and β subunits contain a large extracellular region, single pass transmembrane domain and a short cytoplasmic tail (usually less than 50 amino acids) as shown in **Figure 1.5**.

The extracellular domain (ED) of the α chain is composed of a β propeller domain with seven blades, a thigh domain, and two calf domains each containing two anti-parallel β -sheets²². The α subunit has been compared to a "leg" that has "knee" (genu) located between the thigh and first calf domains. A Ca²⁺ binding site is also found at the genu and may play a role in regulating integrin activation²⁴. EM and crystallography experiments using $\alpha_x\beta_2$ and $\alpha_v\beta_3$ integrins have indicated that this region is bent at a 135 degree angle when integrins are not active^{20,25}. The extension of the 'leg' of the integrin

is associated with a transition from low to high ligand-binding affinity. This model of integrin activation is supported by studies using Fluorescence Resonance Energy Transfer (FRET)-based measurements, EM analysis, NMR, and the mapping of epitope structures that have determined that a bent conformation is associated with a low affinity state in which the binding of integrins to their ligands is not likely to occur^{9,26-34}.

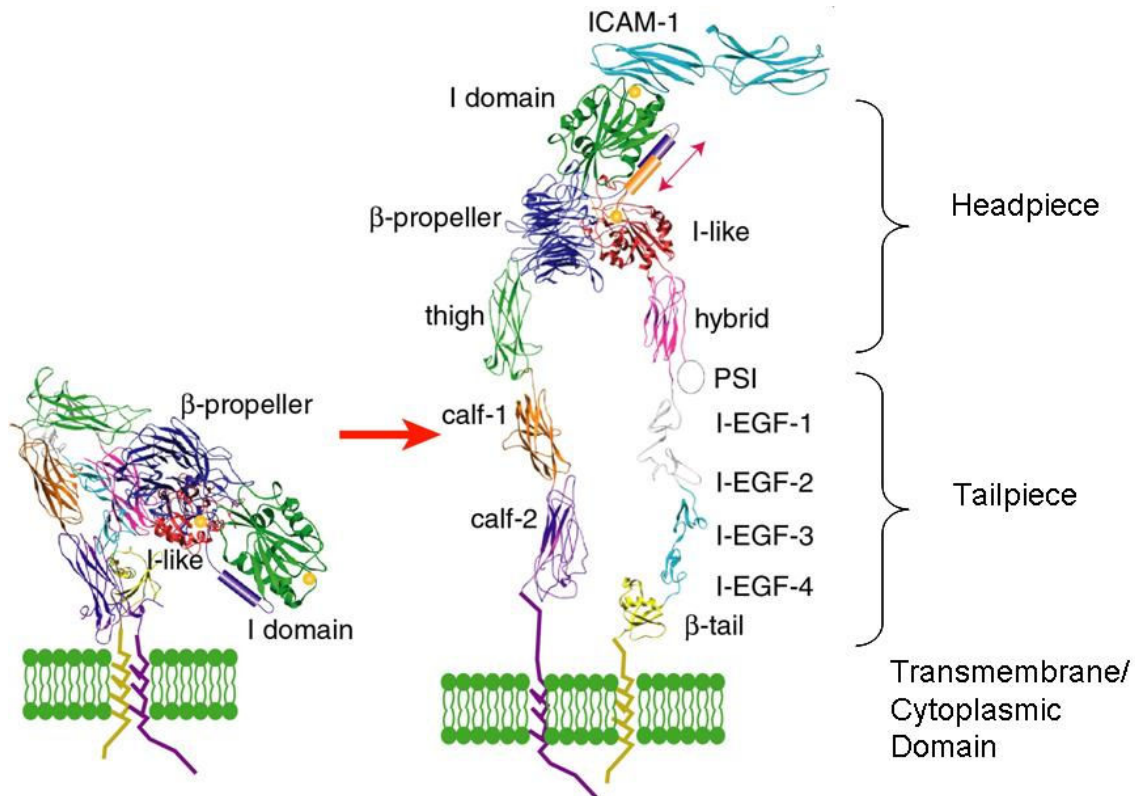


Figure 1.5 Schematic of Integrin Structure showing a Conformational Change as a Result of Activation.

Integrin signaling is bidirectional and can be transmitted from the extracellular environment into the cell cytoplasm (“outside-in signaling”), and from the cytoplasm out to the extracellular domain of the receptor (“inside-out signaling”)¹⁰. Both types of signaling result in a conformational change in the receptor from an inactive bent state to an extended, active state that is associated with increased affinity for ligand-binding. Reprinted from *Current Opinion in Cell Biology*, vol. 15, Carman C.V. and Springer T.A, Integrin avidity regulation: are changes in affinity and conformation underemphasized?, 547-556, Copyright (2003), with permission from Elsevier.

Half of the α subunits, including α_M and α_L , contain an inserted domain (I domain, also known as α_A domain) that is capable of adopting the Rossmann nucleotide-binding fold²³. This α -I domain is the ligand binding site for β_2 integrins and integrins that bind

to collagen. Integrins that lack an I-domain contain an A-domain ligand binding site on their β subunits. Both types of I-domains feature, at their apex, a metal-binding site known as the metal-ion dependent adhesion site (MIDAS). MIDAS is believed to be used by integrins as an anchorpoint for binding to the carboxylate of their ligands¹⁴.

The extracellular domain of the β subunit contains a plexin-semaphorin-integrin (PSI) domain, an I-like (or β A) domain, a hybrid domain formed by two contiguous primary amino acid sequences, four Integrin-epidermal growth factor (EGF) folds and a β tail domain (TD). The divalent cation binding sites on the β subunit I-like domain have also been shown in mutation studies to regulate affinity for integrin ligands³⁵.

The conformation of the integrin changes not only from a bent to extended state but also from a “closed” to “open” one as well^{23,36,37}. The current hypothesis for the regulation of integrin activation theorizes that the affinity of an individual integrin for its ligand depends upon both the extension of the ED and the “openness” of the integrin determined by the separation between the cytoplasmic tails of the α and β subunits. In the open conformation there is a distinct coordination between the metal in the MIDAS, a specific arrangement of the β_6 -strand- α_7 -helix loop and a 10 Å shift of the carboxyl terminal α_7 helix down the side of the I domain that leads to a high affinity state³⁷⁻³⁹. Structural mutations to the cytoplasmic tails, such as the addition of disulfide bonds to lock the integrin into an open conformation, have yielded similar results^{27-29,34,39-42}. Meanwhile the extended/closed and extended/open conformations correspond to intermediate and high affinity states respectively^{25,30,43}.

Many integrins are not constitutively active; they are often expressed on the cell surface in an inactive or “OFF” state in which they do not bind to their ligands. In order

for ligand binding to occur the receptor must be converted to an active state¹⁵. Integrin activation is a highly regulated process that can occur via either “outside-in” or “inside-out” signaling¹⁵. The binding of integrin extracellular domains to ligands and other agonists (phorbol 12-myristate 13-acetate (PMA), Mg^{2+} or Mn^{2+}) and physiological forces can result in a conformational change in the integrin that regulates multiple cellular functions through the conduction of biochemical and mechanical signaling into the cell which is known as “outside-in signaling”. In contrast, integrin activation initiated through “inside-out signaling” is mediated through stimuli received from cell surface receptors including TCR and chemokines receptors that generate intracellular signals as shown in **Figure 1.6**⁴⁴.

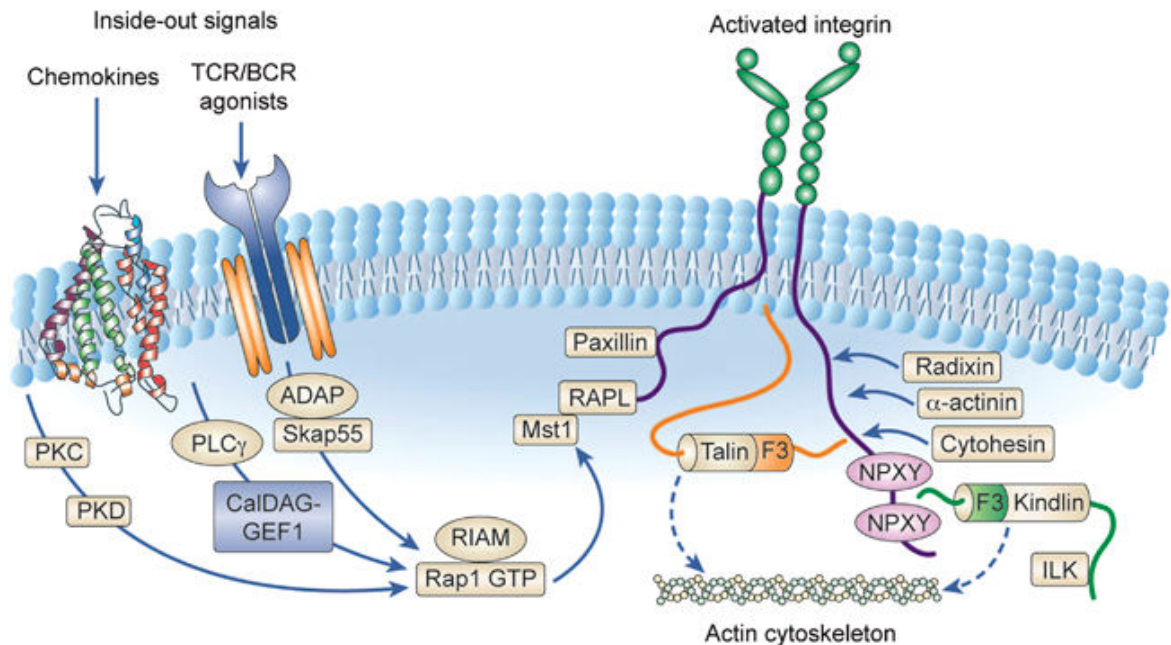


Figure 1.6 Schematic of Integrin Inside-out Signaling

Chemokine and TCR activation transduce signals to guanine nucleotide exchange factors which activate the small GTPase Rap1. Activated GTP-bound Rap1 then signals to its effectors RIAM and RapL which form a complex with the cytoplasmic tails of integrins. This allows a number of other proteins to bind to the tail including Paxillin, Radixin, cytohesin, α -actinin and the kindlins. The cytoplasmic tails of the integrin's α and β subunits separate and change the conformation state of the integrin. This change in conformation is essential for high-affinity ligand binding and coupling to the actin cytoskeleton. Reprinted with permission from Macmillan Publishers Ltd: Immun. And Cell Biol, (Abram C.L. and Lowell C.A. (2009) Immun. And Cell Biol. **87**: 440-442), copyright (2009).

Integrins are capable of bidirectional signaling to the cellular cytoskeleton through associations between their cytoplasmic tails and cytosolic proteins. Much of this signaling transduction is modulated by integrin tail phosphorylation^{45,46}. Cell migration requires coupling between the cytoplasmic tails of integrins and the cytoplasmic adaptor protein paxillin^{47,48}. The association between paxillin and the cytoplasmic tail of the integrin was shown by Han et al. to be inhibited by protein kinase A (PKA)-mediated phosphorylation of Ser⁹⁸⁸ on the integrin⁴⁹.

The overall ability of cells to adhere to integrin ligands depends on both integrin affinity and avidity. Affinity characterizes the strength of a single integrin-ligand bond, while avidity describes the strength of multiple bond interactions, that is, multimeric affinity or functional affinity⁵⁰. Avidity is altered by integrin clustering at Focal adhesions and it is believed that lymphocytes are only able to bind to ligands when LFA-1 is clustered at the cell surface^{51,52}. Some studies have shown that the clustering of LFA-1 is dependent on the presence of lipid raft microdomains in the cell membrane which may serve as platforms where signaling molecules can congregate^{53,54}. Avidity regulated by lipid rafts seems to be dependent on phosphatidylinositol-3 kinase (PI3K) activity and cytoskeleton mobility and is known as ligand-induced active microclustering⁵⁴. In addition, ligand-binding itself can influence integrin clustering through ligand-induced redistribution of integrins to further increase ligand binding⁵⁵. A schematic of modes of cellular integrin reorganization is shown in **Figure 1.7**.

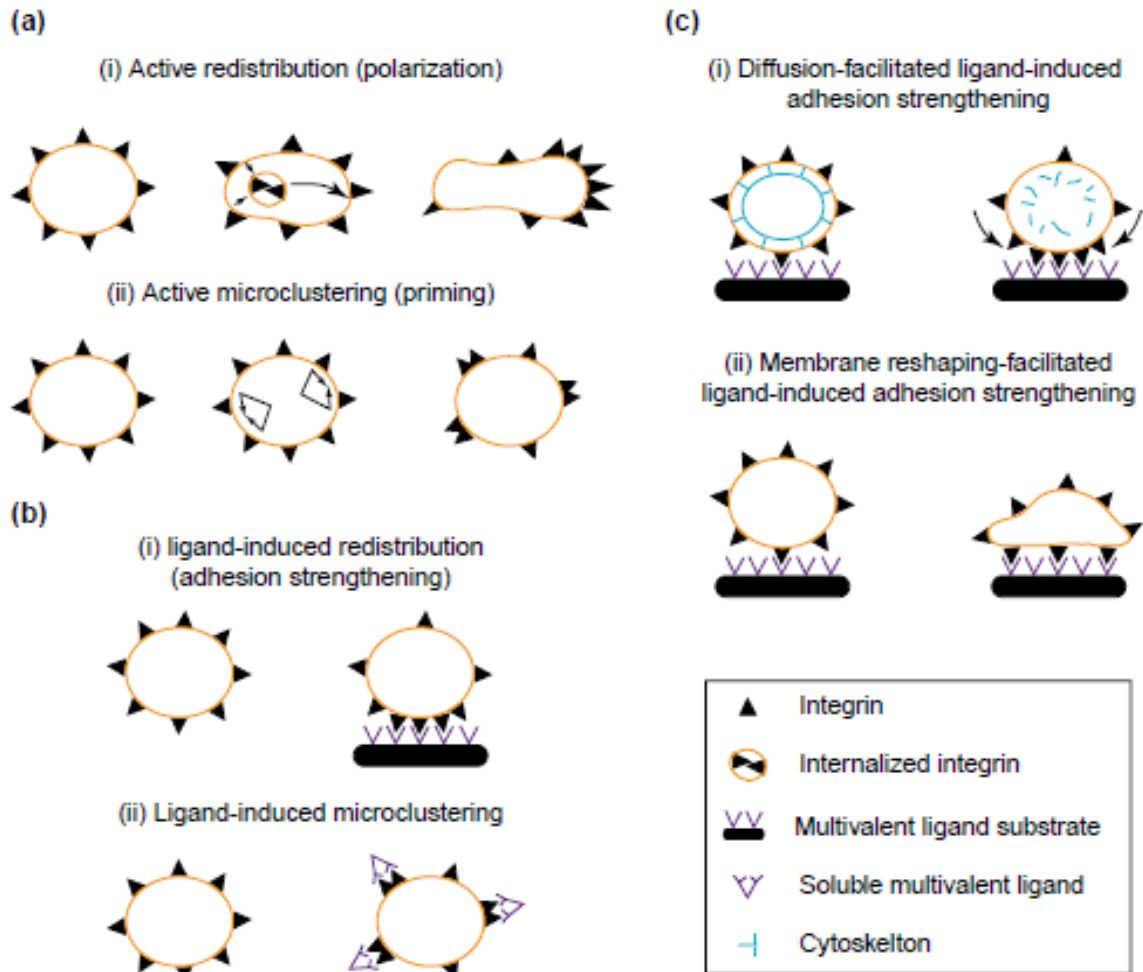


Figure 1.7 Modes of cellular integrin reorganization associated with valency regulation

(a) Ligand independent reorganization. (i) Reorganization may require the active transport of integrins in vesicles to achieve polarization. (ii) Integrins can also be driven into microclusters through associations with lipid rafts. (b) Ligand induced integrin redistribution. (i) Integrins can redistribute to zones where a ligand-contact has already formed in cell-cell or cell-ECM interactions. (ii) Microclustering might occur due to the binding of soluble multivalent ligands to integrins. (c) Adhesion Strengthening is ligand independent and depends upon global and internal cell structure (i) Inside-out signaling is capable of dissociating integrins from the actin cytoskeleton allowing them to redistribute. (ii) Cell deformation arising from spreading can enhance the binding between integrins and their ligands. Post-ligand binding associations between the integrin and actin cytoskeleton can further strengthen adhesion, as seen in focal adhesions. Reprinted from *Current Opinion in Cell Biology*, vol. 15, Carman C.V. and Springer T.A, Integrin avidity regulation: are changes in affinity and conformation underemphasized?, 547-556, Copyright (2003), with permission from Elsevier.

Focal adhesions are macromolecular assemblies that transmit both mechanical force and regulatory signals and often serve as a hub to concentrate and direct signaling proteins. These assemblies can also work to strengthen integrin-mediated adhesion by upregulating integrin clustering. Focal adhesions are sites of tight adhesion between the

ECM and several protein complexes inside the cell including integrins and cytoplasmic proteins such as paxillin, talin, vinculin and α -actinin as depicted in **Figure 1.8**⁵⁶. Paxillin interacts directly with the cytoplasmic tail domain of the integrin subunits (as described earlier in this section) and is phosphorylated upon integrin engagement by the tyrosine kinases Src family kinases (SFK) and focal adhesion kinase (FAK).

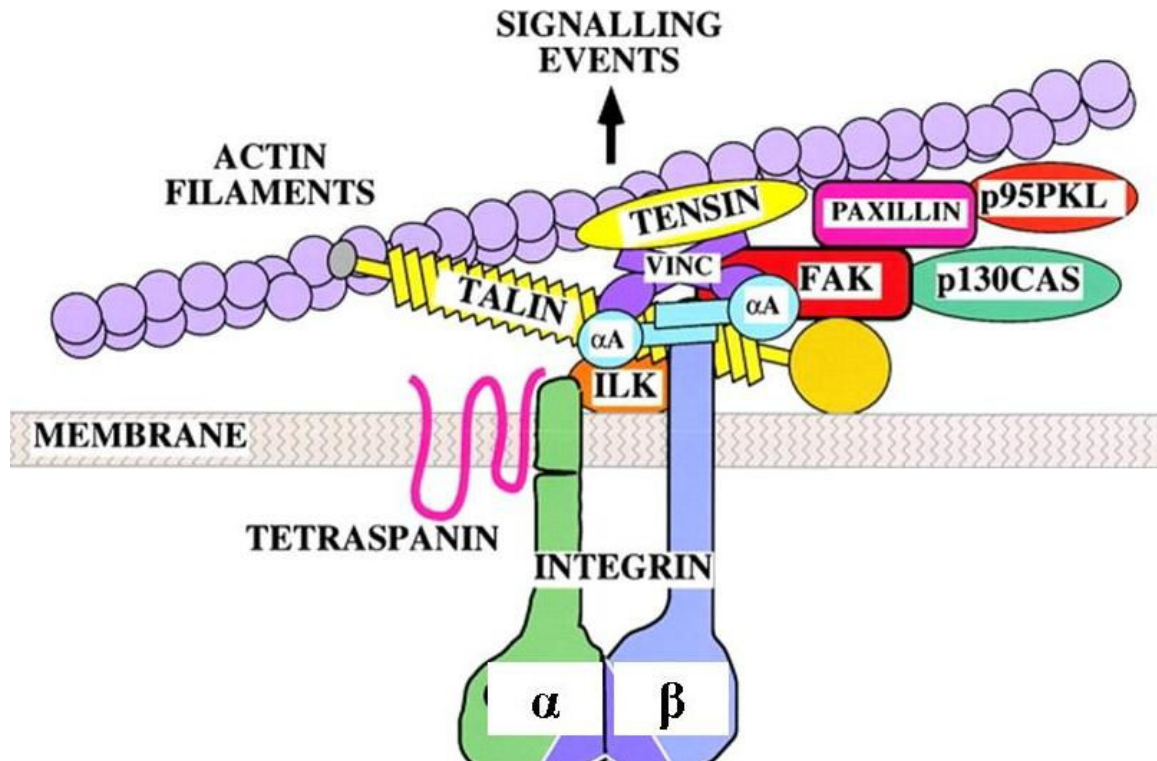


Figure 1.8 Schematic of Focal Adhesion proteins involved in the signaling between integrins and the actin cytoskeleton.

Integrins regulate changes in actin filament organization through adapter proteins including Talin, Tensin, Paxillin, Vinculin (Vinc), α -actinin (αA), and kinases such as Focal Adhesion Kinase (FAK) and integrin-linked kinase (ILK). Reprinted with permission from Rockefeller University Press © 2000. Originally published in *Journal of Cell Biology*:150:F89-F96

Talin is a high-molecular weight integrin-bound protein that is capable of coupling β integrins to the actin cytoskeleton either directly or indirectly by interacting with vinculin and α -actinin^{57,58}. Vinculin (Vinc) binds to both talin and α -actinin as well as paxillin and actin filaments⁵⁹. The binding of Vinc to talin and actin is regulated by polyphosphoinositides.

FAK is a 125 kD protein that promotes the turn-over of cell contacts with the ECM, but is not absolutely necessary for migration. FAK becomes phosphorylated in response to integrin engagement. FAK, SFK and PI3K modulate the actin cytoskeleton through interactions with downstream Rho GTPases as shown in **Figure 1.9**. PI3K catalyzes the phosphatidylinositol 4,5-bisphosphate (PIP₂) to generate the lipid byproduct phosphoinositol 3,4,5-trisphosphate (PIP₃) and can be activated by GPCR signaling. Downstream effectors of PI3K include protein kinase C (PKC) and protein kinase B (PKB also known as Akt). Downstream effectors of PKC include the Raf1/MEK/ERK1/2 MAPK signaling cascade, Rap1 and the substrate protein myristoylated alanine-rich C Kinase substrate (MARCKS)^{44,60,61}. MARCKS phosphorylation is required for integrin avidity changes during PKC-mediated integrin activation^{62,63}. PKC is also known to signal to Rho family GTPases.

The family of Rho GTPases is a family of small (21 kD) signaling G proteins that are downstream of both chemokine receptors and integrin adaptor proteins. They function to regulate changes in actin polymerization through signaling to downstream effectors. These proteins are thought to act like a “switch” because they are only active in their guanosine triphosphate (GTP)-bound form. GTP hydrolysis converts the Rho GTPase to its inactive form and is initiated by GTPase-activating proteins (GAPs). The reaction is reverted by Guanine nucleotide exchange factors (GEFs). Members of the family include Cdc42 (Cell division control protein 42 homolog), Rac1 (Ras-related C3 botulinum toxin substrate 1) and RhoA (Ras homolog gene family, member A).

Cdc42 regulates actin polymerization by directly binding to a Wiskott-Aldrich syndrome protein (WASP) family protein (described in section 1.1.1.3). Cdc42 also

binds to the serine threonine kinase ROCK (Rho-associated coiled coil containing protein kinases), which phosphorylates and activates LIM kinase (LIMK). LIMK is responsible for increasing actin stability by phosphorylating cofilin, thereby inhibiting its ability to depolymerize actin filaments. Another target of Cdc42 is PKC ζ whose signaling is important for establishing cell polarity (discussed in section 1.1.1.3)⁶⁴. Cdc42 also binds to PI3K and p21 activated kinases (PAK), which can also activate LIMK. Signaling via Cdc42 is also required for the formation of thin projections at the leading edge of a cell known as filopodia and the phagosome (described in section 1.1.2).

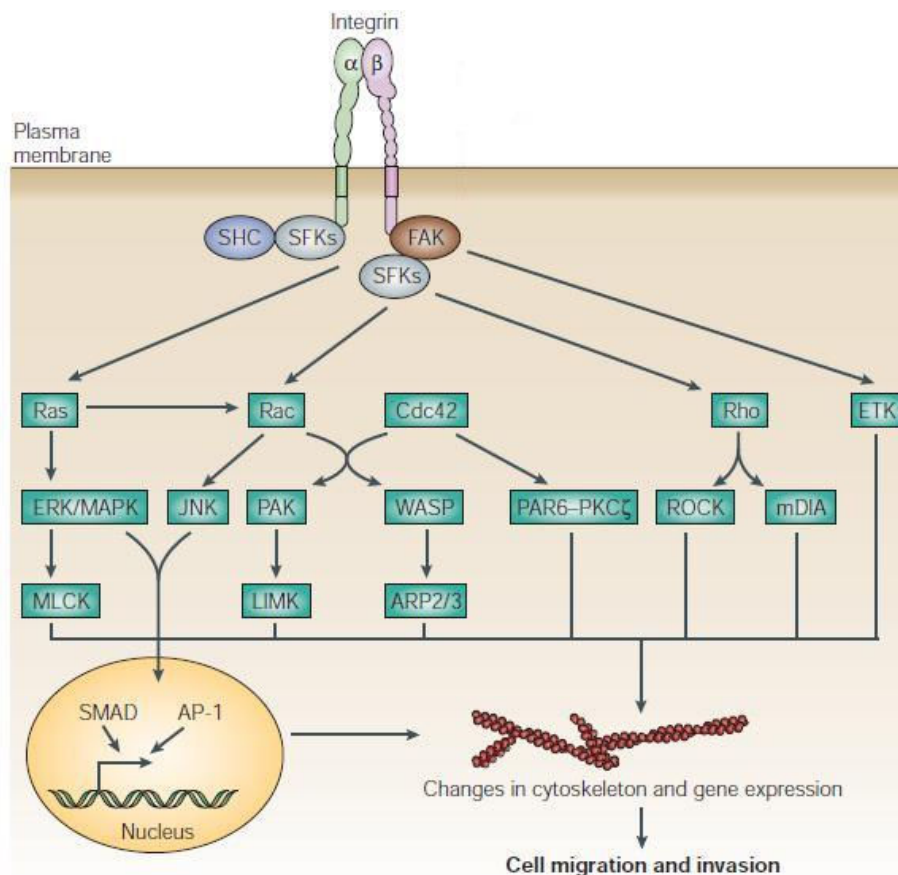


Figure 1.9 Intracellular Signaling Cascade Initiated by Integrin Activation

Integrin activation results in receptor conformational changes that cause signal transduction through Focal Adhesion kinase (FAK) and Src-family kinases (SFKs) to members of the Ras superfamily of GTPases including Rac, Ras, Cdc42 and Rho. These molecules then signal to downstream effectors to stimulate changes in gene expression and the cytoskeleton. Reprinted by permission from Macmillan Publishers Ltd: Nat Rev. Mol. Cell Biol., Guo et al. Nat Rev. Mol. Cell Biol. (10):816-26, copyright (2004).

Like Cdc42, Rac1 is a small (21 kD) GTPase that signals to both WASP and PAK proteins to regulate changes in the actin cytoskeleton⁶⁵. In addition, Rac1 also activates c-Jun N-terminal kinases (JNK) which belong to the mitogen-activated protein kinase (MAPK) family. Rac1's activity is regulated by PI3K in addition to FAK and is involved in the formation of lamellipodia in migrating cells.

The last Rho GTPase, RhoA regulates the formation of actin stress fibers, which are the thinnest filaments of the cytoskeleton. RhoA also activates RhoA Kinase (ROCK) and mDia1 (Diaphanous-related formin 1) which accelerates actin nucleation and the formation of actin filaments (discussed in section 1.1.1.3).

1.1.1.3 Cytoskeletal Reorganization

Rearrangement of the actin cytoskeleton is important for chemotaxis, cell spreading and phagocytosis. A major component of the actin cytoskeleton is actin, a highly-conserved protein that exists in two forms: monomeric globular-actin (G-actin) and filamentous-actin (F-actin). Actin filaments are formed by the reversible endwise polymerization of adenosine triphosphate (ATP)-bound (active) monomers. The ATP-bound actin is more stable than ADP-bound actin.

Actin filaments are polar and the rate of filament elongation depends on whether monomers are added to the barbed (+) end (fast-growing) or pointed (-) end (slow growing). Nucleotide hydrolysis takes place at the (-) end of the filament, causing ADP-actin monomers to dissociate faster from that end of the filament.

Polymerization is regulated by monomer and filament-binding proteins that control the monomer concentration, direct the formation of filaments organize filaments into arrays and depolymerize filaments for monomer recycling. Filament formation is

stimulated by nucleating factors such as the actin-related proteins (Arp2/3 complex), which mimics the structure of a G-actin dimer to initiate the nucleation of actin monomers. Arp2/3 binds to pre-formed actin filaments to form new branches oriented at a 70° angle from the first filament^{66,67}. The nucleating activity of Arp2/3 is activated by members of the WASP. Arp2/3 cofactors Cdc42 and PIP₂ relieve WASP's auto-inhibition, thereby allowing it to activate Arp2/3 as shown in **Figure 1.10**.

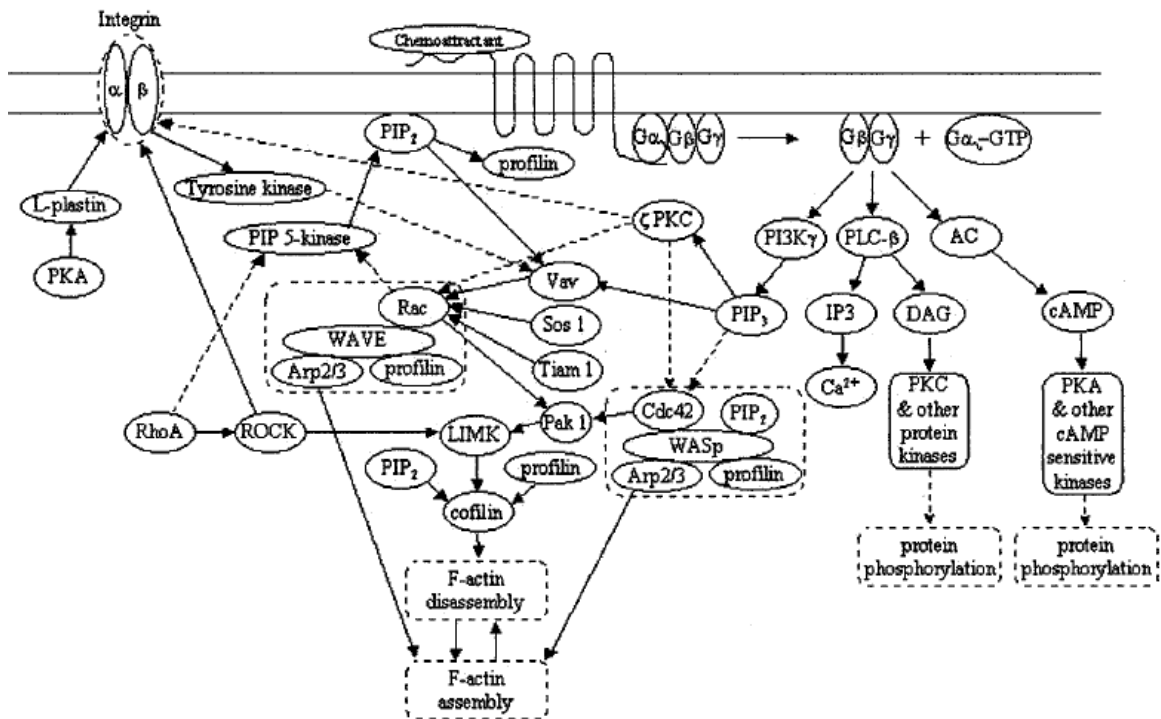


Figure 1.10 Diagram of the interaction of the integrin and chemoattractant GPCR signaling pathways

Both integrins and GPCRs alter actin polymerization through Rac activation. Note that the molecule phorbol 12-myristate 13-acetate (PMA), which activates Protein Kinase C (PKC) is able to activate integrins independent of GPCR-signaling. Reprinted with kind permission from Springer Science and Business Media, *Annals of Biomed. Eng.*, Vol. 30, 2002, 357, *Signaling in the Motility Responses of the Human Neutrophil*, Zhelev, D.V. and Alteraifi, A., Figure 1, © 2002 *Biomedical Engineering Society*.

The nucleating activity of the Arp2/3 complex is counteracted by the protein cofilin, which binds to both G- and F-actin. Cofilin is able to disrupt the actin cytoskeleton by depolymerizing the (-) end and inhibit their reassembly as well as sever

filaments by creating more (+) ends on filament fragments⁶⁸. The accelerated dissociation of the actin filaments allows the newly freed monomers to be recycled at filaments in other locations within the cell. This delicate balance of polymerization and depolymerization is known as actin filament treadmilling and is required for efficient cell migration⁶⁹.

Directional cell migration is important for leukocyte homing and inflammatory responses and requires the establishment of cell polarity^{64,70}. Once polarity is established leading edge protrusions, often seen as broad lamellipodia, are pushed forward by actin polymerization and stabilized by focal adhesions⁷⁰. These connections located at the leading edge of the cell provide traction for the cell to use during migration. In order for the cell to propel forward the focal adhesions at the rear of the cell must simultaneously become dissociated. Several of the signaling molecules required for adhesion and protrusion accumulate at the front of the cell including WASP, profilin, the Arp2/3 complex, PIP3 and Rho family GTPases (Rho, Rac and Cdc42)⁷⁰⁻⁷².

1.1.2 Neutrophil Activation

Neutrophils are produced from myeloid stem cells in the bone marrow and are the most abundant leukocyte subtype present in blood, accounting for approximately 50-70% of all white blood cells⁶⁸. Human neutrophil counts vary, but are normally between $2.5-7.5 \times 10^9/L$ ⁶⁸. The average lifespan of non-activated human neutrophils is 5.4 days, while activated cells survive for 1-2 days after migrating to sites of inflammation^{73,74}.

Neutrophils become activated in response to a variety of stimuli including chemoattractant agents, cytokines, and chemokines⁷⁵. Chemoattractant agents include molecules derived from bacteria such as lipopolysaccharides (LPS) and N-

formylmethionyl peptides (fMLP) and molecules produced by the inflammatory responses of other immune cells such as platelet-activating factor (PAF), Leukotriene B₄ (LTB₄) and the proteolytic fragment of the fifth component of complement (C5a)^{27,677}. Neutrophils stimulated with above the chemoattractants undergo directed cell migration, or chemotaxis towards higher gradients of the chemoattractants. In addition, chemoattractants act as positive feedback mechanisms by increasing the surface expression of β -integrins on neutrophils, which further enhances their motility^{78,79}. Lastly, chemoattractants can promote the activation of oxidase pathways, the desensitization of neutrophilic response to other chemoattractants and the secretion of cytokines⁸⁰.

Cytokines are small molecules produced by leukocytes, including neutrophils, during inflammation and consist of members of the interleukin family (IL-1) and interferons (TNF- α , IFN- γ). TNF- α and IL-1 are produced by macrophages/monocytes in response to LPS^{81,82}. In neutrophils, cytokines promote the expression of CD18, integrin activation and the shedding of L-selectin in addition to adhesion and the release of PAF and other mediators from granule contents.

Chemokines are specific types of cytokines that are small proteins (6 to 15 kD) with similar cysteinyl-containing structures. Chemokines are classified into subgroups based on cysteine motifs in their amino acid motif: C, CC, CXC, or CX₃C, where X is an amino acid⁸³. Chemokines are released from neutrophils, endothelium, platelets, monocytes and macrophages in response to inflammation. Chemokines that elicit responses in neutrophils include: interleukin-8 (IL-8), epithelial cell-derived neutrophil activating peptide-78 (ENA-78), neutrophil-activating peptide-2 (NAP-2), granulocyte

chemotactic peptide-2 (GCP-2), and three forms (α , β and γ) of growth-related oncogenes/melanoma growth stimulating activity (GRO/MGSA)⁷⁷. **Table 1.2** summarizes the effects of chemokines on neutrophils and their sources.

Chemokine	Synonyms	Receptor	Secreted by	Effects on Neutrophils
CXCL1	Growth-related oncogene- α (GRO- α), melanoma growth stimulating activity (MGSA)	CXCR2	Dendritic cells Melanoma cells,	Chemotaxis, Degranulation, Respiratory Burst, Induces expression of CD18, Rise in intracellular free Calcium ⁸⁴⁸⁵⁸⁶⁸⁷
CXCL2	Growth-related oncogene- β (GRO- β), Macrophage inflammatory protein-2 α (MIP-2 α)	CXCR2	Dendritic cells	Chemotaxis
CXCL3	Growth-related oncogene- γ (GRO- γ), Macrophage inflammatory protein-2 β (MIP-2 β)	CXCR2	Stromal cells, Dendritic cells	Chemotaxis
CXCL4	Platelet Factor 4 (PF4)	CXCR3B	Activated platelets	Chemotaxis ⁸⁸⁸⁹
CXCL5	Epithelial Cell-derived neutrophil activating peptide-78 (ENA-78)	CXCR2	Monocytes, Epithelial cells, ECs, mesothelial cells	Chemotaxis, rise in intracellular free calcium, Respiratory burst, induces expression of CD18, Degranulation ⁹⁰⁸⁴⁹¹⁸⁷
CXCL6	Granulocyte chemotactic peptide-2 (GCP-2)	CXCR1, CXCR2	Mesenchymal cells, ECs	Chemotaxis ^{9293,94}
CXCL7	Neutrophil activating peptide-2 (NAP-2), Platelet basic protein (PBP), Connective Tissue activating peptide III (CTAPIII),	CXCR1, CXCR2	Activated platelets	Chemotaxis, Degranulation, Respiratory Burst ^{89 86}
CXCL8	Interleukin-8 (IL-8)	CXCR1, CXCR2	Macrophages, Neutrophils, ECs	Induces expression of CD18 and L-selectin shedding, Chemotaxis, Degranulation, Respiratory Burst ^{8486 9595,9697 8798}

Table 1.2 Chemokines that target Neutrophils and their Function

The Chemokine receptor CXCR2 is able to bind to all neutrophil-activating chemokines with the exception of PF4, which signals to CXCR3B receptors. The receptor CXCR1, on the other hand, only binds to IL-8, NAP-2 and GCP-2. Both receptors belong to the large family of G_i-protein coupled receptors (GPCR) that contain seven transmembrane domains. Once activated GPCR receptors undergo a

conformational change that enables a trimeric GTP-binding protein (G protein) to change its conformation. The G protein can then exchange its guanine diphosphate (GDP) for GTP to become activated. Once activated the G protein can dissociate into its α and $\beta\gamma$ subunits and regulate the activity of other target proteins whose signaling can lead to changes in gene expression, protein translation, and reorganization of the actin cytoskeleton.

Mature neutrophils are highly motile cells that play a major role in host defense against the invasion of microorganisms and in acute inflammation. In addition to releasing cytokines and undergoing chemotaxis towards chemoattractants and cytokines activated neutrophils also shed L-selectin and increase their expression of integrins. L-selectin surface expression is rapidly down-regulated in activated neutrophils by a calmodulin-mediated proteolytic mechanism that cleaves L-selectin at a membrane-proximal site⁹⁹⁻¹⁰¹. This cleavage is mediated by the same enzyme, TACE (TNF- α converting enzyme), that processes pro-TNF and is blocked by inhibitors of zinc-dependent metalloproteases¹⁰². Studies have also observed L-selectin downregulation in PMA-stimulated neutrophils which suggests that PKC signaling transduction activates TACE^{103,104}.

Though small, the cytoplasmic domain of L-selectin is essential for normal L-selectin function. One study by Kansas et al. demonstrated that deletion of the COOH-terminal 11 amino acids of the L-selectin cytoplasmic tail inhibited neutrophil rolling in vivo and the ex vivo binding of lymphocytes to high endothelial venules (HEV) in peripheral lymph node tissue¹⁰⁵. The shedding of L-selectin serves to aid leukocytes in transforming from a rolling to firmly adherent phenotype. This concept is demonstrated

by a study by Hafezi-Moghadam et al. in which L-selectin shedding significantly increased firm adhesion and transmigration of mouse leukocytes on ICAM-1¹⁰⁶.

The shift from a rolling to firmly adherent phenotype is further aided by the simultaneous upregulation in β -integrins expression on neutrophils, including Mac-1. This upregulation is initiated through inside-out signaling as described in section 1.1.1 and shown in **Figure 1.11**¹⁰⁷. PMA has also been shown in studies to upregulate CD11b expression in neutrophils^{103,108-111}. The signal transductions generated by β -integrins can then modulate the adhesion, migration, phagocytosis, respiratory burst and granule release of neutrophils^{112,107}.

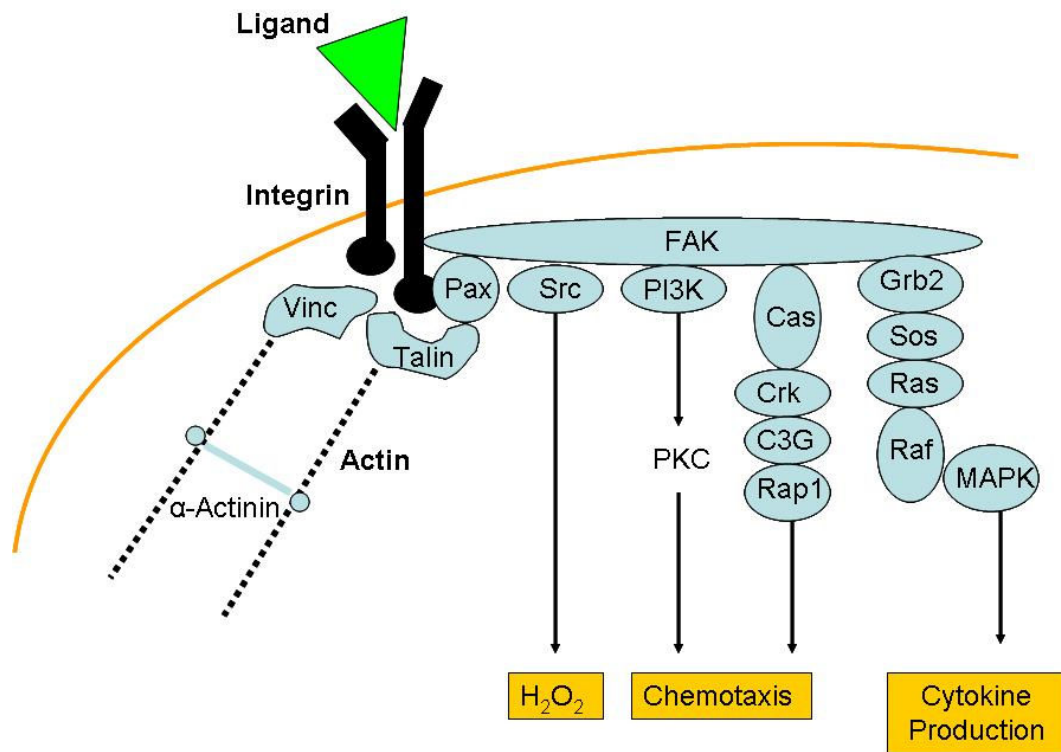


Figure 1.11 Effectors of Outside-in signaling to integrins in Neutrophils.

Schematic of integrin priming by IL-8, PMA (via PKC) and TNF- α , which all commonly signal to Rho GTPase.

Neutrophils also destroy invading pathogens through three processes: phagocytosis, the generation of reactive oxygen species (ROS, also known as respiratory burst), and degranulation. Phagocytosis is the process of engulfing foreign material by

the cell membrane to form an internal phagosome as shown in **Figure 1.12** and is initiated by the attachment of antibodies and opsonins to the surface of the pathogen. Engulfment of the material is facilitated by the actin-myosin contractile system. Once ingested, pathogens are fused with the lysosome to undergo two types of degradation, oxygen-dependent and oxygen-independent. The phagosome membrane is depolarized during superoxide production allowing for the transport of protons and potassium out of the neutrophil and into the phagosome. Once in the phagosome, potassium activates inactive proteases that are released by granules and protons are used in reactions involved in ROS production.

Oxygen-dependent degradation involves the production of ROS, such as superoxide, oxidized halogens and hydroxyl radicals, which are chemically reactive molecules derived from oxygen that contain unpaired valence shell electrons. Oxidants are able to damage a variety of biomolecules, including Deoxyribonucleic acid (DNA)¹¹³¹¹⁴. One pathway for the creation of ROS is through the superoxide-generating enzyme phagocytic Nicotinamide adenine dinucleotide phosphate (NADPH) oxidase (Nox2-based or phox) which catalyzes the one electron reduction of oxygen to O_2^- at the expense of NADPH¹¹⁵. Patients with a defective form of this oxidase suffer from enhanced susceptibility to microbial infections¹¹⁶.

Oxygen-independent degradation of pathogens is known as degranulation and relies on the release of proteins to aid in targeting and killing microbes. Granules can be divided into three categories: peroxidase-positive azurophilic granules, specific granules and gelatinase granules¹¹⁷. Azurophilic granules are the most potent subtype and contain antimicrobial substances such as lytic enzymes and a group of antimicrobial peptides

known as defensins¹¹⁸. These peptides are thought to kill bacteria by forming pores in bacterial membranes¹¹⁹. The microtubule network is involved in directing azurophilic granules to the phagosome. Specific granules fuse with the plasma membrane at any location and hold NADPH oxidase, myeloperoxidase, lysozyme, alkaline phosphatase, and lactoferrin, which sequesters iron to inhibit the growth of bacteria¹²⁰. Gelatinase granules contain receptors involved in directed migration and enzymes that degrade ECM¹²¹.

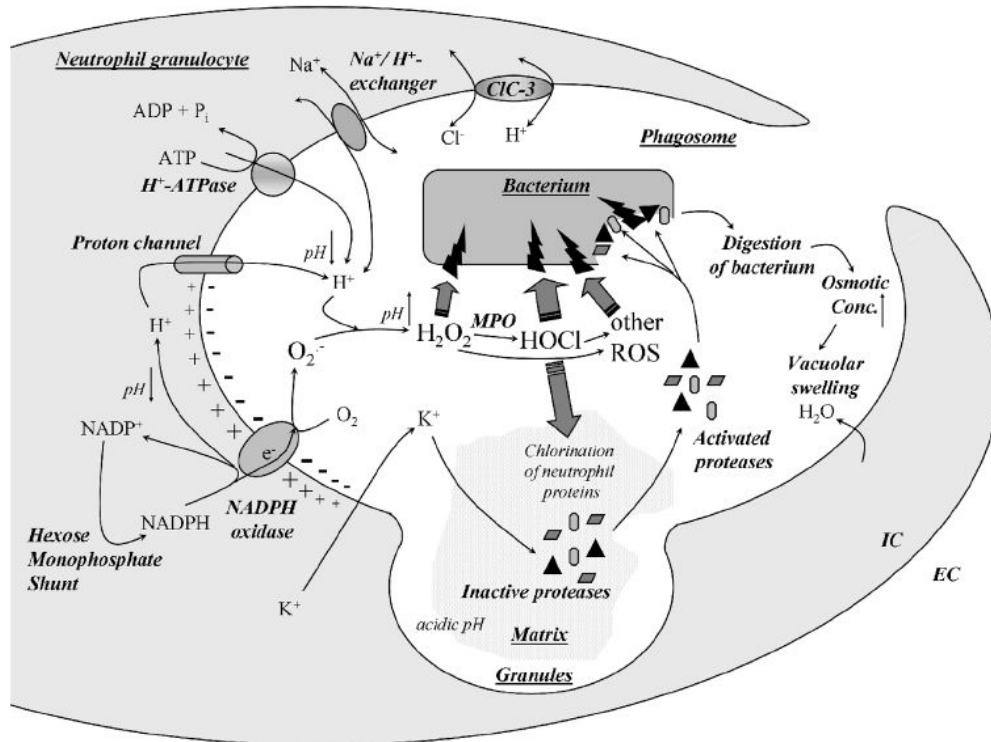


Figure 1.12 Schematic of the Neutrophil Phagosome

Once neutrophils engulf bacteria granules fuse with the phagosome and the enzyme NADPH oxidase is assembled and activated on the phagosomal membrane. The membrane of the phagosome is depolarized after electrons are transported from cytosolic NADPH during the superoxide production. The bacteria are then attacked by the ROS and latent proteases from the granule matrix that are liberated by potassium ions. Reprinted with permission from S. Karger AG Basel. Raba, B. et al: *Egesten A, Schmidt A, Herwald H (eds): Trends in Innate Immunity. Contrib Microbiol. Basel, Karger, 2008, vol 15, pp 164-187.*

1.1.3 Adenosine Receptor Signaling

Adenosine is a purine nucleoside synthesized through the catabolism of adenine nucleotides (ATP, adenosine diphosphate (ADP) and adenosine monophosphate (AMP)) via ectonucleotidases (CD39 or nucleoside triphosphate dephosphorylase and CD73 or 5'-ectonucleotidase)¹²². Endogenous adenosine extracellular concentrations are very low (less than 1 μ M), but increase under metabolically stressful conditions such as acute tissue injury, hypoxia or chronic inflammation¹²³.

Adenosine receptors (ARs) are GPCRs that are either inhibited or stimulated by cyclic AMP (cAMP) accumulation. Four subtypes of adenosine receptors have been identified based on their pharmacological profiles, genetic sequence, affinity for adenosine and G-protein coupling and signaling pathways¹²⁴. Among the 4 AR subgroups (A_1 , A_{2A} , A_{2B} , A_3), the A_1 and A_3 receptor subtypes couple to members of the inhibitory G-protein (G_i) family while the two A_2 receptors primarily couple to members of the stimulatory G protein (G_s) family¹²⁵. Adenosine receptors are widely expressed among different cell types of the immune system including platelets, neutrophils, macrophages, ECs, lymphocytes and NK cells¹²²⁻¹³⁵. Reverse transcriptase polymerase chain reaction (RT-PCR) analysis in human neutrophils has shown that of the four receptor subtypes, A_{2A} receptors have the highest messenger ribonucleic acid (mRNA) expression levels followed by A_3 receptors as shown in **Figure 1.13**¹³⁶¹³⁷.

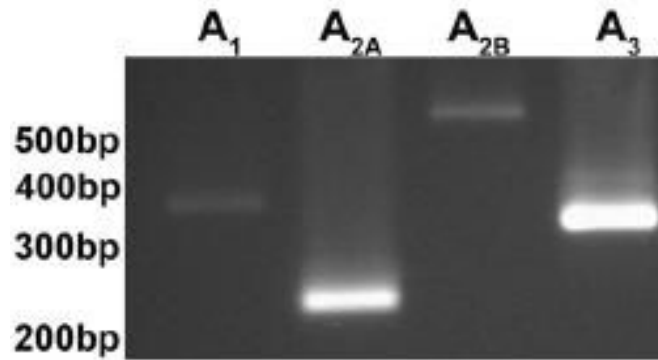


Figure 1.13 Adenosine subtype mRNA expression in LPS-stimulated human Neutrophils

Reprinted with permission from American Society for Microbiology, 2011, Vol. 79 no. 8, p. 3431-3437, Activation of Adenosine A_{2A} Receptors inhibits Neutrophil Transuroepithelial migration, Save S. et al., © 2011

Adenosine A_{2A} receptors are coupled to G_s proteins that activate the transmembrane protein Adenylyl cyclase (AC), which rapidly synthesizes cAMP from ATP. The second messenger cAMP signals to exchange Protein directly Activated by cAMP (EPAC) as shown in **Figure 1.14**. EPAC can then activate the STAT-induced STAT(Signal transducer and activator of transcription) inhibitor known as suppressor of cytokine signaling (SOCS) which negatively regulates cytokine signaling¹³⁸. An increase in cAMP also activates PKA allowing it to dissociate into its regulatory and catalytic subunits. Once PKA is activated by cAMP it phosphorylates other downstream targets such as Rap1 and RhoA.

Other important downstream targets of Adenosine A_{2A} Receptors include members of the Ras/Raf-1/MEK/ERK signaling cascade that are regulated through PKA-dependent and PKA independent pathways that are mediated by Src and Sos (Sons of Sevenless), respectively^{139,140}. Both Sos and Src signal to the GTPase Ras, causing it to exchange its GDP for GTP. Active GTP-bound Ras then proceeds to activate the serine/threonine MAP3K (MAPK kinase kinase) Raf. Raf phosphorylates the tyrosine/threonine MAP2K (MAPK kinase) MEK, which then phosphorylates the

serine/threonine MAPK extracellular signal regulated kinase (ERK1/2). ERK1/2 signaling leads to the activation of transcription factors including myc and the cAMP response element binding (CREB) protein. These transcription factors bind to a specific genetic sequence in the nucleus and result in the altered transcription of genes involved in cell proliferation, differentiation, survival and cytokine production. PKA is also able to phosphorylate CREB directly at Ser¹³³ and CREB has been shown to compete with the nuclear factor- κ B (NF κ B) p65 for the co-factor CREB-binding protein (CBP)¹⁴¹⁻¹⁴⁴.

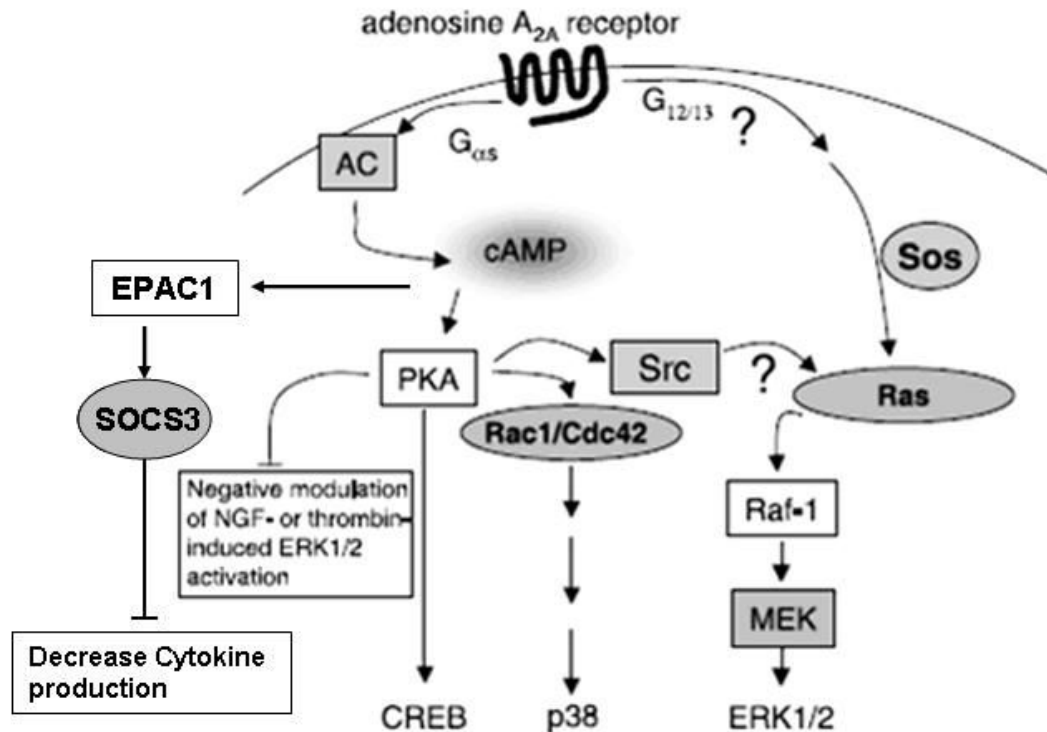


Figure 1.14 Adenosine A_{2A} Receptor Signaling Pathway

Ligation of the Adenosine A_{2A} receptor coupled to G_s proteins activate Adenyl Cyclase (AC) increasing the production of cyclic adenosine monophosphate (cAMP) from adenosine triphosphate (ATP). cAMP activates both EPAC1 and Protein Kinase A (PKA) which transducer signals to other downstream proteins that ultimately lead to the inhibition of inflammation. Reprinted from *Cell Signalling*, Vol 15, Schulte G. and Fredholm B.B., Signalling from adenosine receptors to mitogen-activated protein kinases, 813-827, Copyright (2003), with permission from Elsevier.

Elevated levels of adenosine have been shown to induce angiogenesis, matrix remodeling and vasodilation. Agonist-induced activation of adenosine A_{2A} receptors has been shown to have anti-inflammatory effects in animal models of inflammatory bowel disease¹⁴⁵⁻¹⁴⁸, rheumatoid arthritis¹⁴⁹⁻¹⁵², sepsis¹⁵³ and ischemia-reperfusion injury in the lungs^{154,155} and heart¹⁵⁶⁻¹⁵⁹. In a canine model of coronary ischemia and reperfusion injury the selective A_{2A} receptor agonist CGS21680 (3-[4-[2-[[6-amino-9-[(2R,3R,4S,5S)-5-(ethylcarbamoyl)-3,4-dihydroxy-oxolan-2-yl]purin-2-yl]amino]ethyl]phenyl]propanoic acid) significantly reduced neutrophil accumulation in the nonnecrotic area as well as infarction size and superoxide anion production by activated neutrophils¹⁵⁶. Another study using the same drug in guinea pigs showed that A_{2A} receptor activation during cardiac reperfusion after ischemia increased coronary flow and accelerated the recovery of aortic output¹⁵⁷. Even low, non-vasodilating doses of CGS-21680 were found to reduce infarct size in porcine ischemia-reperfusion models of reversibly and irreversibly injured myocardium¹⁵⁸. Low doses of A_{2A} receptor agonists were also shown to abolish or significantly attenuate post-ischemic impairment in left ventricular function independent of coronary blood flow or other hemodynamic effects in canine models of myocardial ischemia-reperfusion injury¹⁵⁹. In human neutrophils A_{2A} receptor occupancy was found to reduce transuroepithelial migration to uropathogenic *Escherichia coli*¹³⁷ and inhibit respiratory burst activity¹⁶⁰⁻¹⁶³.

One important highly selective Adenosine A_{2A} receptor agonist is (4-{3-(6-amino-9-(5-cyclopropylcarbamoyl-3,4-dihydroxytetrahydrofuran-2-yl)-9H-purin-2-yl)prop-2-ynyl}piperidine-1-carboxylic acid methyl ester), hereafter referred to as ATL313, whose binding affinity for each of the four adenosine receptor subtypes is shown in **Table 1.3**.

Mice pretreated with ATL313, prior to lung ischemia reperfusion injury had decreased vascular permeability, edema, airway resistance and pulmonary artery pressure compared to untreated mice, thereby preventing lung injury and dysfunction¹⁵⁴. ATL313 also attenuated the production of the cytokines IFN- γ and TNF- α and the chemokines CXCL1, CXCL2 and RANTES (Regulated upon activation, normal T-cell expressed, and secreted, CCL5), and reduced the pulmonary infiltration of neutrophils and T cells in mice^{155,164-167}. Santen Pharmaceuticals recently filed an investigational new drug application with the U.S. Food and Drug Administration for the use of ATL313 in primary open angle glaucoma and ocular hypertension¹⁶⁸.

Adenosine Receptor	A ₁	A _{2A}	A _{2B}	A ₃
Adenosine binding Affinity (nM) ¹⁶⁹	54	960	11,500	56
ATL313 binding Affinity (nM) ¹⁶⁴	57 \pm 3	0.7 \pm 0.3	>1000	250 \pm 70

Table 1.3 Binding Affinities of Adenosine and ATL313 for each of the Human Adenosine Receptor Subtypes

Binding data for Adenosine binding to each receptor subtype was determined using Chinese Hamster Ovary cells transfected with human adenosine receptors¹⁶⁹. Binding data are mean \pm SEM for binding of ATL313 to the high affinity conformational state of recombinant human adenosine receptors expressed in HEK239 cells as determined by competition for radioligand binding¹⁶⁴.

1.2 Specific Aims

Although necessary to fight infection, undampened neutrophil activation is also responsible for many inflammatory pathologies and damage to host tissues. An excessive release of pro-inflammatory mediators from neutrophils can contribute to the harmful inflammatory processes and organ dysfunction observed in acute lung injury, sepsis and autoimmune disease such as rheumatoid arthritis and Lupus erythematosus¹⁷⁰⁻¹⁷³.

Adenosine A_{2A} receptor agonist stimulation has been shown to decrease inflammation in animal models of rheumatoid arthritis, sepsis and ischemia-reperfusion injury in the lungs and heart. While the systemic effects of adenosine receptor stimulation *in vivo* are well-established, little is known about the mechanism for

adenosine's effects on the subcellular level. The goal of the present research was to determine the effect of ATL313-stimulation on the expression of neutrophil activation markers and β_2 integrin-mediated adhesion to ICAM-1. The activation markers examined in this study were L-selectin, CD11b, and F-actin each of which represents a different step in the leukocyte adhesion cascade—capture, arrest, and migration respectively.

In the present study the diacylglycerol analogue PMA was chosen to activate the neutrophils because it activates the signal transduction enzyme Protein Kinase C independently of the GPCR signaling cascade. Studies have also shown that PMA-stimulation modulates the expression of Mac-1 and L-selectin in neutrophils¹¹⁰¹⁰⁸¹⁰³¹⁰⁹¹⁰⁴¹¹¹. In order to examine the effect of A_{2A} receptor agonist stimulation on activated neutrophils cells were treated with PMA before being treated with ATL313. Thus, our results indicated whether ATL313 stimulation was able to overcome the pro-inflammatory signaling cascades induced by PMA treatment.

1.2.1 Specific Aim 1 (Chapter 2) To examine the effects of adenosine A_{2A} receptor agonist stimulation on PKC-activated human neutrophils.

Hypothesis: Adenosine A_{2A} receptor agonist stimulation of activated neutrophils will have an anti-inflammatory impact on activation markers. Specifically, CD11b (Mac-1) expression will be reduced and L-selectin expression will be higher than levels seen in activated neutrophils without agonist treatment. In addition, neutrophils treated with an A_{2A} receptor agonist will have reduced levels of actin polymerization.

Overview of Methods: The expression of neutrophil activation markers was assessed using flow cytometry. Isolated neutrophils were left on ice for 1 hour to achieve a basal deactivation level. Cell concentration was determined and neutrophils were diluted to a concentration of $1-2 \times 10^6$ cells/mL. Cells were then stimulated with 50 ng/mL PMA for

10 minutes either with or without sequential treatment of 1 μ M of the adenosine A_{2a} receptor agonist ATL313. Cells that were stimulated with both PMA and ATL313 were washed in between stimulations. Untreated cells and cells treated with 1 μ M ATL313 alone were used as a control. Cells were stained on ice for 30 minutes in the dark with antibodies directed against the neutrophil activation marker Mac-1 at a concentration of 0.2 μ g/100 μ L. Unstained cells were treated with staining buffer alone while cells stained with isotype control antibodies (also at 0.2 μ g/100 μ L) were used as staining controls. Cells were washed and subsequently fixed overnight at 4°C. Neutrophil populations were selected using a gate based upon size and granularity as determined by forward and sidescatter measurements. Gating also resulted in the exclusion of dead cells and non-neutrophil cell types from analysis. At least 10,000 gated events were collected per stimulation. Data was then expressed as a histogram of fluorescence intensity for the fluorochrome used in staining. L-selectin staining was done in a similar manner.

Staining with F-actin required a slightly different procedure. Neutrophils were fixed after stimulation with either Hank's Balanced Saline Solution (HBSS), ATL313, PMA or both ATL313 and PMA. After being washed cells were permeabilized and stained using 0.5 μ M fluorochrome-labeled phalloidin. Phalloidin is not an antibody, and therefore has no isotype control, but it is able to bind preferentially to F-actin and prevent filament depolymerization inside the cell.

The median fluorescence intensity value was determined using Flowjo software and then averaged across neutrophils isolated from different donors on different days. Fold-changes in median fluorescence intensity were calculated relative to unstimulated cells.

1.2.2 Specific Aim 2 (Chapter 3) To describe the effects of adenosine A_{2A} receptor agonist stimulation on the firm adhesion and spreading of neutrophils to ICAM-1

Hypothesis: Adenosine A_{2A} receptor agonist stimulation of activated neutrophils will reduce firm adhesion and spreading on surfaces coated with immobilized ICAM-1.

Overview of Methods: ICAM-1 isolated from human tonsils using R6.5 monoclonal antibody (mAb) bound to sepharose in an immunoaffinity column was immobilized onto a plastic surface at a concentration of 5 µg/mL and nonspecific binding was blocked with 1% Tween 20. Plates coated with ICAM-1 were incorporated as the lower wall in a parallel plate flow chamber and rinsed for 5 minutes before and after each experiment. A new plate was used for each experiment and stimulations were performed in duplicate. The concentration of isolated neutrophils was determined and then diluted to be between $1-2 \times 10^6$ cells/mL. Neutrophils were aliquoted into tubes containing 4×10^6 cells and left on ice for 1 hour prior to stimulation to decrease activation associated with our isolation methods. Neutrophils were kept on ice when not in use and pelleted before each stimulation. Cells were stimulated for 10 minutes with 50 ng/mL PMA with and without cotreatment of 1 µM of ATL313. Unstimulated neutrophils and neutrophils treated with ATL313 alone were also examined.

Cells were introduced to the flow chamber using a syringe pump set to a wall shear stress of 1 dyne/cm². The pump was stopped after an even distribution of cells was observed in the chamber, usually after about 2 minutes of flow. Neutrophils were then allowed to settle for 5 minutes before the shear stress of 1 dyne/cm² was resumed.

The ability of neutrophils to firmly adhere to ICAM-1 was assessed in order to examine the effect of ATL313-stimulation on the second step of the leukocyte adhesion

cascade—integrin-mediated arrest and firm adhesion. This experiment would describe whether treatment with ATL313 would influence integrin activation since only activated integrins promote cell adhesion. The number of neutrophils that firmly adhered to ICAM-1 and resisted detachment during the application of 30 seconds of shear stress at 1 dyne/cm² was quantified by hand from images taken using a handheld camera mounted on a microscope under 10× magnification. The percent of neutrophils that firmly adhered was expressed as the number of cells that remained firmly adhered divided by the number of cells present in the camera's field of view(FOV) before the shear stress began. The average and standard deviation of the percent of neutrophils that firmly adhered was taken across neutrophils isolated on different days from different donors. Fold changes in the percent of cells that firmly adhered were calculated relative to unstimulated cells.

The ability of neutrophils to spread on plates coated with immobilized ICAM-1 was also assessed in order to examine the effect of ATL313 stimulation on actin polymerization. Cells were pelleted and underwent the same stimulations as described above, but were added to plates using a pipette instead of a flow chamber and were aliquoted to contain 1-2x10⁶ cells. Cells were allowed to settle onto the plates for 10 minutes before images were collected. The number of cells that spread on ICAM-1 and became 'phase dark' was quantified by hand for each image. A new plate was used for each stimulation and each treatment was done in duplicate.

The percent of cells that spread on ICAM-1 was determined by dividing the number of cells that spread by the total number of cells present in the image. The percentage of cells that spread was then averaged across neutrophils isolated from

different donors on different days. The fold-change in cell spreading was calculated relative to unstimulated neutrophils.

Chapter 2: The Effect of ATL313 Stimulation on Neutrophil Activation Markers

2.1 Introduction

Neutrophil activation is influenced by exposure to cytokines and chemoattractants and results in the upregulation of integrin expression (such as Mac-1), L-selectin shedding, generation of ROS and phagocytosis. Studies have shown that stimulation with the PKC activator PMA also activates neutrophils^{103,104,108-111}. The simultaneous loss of L-selectin and upregulation of integrin expression aids in the transition between the rolling and firm adhesion steps of the leukocyte adhesion cascade.

The firm adhesion of the cells also requires polymerization of actin monomers at the leading edge in order to become polarized. The formation of F-actin is regulated by signaling through both chemokine receptors via Rho GTPases and integrins via adapter proteins at focal adhesions.

Meanwhile, activation of adenosine A_{2A} receptors has been linked to a reduction in inflammation in animal models of several diseases and conditions including sepsis, inflammatory bowel disease and ischemia-reperfusion injury^{145-148,153-159}. In neutrophils A_{2A} receptor occupancy has been found to decrease cytokine production, inhibit respiratory burst activity¹⁶⁰⁻¹⁶³ and reduce transuroepithelial migration to uropathogenic *Escherichia coli*¹³⁷. The effect of A_{2A} receptor stimulation on other measures of neutrophil activation, including the expression of activation markers involved in adhesion such as CD11b, L-selectin and actin filaments, is currently unknown. The A_{2A} receptor agonist ATL313 is hypothesized to inhibit the loss of L-selectin and upregulation of CD11b and F-actin in human neutrophils. Flow cytometry was used to test this hypothesis on human neutrophils.

2.2 Materials and Methods

2.2.1 Antibodies

Fluorescein Isothiocyanated (FITC)-labeled phalloidin used for detecting F-actin and FITC-labeled anti-mouse IgG were purchased from Sigma-Aldrich (St. Louis MO). Allophycocyanin-cyanine7 (APC-Cy7) labeled anti-human CD11b (Integrin α M), APC-Cy7 labeled anti-rat IgG2b isotype control, and FITC-labeled anti-mouse IgG1 κ isotype control were obtained from Becton Dickenson (BD, Franklin Lakes, NJ). FITC-labeled anti-human CD62L (L-selectin) was purchased from ebiosciences (San Diego, CA).

2.2.2 Small Molecules

The adenosine A_{2A} selective agonist ATL313 (4-{3-(6-amino-9-(5-cyclopropylcarbamoyl-3,4-dihydroxytetrahydrofuran-2-yl)-9H-purin-2-yl)prop-2-ynyl} piperidine-1-carboxylic acid methyl ester) was a gift from the Linden lab. Phorbol 12-Myristate 13-Acetate (PMA) was purchased from Fisher Scientific (Waltham, MA).

2.2.3 Neutrophil Isolation

Peripheral whole blood was isolated from normal healthy consenting adults via ventipuncture using 21G $\frac{3}{4}$ butterfly needles (BD) in conjunction with either 10 ml heparin sodium-coated vacutainers (BD) or a 50 mL syringe (BD) with added Heparin Sodium (10U/mL) (Sagent Pharmaceuticals, Schaumburg, IL). The procedure was performed in accordance with Human Investigation Committee protocol 14591 with approval from the Investigational Review Board at the University of Virginia. Neutrophils were isolated by centrifugation in a differential gradient 1-Step Polymorphs solution (Axis Shield PoC AS, Oslo, Norway) similar to previous methods¹⁷⁴. Briefly, 5 mL of whole blood was layered over 3.5 mL of Polymorphs in a 15 ml conical bottom

tube (Genesee, San Diego, CA) and centrifuged for 50 minutes at 500×g 20°C in a swinging bucket rotor in a table top centrifuge (Sorvall Legend RT, Thermo Scientific, Asheville, NC). After centrifugation the lower band of polymorphonuclear cells were collected into a separate 50 ml tube and washed twice using HBSS (Gibco, Grand Island, NY) with 1% Human serum albumin (HSA) (Gemini Bioproducts, Sacramento, CA).

Alternatively, Neutrophils were also isolated using both centrifugation and sedimentation similar to previous methods¹⁷⁵¹⁷⁶. Whole blood was deposited into 50 ml centrifuge tubes with equal volumes of a sterile-filtered solution of 3% Dextran 500 (Sigma) /0.9% NaCl(Baxter, Deerfield, IL), and inverted gently before being allowed to settle for 20 minutes at room temperature (RT). The top layer of blood was then removed and centrifuged at 200×g for 10 minutes at 20°C. The pellet was subsequently resuspended in 35 ml of Dulbecco's phosphate buffered saline (DPBS) (Gibco) containing 0.1% D-glucose (J.T. Baker, Phillipsburg, NJ). A layer of 10 ml of Ficoll-paque Plus (GE Healthcare, Piscataway, NJ) was then carefully laid underneath the solution before being centrifuged for 30 minutes at 200×g at 20°C. During centrifugation the cells are separated based on their density, with granulocytes (neutrophils) and red blood cells sedimenting together into the pellet as shown in **Figure 2.1**. Afterwards, the supernatant was removed.

For both procedures red blood cells were lysed by resuspending the pellet in 20 ml of sterile de-ionized water for 30 seconds. Cells were then mixed gently with 20 ml of 1.7% NaCl before being centrifuged at 200×g for 10 minutes at 20°C. The pellet was then resuspended in 10 ml DPBS and the cell concentration was quantified using a hemacytometer (Reichert, Buffalo, NY). DPBS was added to the cells until a cell

concentration of $1-2 \times 10^6$ cells/mL was achieved. Neutrophils were left on ice for 1 hour to reduce basal activation. All unfixed neutrophils were used the same day they were isolated.

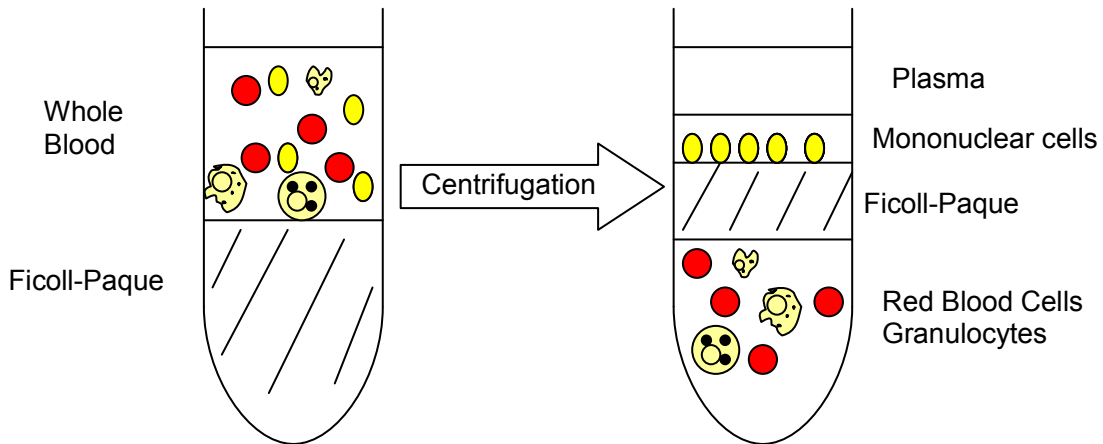


Figure 2.1 Ficoll-Paque Gradient Separation of Whole Blood

Whole blood layered on top of Ficoll-paque separates into different fractions (plasma, mononuclear cells, and red blood cells and granulocytes) based on cellular density after centrifugation.

2.2.4 Flow Cytometry

Isolated neutrophils were treated for 10 minutes at RT with either 50 ng/ml PMA or 100 nM ATL313. Some cells were treated with 50 ng/mL PMA for 10 minutes, washed and then incubated with 100 nM ATL313 for an additional 10 minutes. Untreated cells were stimulated with HBSS with 1% HSA, which was the carrier solution for each of the stimulants. Cell solutions at concentrations of $1-2 \times 10^6$ cells/mL were incubated with antibodies or isotype controls in the dark on ice for 30 minutes at concentrations of 0.2 $\mu\text{g}/100 \text{ uL}$ in HBSS with 1% HSA. Staining for F-actin was done using 0.5 μM FITC-labeled phalloidin according to methods described previously¹⁷⁷. Unstained cells were incubated with 100 μL of HBSS with 1% HSA in the dark on ice for 30 minutes. Cells were then washed once with HBSS and fixed on ice for 10 minutes using a fixation buffer (4% formaldehyde (Polysciences Inc, Warrington, PA), 1% HSA

and HBSS). Cells to be stained for F-actin were fixed for 10 minutes at RT and permeabilized with 5 g/L saponin (MP biomedical, Solon, OH) in HBSS at RT for 3 minutes before being stained¹⁷⁴. Cells were washed and resuspended in HBSS before being analyzed on a FACScan or Cyan Flow Cytometer (BD) using Cellquest Pro software (BD). Cells were gated based on their forward and side scatter measurements and 10,000 gated events per sample were collected to be analyzed. Data analysis was performed using Flowjo version 7.6.1 software (Tree Star Inc, Ashland, OR).

2.3 Results

2.3.1 ATL313 Stimulation Does Not Alter the Surface Expression of Mac-1 (CD11b) on Neutrophils

To determine the appropriate PMA incubation time period the Mac-1 staining of unstimulated neutrophils was compared to neutrophils stimulated with PMA for 0, 5, 10, 15, 30 and 60 minutes. Surface expression of CD11b on PMA-stimulated neutrophils was found to be time-dependent, with the majority of the increased expression occurring within 10 minutes as shown in **Figure 2.2**.

Neutrophils were stimulated at RT for 10 minutes with HBSS, 50 ng/mL PMA, 1 μ M ATL313, or both 1 μ M ATL313 and 50 ng/ml PMA. After stimulation, cells were stained with either APC-Cy7-labeled anti-CD11b or APC-Cy7-labeled rat anti-IgG2b κ isotype control. HBSS was added to unstained cells during cell staining. Fixed cells were analyzed on a BD Cyan flow cytometer and gated based on their forward and side scatter measurements.

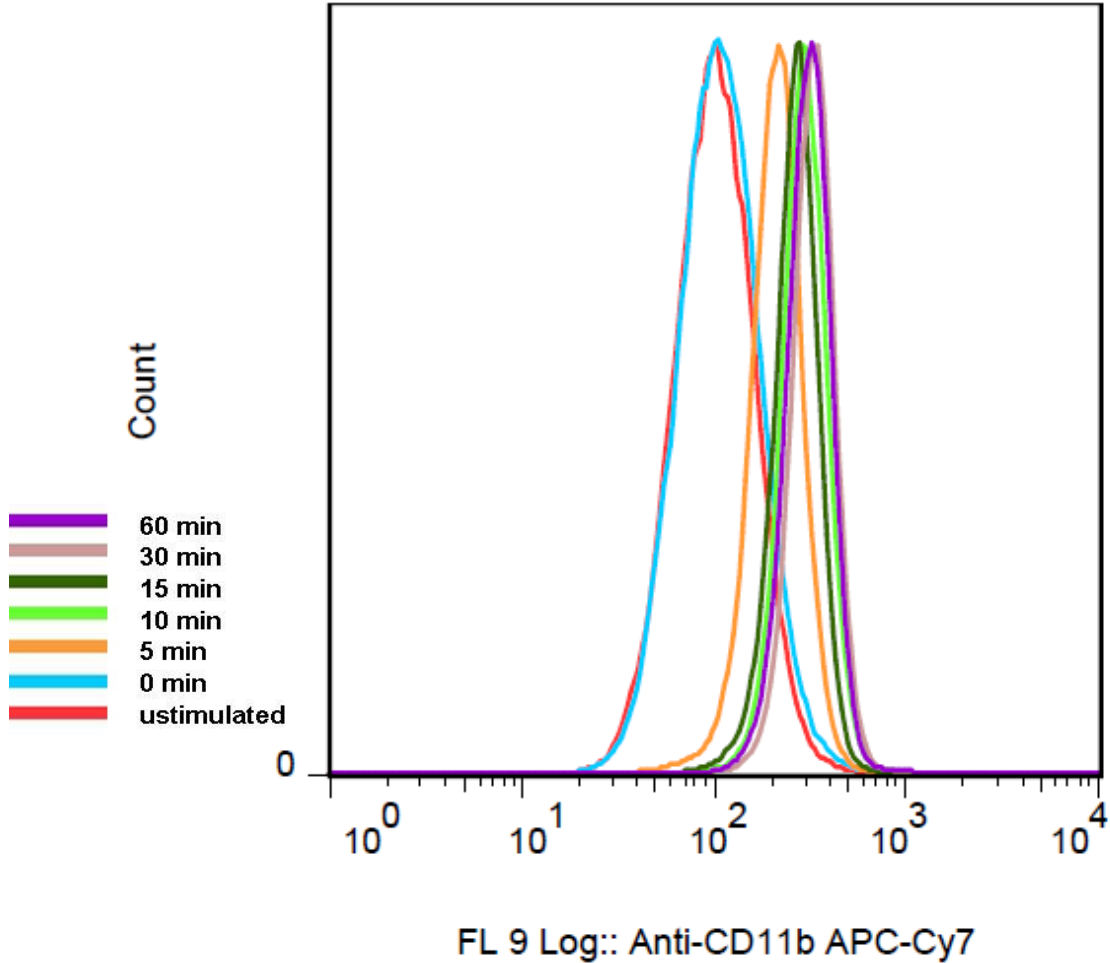


Figure 2.2 Histogram of APC-Cy7-labeled CD11b Fluorescent Intensity for Neutrophils stimulated with PMA for various time periods.

Gated neutrophils accounted for between 89 and 93% of cell data collected.

Figure 2.3 shows a representative histogram of the fluorescent intensity for APC-Cy7 anti-CD11b stained neutrophils for each of the four stimulations. Neutrophils incubated with 50 ng/mL PMA exhibited a 2.26 ± 0.53 fold average increase in CD11b median fluorescence intensity compared to unstimulated cells ($p=0.030$). Similarly, stimulation with 50 ng/mL PMA followed by 1 μ M ATL313 resulted in a 2.51 ± 0.63 fold average increase in CD11b median fluorescence intensity compared to unstimulated cells ($p=0.025$). Neutrophils treated with 1 μ M ATL313 were not statistically different from unstimulated cells as shown in **Figure 2.4**.

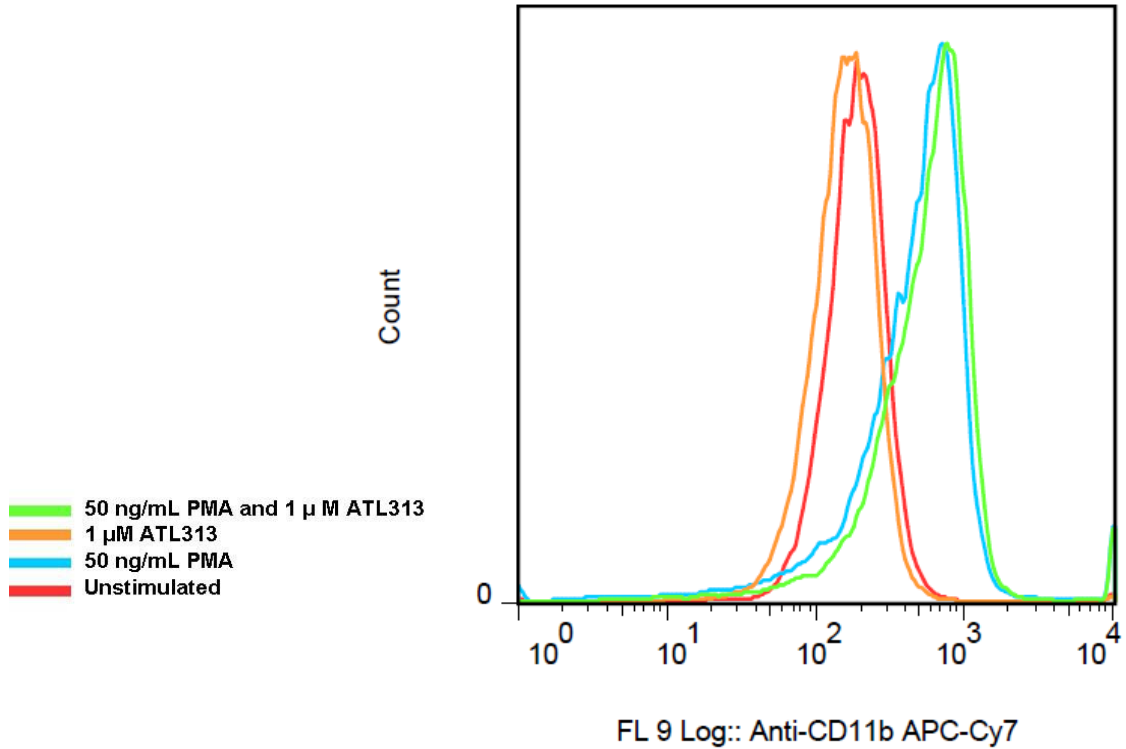


Figure 2.3 Histogram of APC-Cy7-labeled CD11b Fluorescent Intensity for Stimulated cells.
Representative of 4 experiments

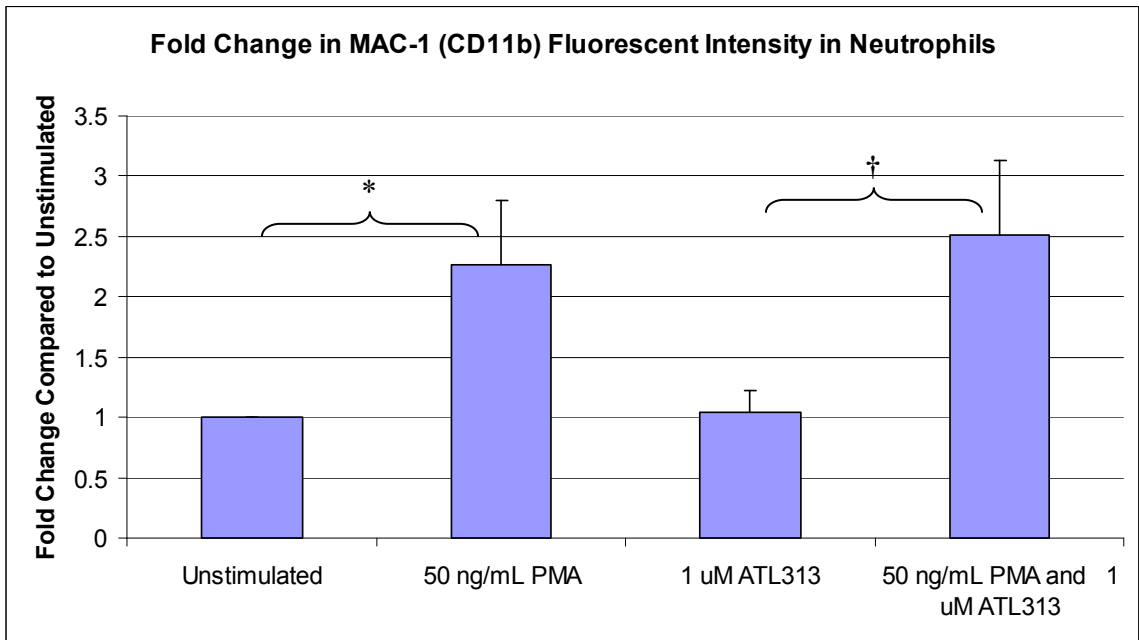


Figure 2.4 Fold Change in median Mac-1 Fluorescent Intensity in Neutrophils

PMA increased CD11b expression 2.26-fold compared to unstimulated cells (*, $p=0.030$). Cells treated with both ATL313 and PMA increased CD11b expression 2.51-fold compared cells treated with ATL313 alone (\dagger , $p=0.0417$). Fold changes were calculated relative to unstimulated neutrophils. Error bars are the standard deviation of the mean of 4 experiments.

2.3.2 ATL313 Stimulation Does Not Alter L-selectin Shedding in Neutrophils

Neutrophils were stimulated at RT for 10 minutes with HBSS, 50 ng/mL PMA, 1 μ M ATL313, or both 1 μ M ATL313 and 50 ng/ml PMA. After stimulation, cells were stained with either FITC-labeled anti-CD62L or FITC-labeled mouse anti-IgG1 κ isotype control. HBSS was added to unstained cells during cell staining. Fixed cells were analyzed on a BD FACsCalibur flow cytometer and gated based on their forward and side scatter measurements.

Gated neutrophils accounted for between 89 and 96% of cell data collected. **Figure 2.5** shows a representative histogram of the fluorescent intensity for FITC anti-CD62L stained neutrophils for each of the four stimulations. Neutrophils incubated with 50 ng/mL PMA exhibited a 5.25 ± 1.58 fold average decrease in FITC median fluorescence intensity compared to unstimulated cells ($p < 0.0005$). Similarly, stimulation with 50 ng/mL PMA followed by 1 μ M ATL313 resulted in a 5.29 ± 2.13 fold average decrease in CD11b median fluorescence intensity compared to unstimulated cells ($p = 0.0018$). Neutrophils treated with 1 μ M ATL313 were not statistically different from unstimulated cells as shown in **Figure 2.6**.

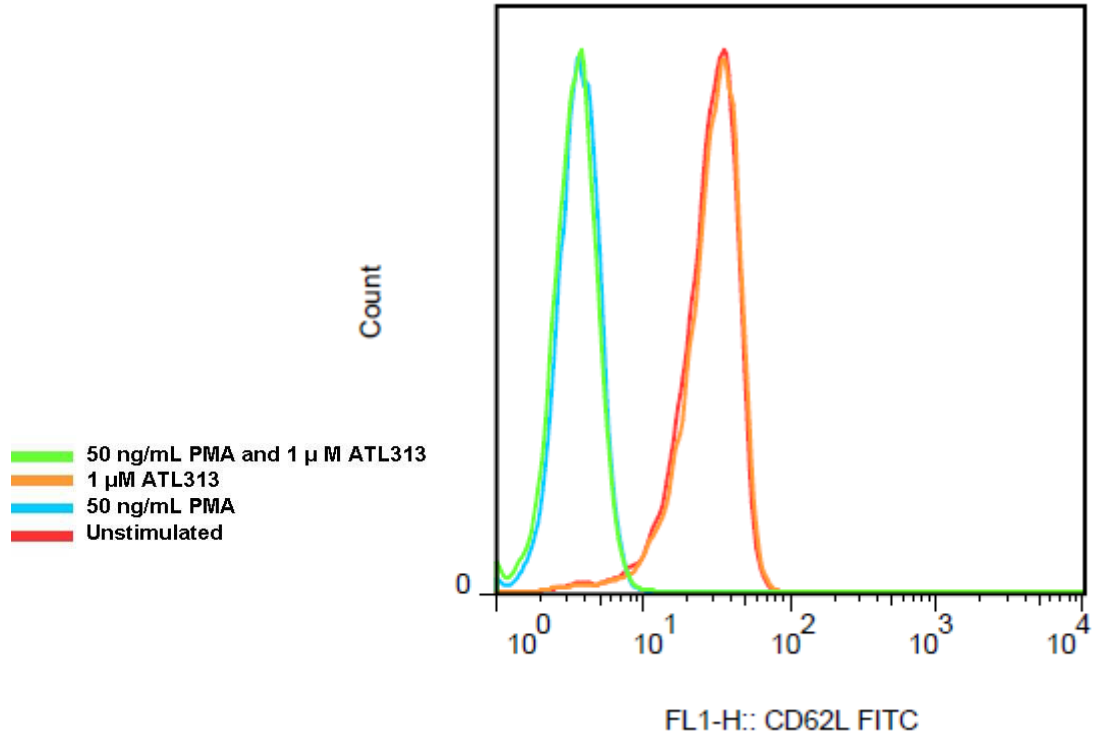


Figure 2.5 Histogram of FITC-labeled CD62L Fluorescent Intensity for Stimulated Cells Representative of 7 experiments.

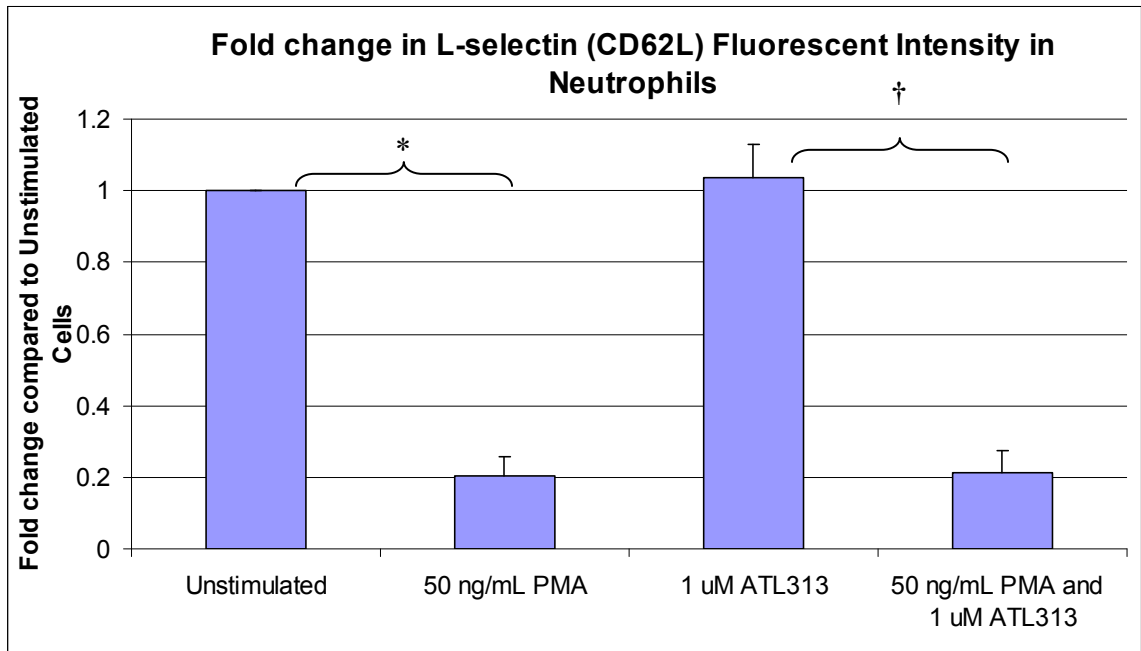


Figure 2.6 Fold Change in median L-selectin Fluorescent Intensity in Neutrophils Neutrophils stimulated with PMA had 5.25-fold lower expression levels of L-selectin compared to unstimulated cells (*, $p < 0.0001$). Cells stimulated with both PMA and ATL313 had 5.29-fold lower L-selectin expression levels compared to cells treated with ATL313 alone (†, $p < 0.0001$). Fold changes were calculated relative to unstimulated neutrophils. Error bars are the standard deviation of the mean of 7 experiments.

2.3.3 ATL313 Stimulation Does Not Alter the Concentration of Filamentous Actin in Neutrophils

Neutrophils were stimulated at RT for 10 minutes with HBSS, 50 ng/mL PMA, 1 μ M ATL313, or both 1 μ M ATL313 and 50 ng/ml PMA. After stimulation, cells were fixed for 10 minutes at RT and then permeabilized for 3 minutes at RT. Neutrophils were then stained with FITC-labeled phalloidin, which binds more tightly to actin filaments (F-actin) than actin monomers. HBSS was added to unstained cells during cell staining. Fixed cells were analyzed on a BD FACsCalibur flow cytometer and gated based on their forward and side scatter measurements.

Gated neutrophils accounted for between 91 and 96% of cell data collected. **Figure 2.7** shows a representative histogram of the fluorescent intensity for FITC-labeled F-actin in neutrophils for each of the four stimulations. Neutrophils incubated with 50 ng/mL PMA exhibited a 1.49 ± 0.24 fold average decrease in FITC median fluorescence intensity which was not statistically significant compared to unstimulated cells. Stimulation with 50 ng/mL PMA followed by 1 μ M ATL313 resulted in a 1.68 ± 0.12 fold average decrease in F-actin median fluorescence intensity compared to unstimulated cells ($p=0.010$). Neutrophils treated with 1 μ M ATL313 were not statistically different from unstimulated cells as shown in **Figure 2.8**.

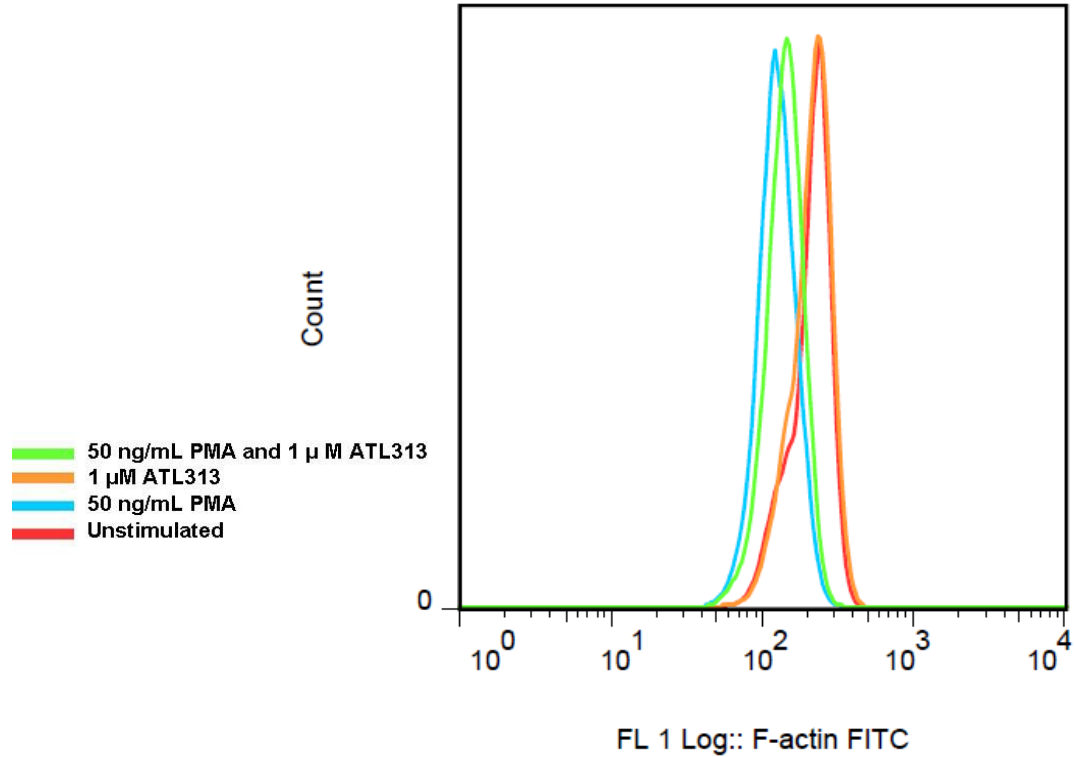


Figure 2.7 Histogram of FITC-labeled F-actin Fluorescent Intensity for Stimulated Cells.
Representative of 3 experiments.

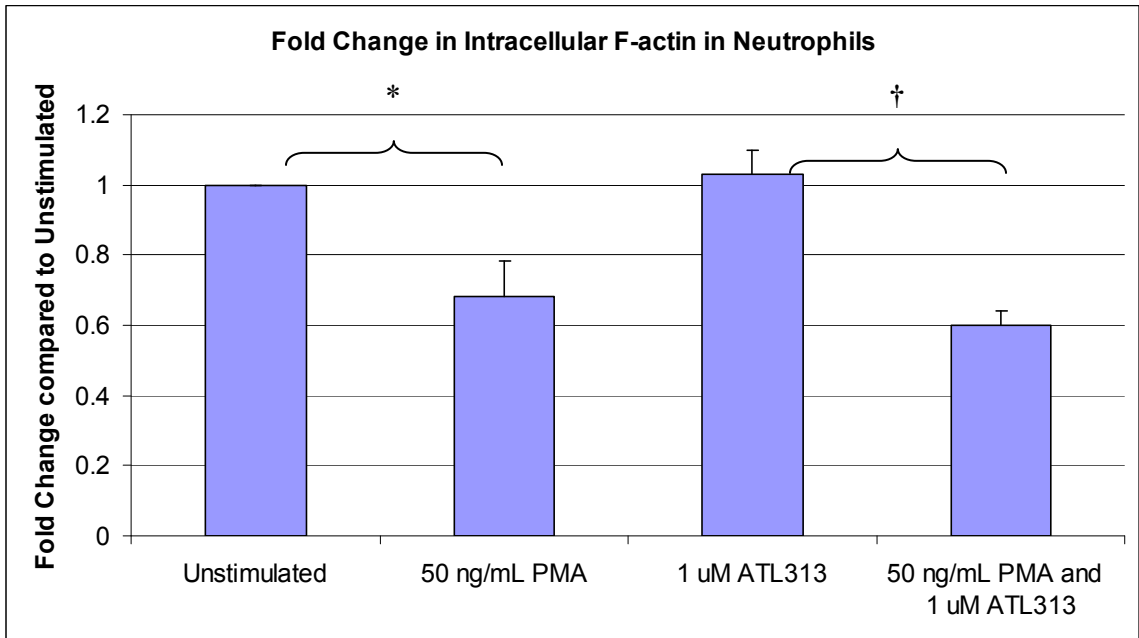


Figure 2.8 Fold Change in Median F-actin Fluorescent Intensity in Neutrophils.

PMA stimulation decreased F-actin expression 1.49-fold compared to unstimulated cells (*, $p=0.032$). Cells stimulated with both PMA and ATL313 had lower F-actin expression levels compared to cells treated with ATL313 alone (†, $p=0.0142$). Fold changes were calculated relative to unstimulated neutrophils. Error bars are the standard deviation of the mean of 3 experiments.

2.4 Discussion

Neutrophils become activated in response to a variety of inflammatory stimuli produced by damaged tissues, pathogens and other leukocytes including chemoattractant agents, cytokines, and chemokines. Neutrophils respond to these extracellular signals by releasing their own cytokines, migrating towards higher gradients of chemoattractants, increasing the surface expression of β -integrins (Mac-1), shedding L-selectin, and undergoing processes that aid in the destruction of foreign pathogens^{78,79,98,103,108-110,178,179}.

The diacylglycerol analogue PMA is capable of activating the signal transduction enzyme Protein Kinase C independently of the GPCR signaling cascade. PKC has many effectors including Rac and Cdc42, which upregulate F-actin assembly. Studies have also shown that PMA-stimulated neutrophils modulate the expression of Mac-1 and L-selectin^{103,104,108-111}.

Meanwhile, Adenosine A_{2A} receptor agonists, such as ATL313, have been shown to exert a systemic anti-inflammatory response in animal models. ATL313 stimulation has resulted in the attenuation of the production of cytokines and chemokines and the prevention of injury in mouse models of heart and lung ischemia reperfusion injury¹⁵⁴⁻¹⁵⁹. In neutrophils occupancy of Adenosine A_{2A} receptor has been shown to inhibit the secretion of granules and oxidative burst^{63,180-183}. Despite extensive use in *in vivo* models of inflammation and disease the effects of Adenosine A_{2A} receptor stimulation on neutrophil activation markers related to cell adhesion has not been well-characterized.

The purpose of the present study was to assess the effect of Adenosine A_{2A} receptor stimulation on the expression of neutrophil activation markers. We focused on

the activation markers L-selectin, CD11b and F-actin, representing the rolling, arrest and spreading steps of the leukocyte adhesion cascade, respectively. Flow cytometry was used to assess the expression of these markers on neutrophils stimulated with PMA with or without ATL313. It is important to note that the results obtained are specific to the A_{2A} receptor agonist ATL313. Other agonists will have different AR specificities and signaling kinetics.

Neutrophils stimulated with the A_{2A} Receptor agonist ATL313 did not alter the expression of neutrophil activation markers as hypothesized. Neutrophils incubated with 1 μ M ATL313 for 10 minutes exhibited expression levels of CD11b, L-selectin and F-actin that were not statistically different from unstimulated cells as determined using a student's paired T-test. Similarly, neutrophils treated with ATL313 in combination with 50 ng/mL PMA were not statistically different from cells stimulated with PMA alone.

One possible explanation for the lack of alteration in the expression of activation markers may be due to a time-dependent attenuation of the effects of ATL313. Adenosine A_{2A} receptor signaling may be rapidly downregulated within 10 minutes of ATL313 stimulation by endogenous adenosine deaminase, however this seems unlikely since other studies using Adenosine A_{2A} receptor agonists have utilized incubation periods ranging from 5 minutes to 3 hours and still observed an anti-inflammatory response.

The failure of ATL313 stimulation to alter neutrophilic L-selectin shedding mediated through PKC activation suggests that adenosine A_{2A} receptor mediated signaling does not impair TACE metalloprotease activity.

Furthermore, it should be noted that changes in the surface expression level of β integrins do not describe their affinity state or signaling capacity. Therefore, it is possible that despite the costimulation of ATL313 and PMA showing similar surface expression levels of CD11b in comparison to PMA-stimulated cells the actual adhesive capabilities of the integrin may be lower, depending on its conformational state (affinity) and level of integrin clustering on the cell membrane (avidity). One possible means of altering integrin affinity is through signaling via adaptor proteins such as talin and RAPL, which act to destabilize the association between the integrin's α and β subunits' cytoplasmic and transmembrane domains⁵⁰. It is also possible that A2a receptor occupancy disrupts the ligand-independent mobilization of β_2 integrins through changes in lipid rafts or their cytoskeletal attachment both of which are important for regulating integrin clustering^{53,63}. One likely mechanism for altered avidity is through PKA-mediated phosphorylation of the integrin's cytoplasmic tail, which has been shown to occur in α_4 integrins^{47,49,50,180-182}.

In addition measurements of F-actin polymerization assessed by flow cytometry are purely quantitative and do not describe the quality of the structural organization of the actin cytoskeleton or level of cell deformability both of which are essential for proper cell spreading and migration. Thus, the intracellular organization of actin filaments in ATL313-stimulated neutrophils may be altered in comparison to neutrophils with activated PKC. The actin filaments in ATL313-stimulated neutrophils may be distributed differently than in untreated cells, making it impossible for cells to efficiently polarize, adhere, and migrate. A_{2A} receptor occupancy could also disrupt the binding between adapter proteins, integrins and the actin cytoskeleton which is required for the formation of focal adhesions and eventual polarization and migration of the cell.

Chapter 3: ATL313 Stimulation Decreases β_2 -Dependent Adhesion of Neutrophils to ICAM-1

3.1 Introduction

Adhesion between cells and cells and the ECM is regulated by adhesion molecules called integrins, which contain an α and β subunit. Integrin-ligand binding depends on many factors including the affinity and avidity of the integrin. An individual integrin's affinity is determined by the conformational state of its α and β subunits. The protein is thought to exist in three potential states: bent/closed, extended/closed and extended/open which correspond to low, intermediate and high binding affinity states. In the bent state the ligand-binding headpiece that contains the α subunit β -propeller and β I domain is snuggled close to the lower legs of the integrin, thereby preventing effective ligand binding⁵⁰. Extension of the legs exposes this region slightly, while an opening of the cytoplasmic domains further exposes the MIDAS on the integrin.

The adhesiveness of integrins is also controlled by ability to redistribute on the cell membrane and form clusters at focal adhesions. The avidity of integrins is regulated by connections to the actin cytoskeleton through adaptor proteins and ligand-binding. PMA is known to upregulate LFA-1 avidity¹⁸³.

Integrins expressed on the surface of activated neutrophils mediate their adhesion to the endothelium. Neutrophils then use complexes of integrins and the actin cytoskeleton, known as focal adhesions, to gain traction during migration towards sites of inflammation. Once the neutrophils reach the damaged tissue they release pro-inflammatory mediators to destroy pathogens, which, if left unchecked, can damage host tissues and contribute to diseases such as sepsis and acute lung injury.

Despite many *in vivo* experiments showing that adenosine A_{2A} receptor activation decreases inflammation, the consequences of A_{2A} receptor signaling on cell adhesion are currently unknown. The aim of this study was to explore whether the A_{2A} receptor agonist ATL313 was capable of reducing the β_2 integrin-mediated adhesion and spreading of PMA-stimulated neutrophils on ICAM-1.

3.2 Materials and Methods

3.2.1 Cell Lines

The human Burkitt's Lymphoma Lymphoblast Raji cell line (ATCC, Manassas, VA) was grown using RPMI-1640 Medium (Gibco) supplemented with 10% fetal bovine serum (FBS) (Atlanta Biologicals, Lawrenceville, GA) and 1% Penicillin/Streptomycin (Gibco) in T-75 tissue culture-treated flasks (BD) with 5% CO_2 in an incubator (Queue Stabitherm, Thermo) at 37°C. The mouse B Lymphocyte hybridoma R6.D6.E9.B2 cell line (ATCC) was also grown in RPMI-1640 medium with 2mM L-glutamine, 10 mM 4-(2-hydroxyethyl)-1-piperazineethanesulfonic acid (HEPES), 1 mM Sodium Pyruvate, 4.5 g/L glucose, 1.5 g/L sodium bicarbonate and supplemented with 10% FBS and 1% Penicillin/Streptomycin. Cell Lines were split when they reached a concentration of $1-2 \times 10^6$ cells/mL.

3.2.2 Anti-human ICAM-1 mAb R6.5

The anti-ICAM-1 R6.5 mouse IgG2a κ mAb was isolated from the supernatant of the R6.D6.E9.B2 (HB9580) cell line according to previous methods^{184,185}. The cells were centrifuged for 10 minutes at 1500xg at RT and the pellet was discarded. Supernatant was stored under sterile conditions at 4°C until about 1 Liter was collected. The mAb supernatant was then centrifuged at 130,000 x g at 4°C for 1 hour in a Sorvall RC 5C

Plus centrifuge (Thermo). The mAb supernatant was adjusted to pH 7.4 by adding 1M NaOH(Sigma).

Protein-A Sepharose CL-4B (GE Healthcare) was allowed to swell in Distilled Water (DW) and then washed 3 times before being de-gassed. Protein-A Sepharose column was prepared by adding the slurry to a 1.0 x 20 cm glass chromatography column made by Biorad (Hercules, CA) and adding DPBS pH 8.0 to pack the column. The mAb supernatant was layered onto the resin bed and passed through the column at a flow rate of 1 mL/minute using a syringe pump (Harvard Apparatus PHD 2000, Holliston, MA). The column was then washed with 5 column volumes of phosphate buffered saline (PBS) (137 mM Sodium Chloride (EMD Serono, Rockland, MA), 2.68 mM Potassium Chloride (Sigma), 1.76 mM Monopotassium phosphate (Mallinckrodt, St. Louis, MO) and 10.14 mM Sodium Phosphate dibasic(Fisher) in DW) pH 8.0.

Antibody fractions were eluted with 0.1 M citric acid (Sigma) at pH 4.0 and aliquoted into tubes containing 50 μ L of 2M Tris(hydroxymethyl)aminomethane (Tris) Base Buffer (Sigma). Silver staining data of the collected elution fractions is shown in Appendix A. The column was cleaned with 1 column volume of 3 M potassium thiocyanate (Sigma) before reequilibrating in 3 column volumes of PBS pH 7.3. The clean column was stored at 4°C for re-use.

3.2.3 ICAM-1

ICAM-1 was purified from human tonsils provided by the Biorepository and Tissue Research Facility at the University of Virginia according to previous methods¹⁸⁶¹⁸⁷. Tonsil samples were stored at -80°C prior to coarse slicing with a sterile surgical carbon steel #10 blade (Premiere, Hatfield, PA). Sliced samples were

homogenized in a lysis buffer consisting of HBSS with 50nM Tris-HCL (Sigma), 2% Nonyl Phenoxyethoxyethanol (NP-40) (US Biologicals, Boston, MA), 150 nM NaCl, 1 mM MgCl₂(Sigma), 0.02% NaN₃, and a protease inhibitor cocktail containing 10 μ g/ml Aprotinin, 10 μ g/ml Pepstatin, 10 μ g/ml Leupeptin, 1 mM phenylmethylsulfonyl fluoride (PMSF), 1 mM Benzamidine, and 5 mM Iodoacetamide (Roche Diagnostics, Indianapolis, IN) using a T8.01 Netzgerat Homogenizer (IKA Labortechnik, Wilmington, NC). The samples were then allowed to incubate with lysis buffer on ice for 3 hours. After the incubation the samples were centrifuged for 1 hour at 8000 \times g at 4°C and the lysate was decanted into a beaker. The supernatant was then centrifuged at 14000 rpm for 1 hour at 4°C and then aliquoted before being stored at -80°C.

The anti-human ICAM-1 R6.5 antibody was covalently linked to sepharose for use in an immunoaffinity chromatography column according to previous methods¹⁸⁸. Briefly, the R6.5 antibody was dialyzed against 0.1 M NaHCO₃/0.5 M NaCl at 4°C with 3 buffer changes during 24 hours. Aggregates were removed by centrifugation at 100,000 \times g for 1 hour at 4°C. The supernatant was saved and the A280 was measured at 562 nM on a Genesys5 Spectrophotometer (Spectronic, Madison, WI) to determine the antibody concentration. The supernatant was diluted with 0.1 M NaHCO₃/0.5 M NaCl until a concentration of 5 mg/ml was achieved. Cyanogen Bromide (CNBr)-activated Sepharose-4B (Amersham Pharmacia Biotech, Uppsala, Sweden) was weighed and suspended in 1 mM HCl and allowed to settle for 15 minutes. The Solution was centrifuged for 5 minutes at 1200 rpm, washed with 1 mM HCl and then washed once more with ice-cold 0.1 mM HCl. The sepharose was then resuspended in 0.1 M

NaHCO₃/0.5 M NaCl buffer and stored at 4°C until needed. The antibody solution was mixed for 2 hours with sepharose before adding 0.05 M glycine (pH 8.0) (Sigma). The solution was then centrifuged at 1300 rpm for 5 minutes and stored in TSA solution (0.01 M Tris-Cl (pH 8.0), 0.14 M NaCl, 0.025% sodium azide).

The precolumn and antibody-sepharose columns were set up in series according to previous methods¹⁸⁹. Both columns were washed in the following order:

*10 column volumes of wash buffer (TSA solution with 0.5% Triton-X-100, 0.5% sodium deoxycholate)

*5 column volumes of TTS buffer (pH 8.0) (50 mM Tris-Cl, 0.1% Triton-X-100, 0.5 M NaCl)

*5 column volumes of TTS buffer (pH 9.0)

*5 column volumes of triethanolamine solution (50 mM Triethanolamine (pH 11.5) (Fisher), 0.1% Triton-X-100 (Biorad), 0.15 M NaCl)

*5 column volumes of wash buffer.

The tonsil lysate was applied to the pre-column and allowed to flow through the antibody-sepharose column at a flow rate of 5 column volumes/hr. The columns were then washed in the following order:

*5 column volumes of wash buffer

*5 column volumes of TTS buffer (pH 8.0)

*5 column volumes of TTS buffer (pH 9.0).

The antigen was then eluted with 5 column volumes of the triethanolamine solution and the fractions were neutralized by collecting them in tubes containing 0.2 vol of 1 M Tris-

Cl (pH 6.7). The column was then washed with 5 column volumes of TSA solution. Silver staining data of the collected elution fractions is shown in Appendix C.

3.2.4 Preparation of Adhesion Substrates

ICAM-1 isolated from tonsils was diluted in DPBS and adsorbed onto non-tissue culture treated 35 x 10 mm petri dishes (BD Falcon, Franklin Lakes, NJ) or to 100 x 15 mm petri dishes (Genesee, San Diego, CA) for 2 hours at RT under high humidity conditions. The dishes were washed three times with 1 ml of DPBS. Nonspecific adhesion was prevented by blocking the dishes overnight in a solution of 1% Tween 20 (Sigma) in DPBS at 4°C. The dishes were then incorporated as the lower wall of a parallel plate flow chamber and mounted over an inverted phase-contrast microscope (Diaphot-300, Nikon, Garden City, NJ) set to 10× magnification.

3.2.5 Flow Chamber Set-up

Experiments were done using a cast acrylic parallel plate flow chamber purchased from Glycotech (Rockville, MD) as shown in **Figure 3.1**. The chamber has a 35 mm diameter and a height of 9.0 mm. The chamber was attached to a polystyrene dish coated with an integrin ligand by using a vacuum to seal a gasket between the dish and chamber. The 0.01 inch thick silicon rubber gasket had a 5.0 mm x 19.0 mm window in the center where the cells would be allowed to interact with the surface of the plate. Cells entered the chamber through tubing connected to an inlet port on one side of the chamber and exited through an outlet port on the opposite side of the chamber. Silastic tubing (Glycotech) with an inner diameter of 1/16 in and an outer diameter of 1/8 in was connected to the inlet and outlet ports. The inlet port's tubing was placed in a tube containing the cell suspension or HBSS to be perfused into the chamber. The outlet port

tubing was connected to a 60 ml syringe (BD) attached to a syringe pump. The wall shear stress of the solution was controlled by adjusting the flow rate of the pump as calculated in Appendix C.

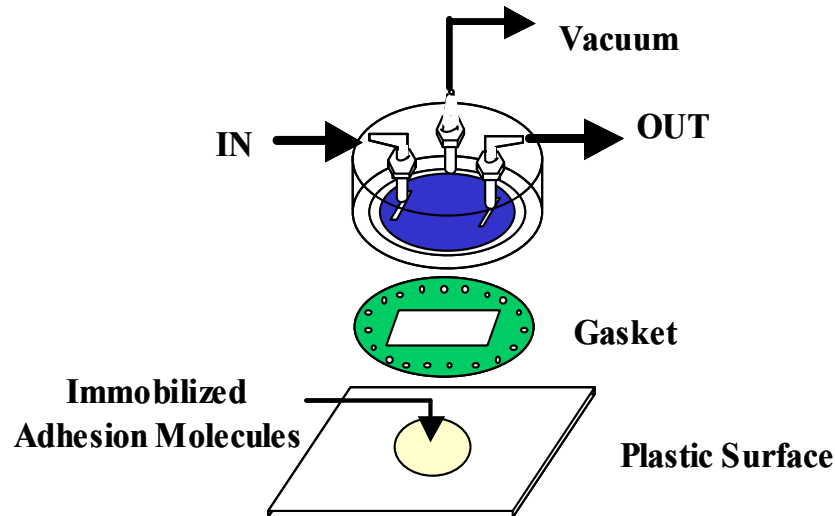


Figure 3.1 Flow chamber Set-up

3.2.6 Shear Stress Detachment after Static Adhesion Assay

Neutrophils were isolated as described in section 2.2.3. Cells were washed and incubated in 100 μL of either 50 ng/mL PMA in HBSS, 1 μM ATL313 in HBSS, or HBSS alone for 10 minutes. Some cells were treated with 50 ng/ml PMA in HBSS for 10 minutes, washed, and then treated with 1 μM ATL313 in HBSS for an additional 10 minutes. Cells were resuspended in HBSS with Ca^{2+} and Mg^{2+} at a concentration of $1\text{-}2 \times 10^6$ cells/ml prior to introduction into the parallel plate flow chamber. Flow was stopped and the neutrophils were allowed to settle for 5 minutes before being introduced to a shear stress of 1 dyne/cm². Pictures of the cells before the start of flow and after 30 seconds of shear stress were recorded using a high-definition camera (Canon Vixia HFS21, Lake Success, NY) mounted onto the microscope. The number of neutrophils

that remained bound was quantified and expressed as a percentage of the neutrophils originally in the field of view (1.012 mm \times 0.7675 mm) before the introduction of flow. A new dish was used for each condition and the chamber and tubing were rinsed for 5 minutes at 1 dyne/cm² before and after setting up each dish.

3.2.7 Static Adhesion Assay to Assess Cell Spreading

Isolated human neutrophils were treated as described in section 3.2.6. Cells were washed and resuspended in HBSS with Ca²⁺ and Mg²⁺ at a concentration of 1-2x 10⁶ cells/ml prior to being pipetted onto dishes coated with 5 μ g/mL ICAM-1. Pictures were taken after 10 minutes to assess the number of cells that spread.

3.3 Results

3.3.1 ATL313 Stimulation Decreases Neutrophil Firm Adhesion on ICAM-1 During a Shear Detachment Assay After Static Adhesion

Neutrophils were incubated at RT for 10 minutes with HBSS, 50 ng/mL PMA, 1 μ M ATL313 or both 50 ng/mL PMA and 1 μ M ATL313. After stimulation cells were introduced to a parallel plate flow chamber whose lower wall contained absorbed ICAM-1. A shear stress of 1 dyne/cm² was applied after cells had settled for 5 minutes to dislodge non-adherent cells. Pictures were taken before and after 30 seconds of shear stress to determine the percent of cells that remained in the field of view.

Incubation with 50 ng/mL PMA for 10 minutes increased the percentage of cells that adhered to ICAM-1 during static adhesion 1.44-fold compared to unstimulated cells, which was not found to be statistically significant. In contrast, ATL313 stimulation decreased the percent of neutrophils after 30 seconds of shear stress was applied 4.2-fold compared to untreated cells ($p=0.0032$) as shown in **Figure 3.2**. Furthermore, stimulation with PMA was not able to abolish the effects of treatment with ATL313 when

neutrophils were treated with both PMA and ATL313. Costimulation of PMA and ATL313 resulted in a 10.9-fold decrease in firm adhesion compared to cells treated with PMA alone ($p=0.001$).

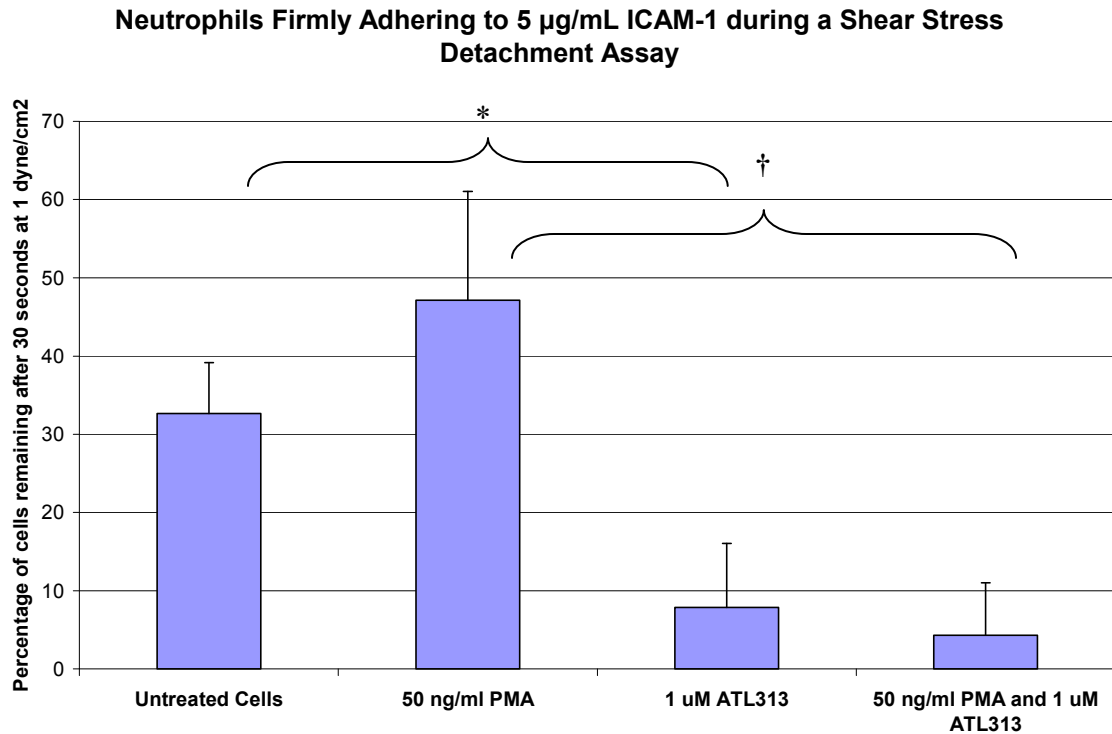


Figure 3.2 Effect of PMA and ATL313 Stimulation on the Static Adhesion of Neutrophils to ICAM-1 ATL313 stimulation lead to a 4.2fold decrease in firm adhesion compared to unstimulated cells(*, $p=0.0032$). Costimulation of PMA and ATL313 resulted in a 10.9fold decrease in firm adhesion compared to cells treated with PMA alone (\dagger , $p=0.001$). Error bars are the standard deviation of the mean of 6 experiments.

3.3.2 ATL313 Decreases Neutrophil Spreading on ICAM-1 during Static Adhesion Assays

Neutrophils were stimulated at RT for 10 minutes with HBSS, 50 ng/mL PMA, 1 μM ATL313 or both 50 ng/mL PMA and 1 μM ATL313. ICAM-1 was adsorbed onto plates and cells were allowed to settle on the surface for 10 minutes. Examples of spreading untreated neutrophils and neutrophils stimulated with 50 ng/mL are shown in **Figure 3.3**. The number of neutrophils that became phase dark after 10 minutes was quantified for multiple plates.

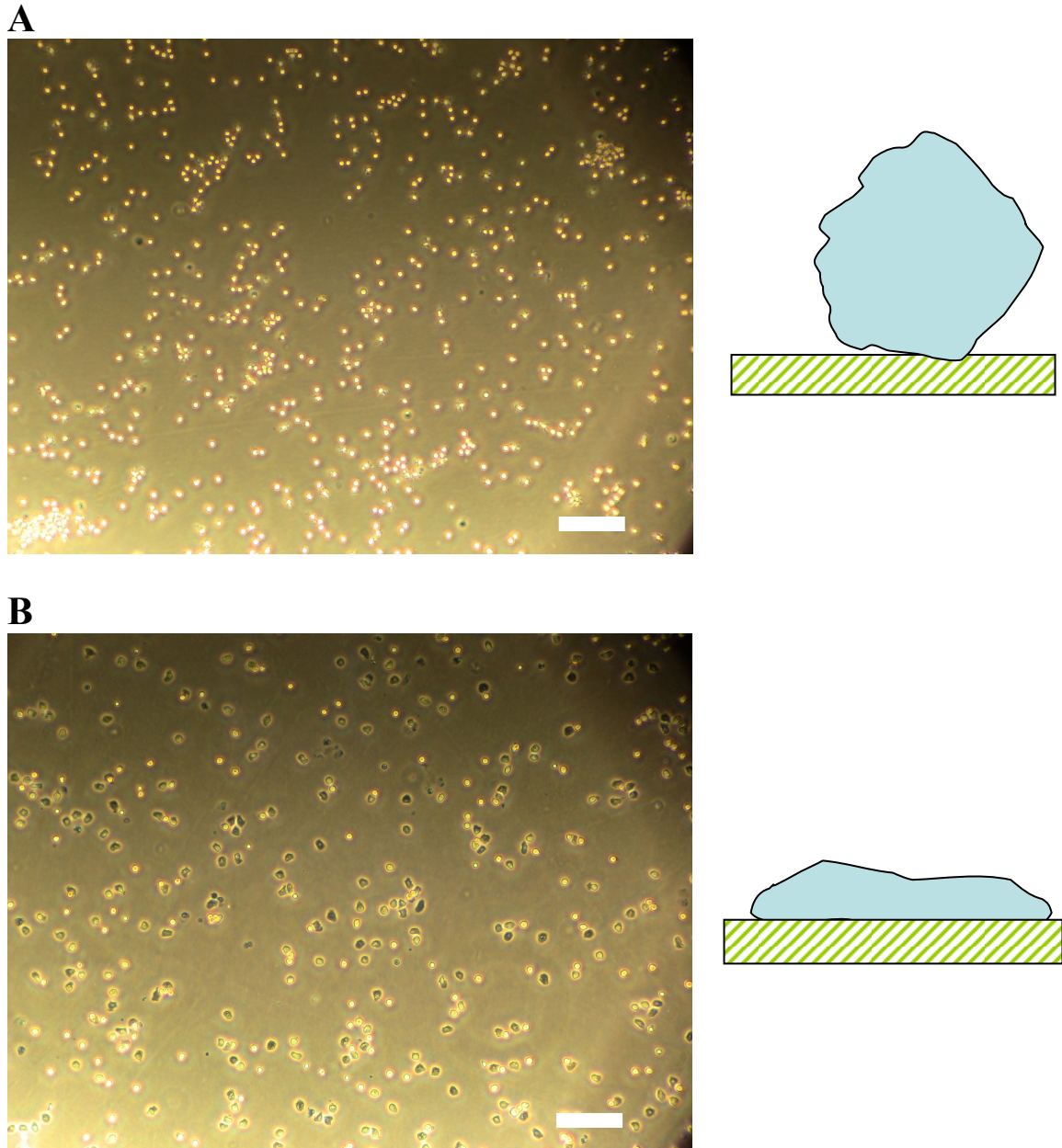


Figure 3.3 Neutrophils Spreading on Plates coated with ICAM-1

(A) Unstimulated Neutrophils do not spread appear on ICAM-1 after a 10 minute incubation and appear round, white and phase bright. (B) Neutrophils stimulated with 50 ng/mL PMA spread on ICAM-1 after 10 minutes. Schematics of a round, non-spreading neutrophil and a firmly adhering, spreading neutrophil are shown. Bar is 0.1 mm.

Neutrophil spreading on ICAM-1 increased 16.7fold when cells were stimulated with 50 ng/mL PMA compared to unstimulated cells ($p=0.0037$) as shown in **Figure 3.4**.

Treatment with ATL313 resulted in a 10.6-fold decrease in the ability of PMA-stimulated

neutrophils to spread on ICAM-1 ($p=0.0052$). No statistical differences were found between untreated neutrophils and cells treated with ATL313 with or without PMA.

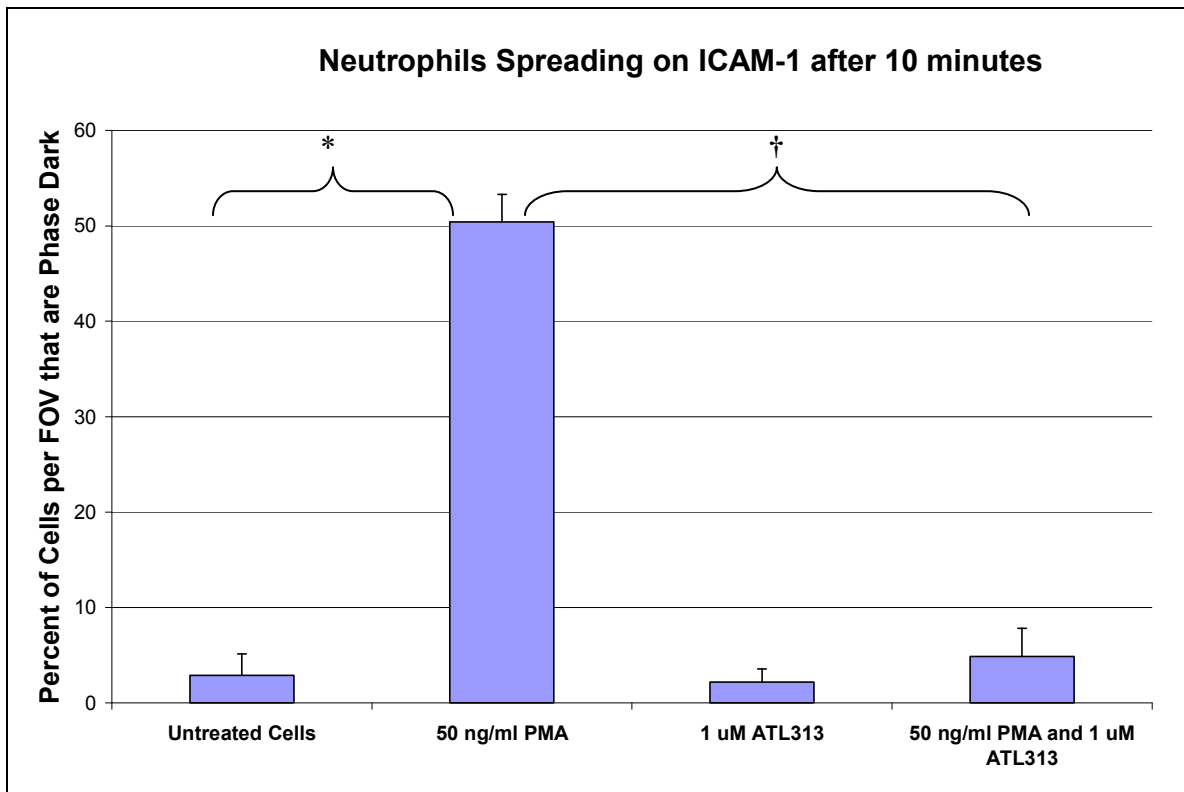


Figure 3.4 Stimulation with 1 μ M ATL313 (alone or with 50 ng/mL PMA) decreases the percent of neutrophils per field of view that spread on ICAM-1

Stimulation with PMA increased spreading on ICAM-1 16.7-fold compared to untreated cells (*, $p=0.0037$). Costimulation of PMA and ATL313 led to a 10.6-fold decrease in spreading compared to cells treated with PMA alone (\dagger , $p=0.0052$). Error bars are the standard deviation of the mean of 3 experiments.

3.4 Discussion

PMA-stimulation resulted in a 1.44-fold increase in the average number of firmly adhering cells after 30 seconds of shear stress and a 16.7-fold average increase in the average number of cells that spread on ICAM-1 after a 10 minute incubation compared to untreated cells. In comparison to neutrophils treated with PMA alone, cells treated with both ATL313 and PMA experienced a 10.6-fold average decrease in cell spreading on ICAM-1 and an average 10.9-fold decrease in the average percent of cells that firmly adhered after 30 seconds of shear stress.

Each of our adhesion experiments was capable of illustrating a different stage of the adhesion cascade. The shear detachment assay describes the integrin-mediated adhesion step of the cascade. Meanwhile, the static adhesion assay depicts the early stages of cell migration in which the actin-cytoskeleton pushes the lamellipodia forward through focal adhesion interactions between integrins, F-actin and adaptor proteins. It is important to note that while all spreading cells were adherent, not all adherent cells were spreading.

Our data indicates that ATL313-stimulation inhibits PKC-activation-mediated adhesion of human neutrophils to the β_2 integrin ligand ICAM-1 through an unknown mechanism. In the shear stress detachment assay stimulation with ATL313 was able to decrease firm adhesion compared to unstimulated cells. This suggests that A_{2A} receptor stimulation disrupts integrin-mediated firm adhesion under physiological shear stress. It is possible that the sudden introduction of flow induced integrin activation in untreated cells through mechanical stimulation of the receptors. ATL313-treated cells may have been able to resist integrin receptor mechanical stimulation because of the inhibition of adaptor proteins or reduced integrin avidity and/or affinity.

These results are specific to ATL313 and may be different for other A_{2A} receptor agonists that have unique kinetics and specificities for each of the AR subtypes. We hypothesize that Adenosine A_{2A} receptor signaling alters either the organization of the actin cytoskeleton or the affinity, conformation and/or avidity of β_2 integrin.

A_{2A} receptor occupancy may interfere with the organization of the actin cytoskeleton by inhibiting cytoskeleton adaptor proteins found at focal adhesions, interfering with the signaling of Rho GTPases or altering the activity of kinases such as

PI3K. These targets might not necessarily change the amount of F-actin present in the cell but could instead induce a loss of polarity or a change in cell deformability.

Disruptions in the actin cytoskeleton could also alter integrin activation. If the integrins are bound too tightly to F-actin then they cannot diffuse to cluster together and increase avidity, which would prevent spreading. On the other hand, a complete lack of focal adhesions would also prevent spreading as well since integrin-ligand interactions would no longer be integrated to the actin cytoskeleton.

In addition, A_{2A} receptor signaling may interfere with the affinity of the β_2 integrin by blocking its transition from a bent to extended conformation. Furthermore, ATL313-stimulation could also disrupt the integrin's shift from a closed to open conformation, although this seems less likely since it would mean that the integrin was able to bind to its ligand in the intermediate-affinity (extended/closed) state.

It is also possible that the integrins on the neutrophils are phosphorylated by activated PKA. Recent work by Goldfinger et al. discovered that cytoplasmic domain of α_4 integrins ($\alpha_4\beta_1$ and $\alpha_4\beta_7$) is phosphorylated by PKA at the leading edge of protrusive lamellipodia¹⁸¹. This phosphorylation inhibits paxillin binding and is necessary for efficient migration since both global α_4 phosphorylation or global inhibition of α_4 phosphorylation would impair migration. It seems probable that α_L integrins are also phosphorylated by PKA, but this mechanism would not completely explain the loss of adhesion between the integrin $\alpha_L\beta_2$ and its ligand ICAM-1 since studies have also found that blocking PKA inhibits protrusions and cell migration as well^{181,190,191}.

Chapter 4: Conclusions

4.1 Concluding Remarks

Neutrophils are the first leukocytes that infiltrate inflamed tissues and become activated in response to a variety of inflammatory stimuli including chemoattractants, cytokines, and chemokines. Once activated neutrophils release their own cytokines, migrate towards chemoattractants, increase their expression of β_2 integrins, shed L-selectin and undergo processes that aid in the destruction of pathogens. The migration of leukocytes to inflamed tissues is a multi-step process that involves specific ligand-receptor interactions between adhesion molecules expressed on the surface of both endothelial cells and the leukocytes. Once activated neutrophils' immune response can damage host tissues and lead to sepsis, acute lung injury and rheumatoid arthritis if left unhindered¹⁷⁰⁻¹⁷³.

Adenosine A_{2A} receptors have been shown to exert anti-inflammatory effects in animal models of of inflammatory bowel disease¹⁴⁵⁻¹⁴⁸, rheumatoid arthritis¹⁴⁹⁻¹⁵², sepsis¹⁵³ and ischemia-reperfusion injury in the lungs^{154,155} and heart¹⁵⁶⁻¹⁵⁹. In spite of the wealth of knowledge collected using *in vivo* studies little is known about the effects of Adenosine A_{2A} receptor occupancy on cell adhesion and neutrophil activation.

The aim of the present study was to examine the effects of the Adenosine A_{2A} receptor agonist ATL313 on β_2 integrin-mediated adhesion to ICAM-1 and the expression of activation markers relevant to the leukocyte adhesion cascade (CD11b, L-selectin, and F-actin) in human neutrophils. It is important to note that the data in this study is specific to the agonist ATL313 and that other A_{2A} receptor agonists might produce different results based on their own diverse kinetics and AR specificities. In

addition, ATL313 was studied in this research as a treatment for pre-existing inflammation and not as a prophylactic.

Expression of neutrophil activation markers was assessed using fluorochrome-labeled antibodies against CD11b, L-selectin and F-actin in flow cytometry experiments. Isolated neutrophils were incubated with 50 ng/mL PMA for 10 minutes with or without costimulation of 1 μ M ATL313. Controls for the experiment included fluorochrome-labeled isotype controls, unstained cells and untreated cells. PMA-stimulation produced an average 2.26-fold average increase in CD11b, a 5.25-fold average decrease in L-selectin and a 1.49-fold average decrease in F-actin median fluorescent intensity compared to untreated cells. ATL313 treatment, alone or in conjunction with PMA, was not statistically different from untreated and PMA stimulated cells, respectively. This suggests that Adenosine A_{2A} receptor occupancy does not change the expression level of CD11b, L-selectin, or F-actin in neutrophils. Therefore, adenosine A_{2A} receptor signaling does not appear to disrupt the activity of TACE, the metalloprotease involved in L-selectin shedding. This does not imply, however, that ATL313 did not elicit an anti-inflammatory response despite the failure to change expression levels of these markers.

The LFA-1 ligand ICAM-1 was immobilized onto plastic dishes used in static adhesion and detachment assays to determine the effect of ATL313 stimulation on the β_2 integrin-mediated adhesion of human neutrophils. Stimulated cells were allowed to settle onto plates coated with ICAM-1 for 5 minutes. The average number of cells that remained attached to the plates after 30 seconds of shear stress at 1 dyne/cm² was quantified. The percentage of neutrophils per FOV that spread on ICAM-1 coated surfaces after a 10 minute incubation was also determined.

Activation of the PKC pathway via PMA lead to an average 1.44-fold increase in the average number of firmly adherent cells after 30 seconds of shear stress and a 16.7-fold average increase in cell spreading after a 10 minute incubation on ICAM-1 compared to untreated cells. In comparison to neutrophils treated with PMA alone, cells treated with both ATL313 and PMA experienced a 10.6-fold average decrease in cell spreading on ICAM-1 and an average 10.9-fold decrease in the average percent of cells that firmly adhered after 30 seconds of shear stress. These results suggest that ATL313 is able to inhibit PKC-activation-mediated adhesion of neutrophils to the β_2 integrin ligand ICAM-1. The specific signaling mechanism involved in this inhibition remains to be elucidated.

4.2 Future Directions

The results of this study demonstrate the effects of Adenosine A_{2A} receptor activation at the cellular level in human neutrophils; however more studies are needed to examine the effects of this stimulation on the signaling cascades involved in neutrophil activation, integrin-mediated adhesion and cytoskeletal reorganization.

Our results show that Adenosine A_{2A} receptor occupancy does not alter the expression of β_2 integrins (Mac-1), yet is capable of inhibiting β_2 integrin-mediated adhesion of neutrophils to the ligand ICAM-1. We would like to examine whether this loss of adhesion is due to (1) the failure of β_2 integrins to change from a bent (inactive) to extended (active) conformation or (2) a decrease in integrin clustering on the cell membrane. Two small antibodies currently exist, KIM127 and CMBR1/5, which are capable of detecting the extended conformation of LFA-1 and Mac-1, respectively¹⁹²⁻¹⁹⁴. It would be interesting to use these antibodies to examine whether ATL313-mediated

signaling is capable of preventing the transition from a bent to extended conformation. This can be done using fluorescently labeled KIM127 and CMBR1/5 in flow cytometry experiments with the same methods used in section 2.2.4 of the present study.

It is possible that A_{2A} receptor signaling deactivates the integrin subunits by changing their conformation from open (high-affinity) to closed (intermediate or low affinity) configurations. This can be tested using integrins whose α and β subunits are each fused to a fluorescent protein in FRET experiments. One of the subunits would be bound to a donor fluorescent protein while the other would be bound to an acceptor fluorescent protein. When the α and β subunits are in the open confirmation, the donor emission is detected upon the donor excitation. On the other hand the acceptor emission is detected when the two subunits are in close proximity (closed configuration). Therefore, we should be able to detect whether A_{2A} receptor occupancy results in the integrin changing from the open to closed conformation.

Integrin-mediated adhesion is also modulated by changes in avidity through integrin clustering and increased lateral mobility on the cell membrane. Recent studies have suggested that treatment with low non-cytoskeleton-disrupting doses of Cytochalasin D (0.3-1 $\mu\text{g}/\text{mL}$) can induce the clustering of integrins by releasing them from cytoskeletal constraints for avidity effects¹⁹⁵. One future study could use ATL313 stimulation in conjunction with Cytochalasin D treatment and observe using confocal laser microscopy whether the clustering of fluorescently-labeled antibody-bound integrin is altered.

The reduction in β_2 integrin-mediated adhesion in neutrophils incubated with ATL313 may be due to changes in actin cytoskeleton organization, altered integrin

affinity/avidity or both. To determine if changes in the integrin conformation state are responsible for the reduction in adhesion we can use selective antibodies that lock the integrin subunit into an extended (activated) conformation. One such antibody is the noncross-linking mAb CBR LFA1/2, which activates beta2 integrins¹⁹⁶. If, despite being locked in a high-affinity binding state, the integrin binding of ATL313-stimulated cells to β_2 ligands is still reduced, then it is likely that only changes in the actin cytoskeleton are responsible for our results. This concept could also be examined using integrins whose I-domain has been locked into an open configuration using disulfide bonds^{27,29,34,41}.

It is also possible that the observed decrease in LFA-1 mediated adhesion of ATL313-stimulated neutrophils to ICAM-1 is the result of changes to the actin cytoskeleton. A couple scenarios are possible that could produce the same outcomes. First, Adenosine A_{2A} receptor occupancy may change the spatial distribution of intracellular actin filaments without having an effect on the total amount of F-actin in the cell. These changes could also lead to a loss in cell polarity which is required for efficient chemotaxis. This hypothesis could be tested by staining ATL313-treated neutrophils for F-actin and observing their distribution using fluorescent microscopy.

Second, Adenosine A_{2A} receptor activation may change cell deformability due to decreased treadmilling. A couple different experiments can be utilized to assess the stiffness of ATL313-treated cells: micropipette aspiration and Cytochalasin D treatment. The former experiment would involve testing the forces required to aspirate neutrophils treated with an Adenosine A_{2A} receptor agonist into a glass micropipette as done by previous lab members. The force, F , required to aspirate the cells can be calculated using the following equation¹⁹⁷:

$$F = \pi R_p^2 \Delta p \left(1 - \frac{4}{3} \bar{\varepsilon} \right) \left(1 - \frac{U_t}{U_f} \right),$$

where Δp is the suction pressure measured using a manometer connected to a force transducer. R_p is the radius of the micropipette, U_t is the velocity of the force transducer during adhesion and U_f is the velocity of the transducer when it is moving freely under the same pressure Δp . For a transducer with radius R_s

$$\bar{\varepsilon} = \frac{(R_p - R_s)}{R_s}$$

The calculated force would be lower if the cell was more deformable. This experiment could also be done in conjunction with high doses of Cytochalasin D, which would result in the inhibition of actin polymerization within the cell. This treatment could be used both as a positive control for deformable cells and as a possible means of counteracting the effects of A_{2A} receptor signaling.

Our work has demonstrated that ATL313 is capable of inhibiting PKC-dependent firm adhesion and spreading on ICAM-1 in human neutrophils. However, the precise interactions between the A_{2A} receptor and PKC signaling cascades are currently unknown. A schematic of the possible intersections of the A_{2A} , integrin and PKC signaling cascades is shown in **Figure 4.1**. These interactions can be probed by treating neutrophils with pharmacological inhibitors of effectors downstream of PKC, such as the Ras inhibitor Trans farnesylthiosalicylic acid. Molecular inhibitors of PKA, including H-89 and Rp-8-Rb-cAMP, which prevent the phosphorylation and dissociation of PKA respectively, could be used to determine whether the effects of ATL313 stimulation are due to PKA-dependent or independent signaling.

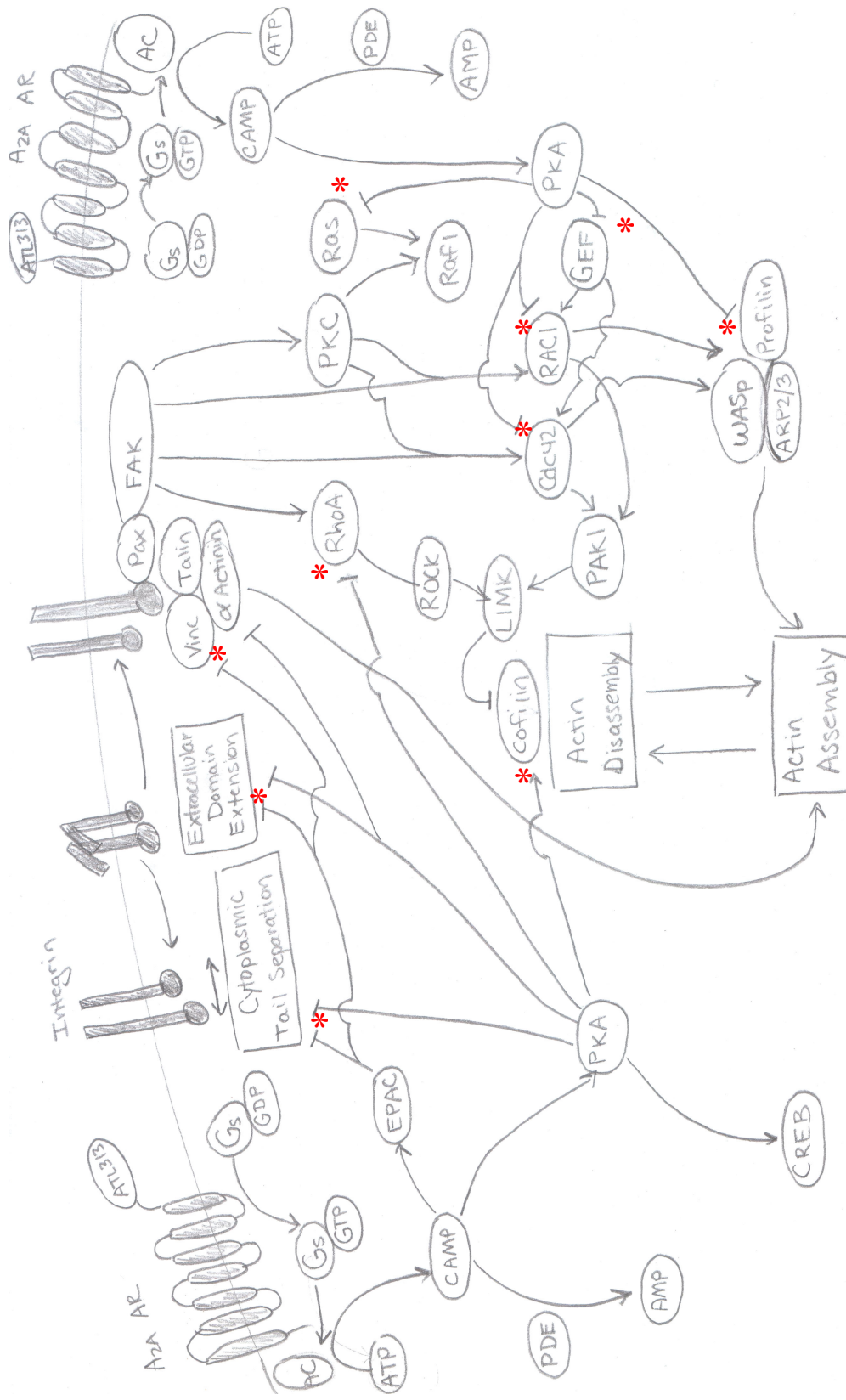


Figure 4.1 Schematic of the Signaling Cascades involved in A_{2A} Receptor and Integrin Activation. Adenosine A_{2A} receptor stimulation via the agonist ATL313 may be altering the organization of the actin cytoskeleton or modulating integrin affinity and/or avidity. Places where A_{2A} receptor signaling is hypothesized to be inhibiting pro-inflammatory pathways are marked with a * symbol.

Appendix

Appendix A. Silver Staining of R6.5 Elution Fractions

Elution fractions were analyzed for the presence of the human ICAM-1 mAb R6.5 using silver staining. A 10% separating gel was created using 30% Acrylimide Bis(Biorad), 10% Ammonium persulfate (APS) (Biorad), Tetramethylethylenediamine (TEMED) (Biorad), 1.5 M Tris pH 8.8 (Sigma), 10% Sodium dodecyl sulfate (SDS) (Biorad), and DW and loaded into a 1 mm glass gel template made by Biorad. The separating gel was allowed to harden before the 4% stacking gel composed of 30% Acrylimide Bis, 10% APS, TEMED, 1 M Tris pH 6.8, 10% SDS, and distilled water was added on top of it. A small plastic insert(Biorad) was used to form 15 wells in the stacking gel. Samples and controls were mixed with distilled water and 5X sample buffer (60 mM Tris-Cl pH 6.8, 50% glycerol (Fisher), 0.1% Bromophenol Blue(Sigma), 2% SDS, 710 mM β -mercaptoethanol(Biorad), and DW) and boiled for 5 min at 100°C prior to loading into the gel. A Novex Sharp pre-stained standard protein marker (Invitrogen, Grand Island, NY) was also loaded into the gel. Gels were run with 1X SDS glycine buffer(25 mM Tris, 192 mM glycine (Sigma), 0.1% SDS, and DW) for 2-3 hours at 100V using a Mini Protean Tank Holder and Biorad Power Pac HC power supply.

After the gel was removed from the tank it was placed in a pyrex glass container under agitation with 100 mL fixation buffer (50% methanol (Fisher), 10% Acetic Acid (Fisher), 40% DW) for 30 min at RT. Next the gel was incubated in 100 ml de-staining solution (5% Methanol, 7% acetic acid, and 88% DW) for 30 minutes under agitation at RT. A 10% Glutaraldehyde (Fisher) solution in DW was then incubated with the gel for

10 minutes at RT. The gel was then washed thoroughly in several changes of Milli-Q water for 2 hours to ensure low background levels. A 5 ug/ml Dithiothreitol (DTT) solution (Biorad) was then added for 30 minutes at RT under agitation. A 0.1% Silver Nitrate (Fisher) solution was added to the gel and agitated for 30 minutes at RT. The gel was then quickly washed once with a small amount of water before being washed twice for about 15 seconds with carbonate developing solution consisting of 3% Sodium Carbonate (Fisher) and 0.0185% formaldehyde in DW. The gel was then soaked in 100 mL carbonate developing solution and agitated slowly until the desired level of staining was achieved. The reaction was stopped by adding 5 ml of 2.3 M citric acid (Sigma) for 10 minutes and rocking slowly at RT. Lastly the gel was washed several times in water under slow agitation for 30 minutes before being preserved in between two clear mylar preserving sheets (GE Healthcare) and placed in a sealed pouch (Kapak, Minneapolis, MN). Finally the gel was imaged on a Canoscan N1220U model Scanner (Canon).

Images of gels are shown in **Figure A.1 (A and B)** below. Fractions 6-34 had positive staining for R6.5 and were pooled together to be covalently linked to sepharose for use in the isolation of ICAM-1 from human tonsils via immunoaffinity chromatography.

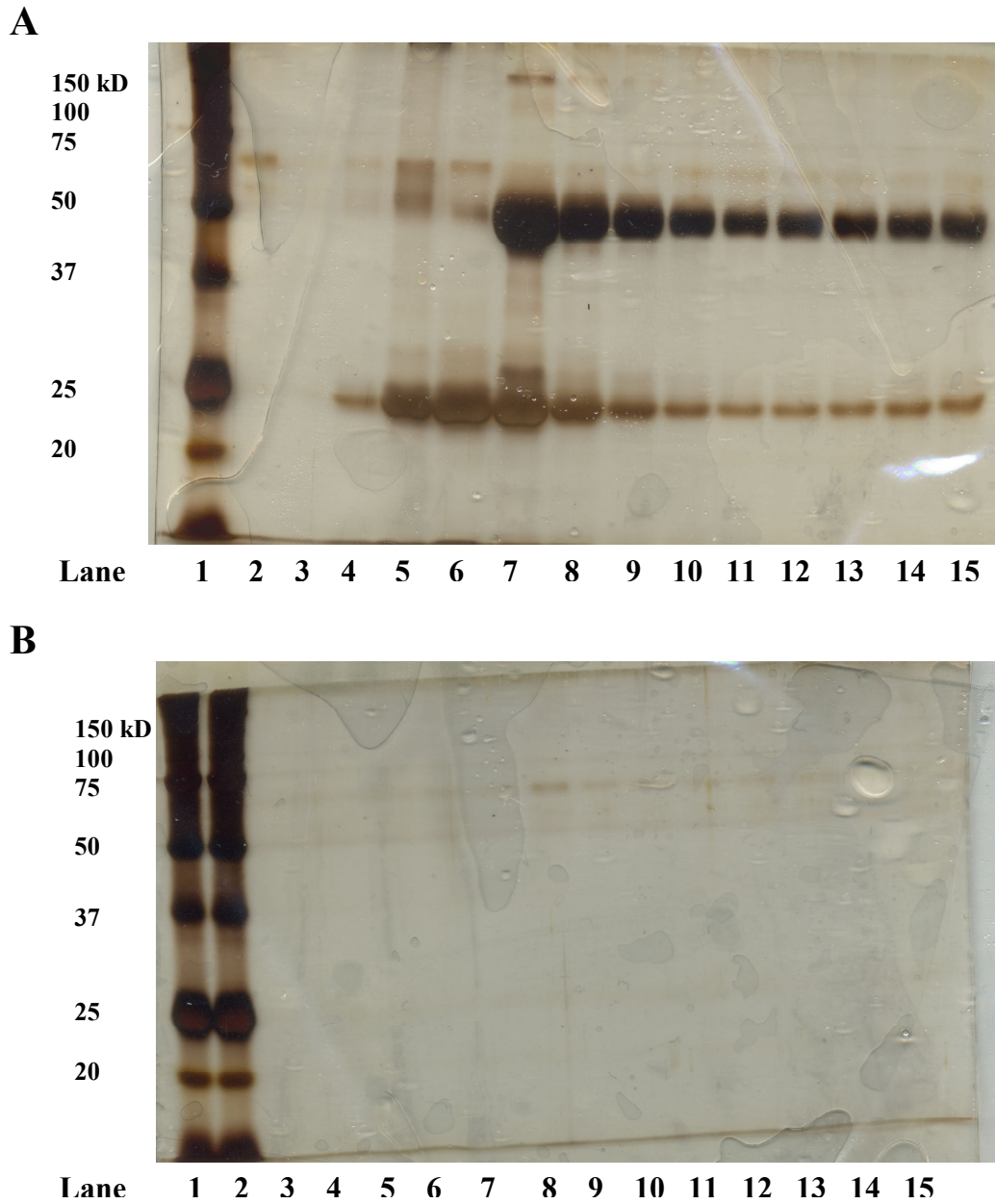


Figure A.1 Images of elution fractions used in SDS-PAGE Gels

(A) Gel containing HB9580-isolated R6.5 fractions 1-14 in lanes 2-15. Lane 1 is the protein marker

(B) Gel containing HB9580-isolated R6.5 fractions 38-50 in lanes 3-15. Lanes 1 and 2 contain the protein marker

Appendix B. Confirmation of the isolation of functional mAb R6.5 using Flow Cytometry

The R6.5 Ab was obtained from Boehringer Ingelheim (Ridgefield, CT) or isolated using affinity chromatography from the HB9580 cell line. Raji cells were incubated with 1 µg/100 µL R6.5 mAbs in staining solution (Sodium Azide (Sigma), 0.75% FBS, HBSS) for 20 minutes on ice. Following staining cells were washed twice with staining solution before incubation with FITC-labeled anti-IgG whole molecule secondary antibody in staining solution on ice for 20 minutes. Cells were washed once with staining solution and then fixed for 10 minutes at RT using fixation solution (5% formaldehyde, 1% Bovine serum albumin (BSA), Sodium Azide). Unstained cells and cells stained with secondary antibody alone were used as controls.

Cells were washed and resuspended in HBSS before being analyzed in a FACsCalibur flow cytometer. Cells were gated based on forward and side scatter measurements and 10,000 gated events were collected. Staining for ICAM-1 in Raji cells was similar for all sources of the mAb R6.5 as shown in **Figure A.2** below, indicating that R6.5 was properly isolated from the HB9580 cell line.

Raji cells stained with Primary Abs to ICAM1 (R6.5) followed by FITC anti-mouse IgG whole molecule secondary staining

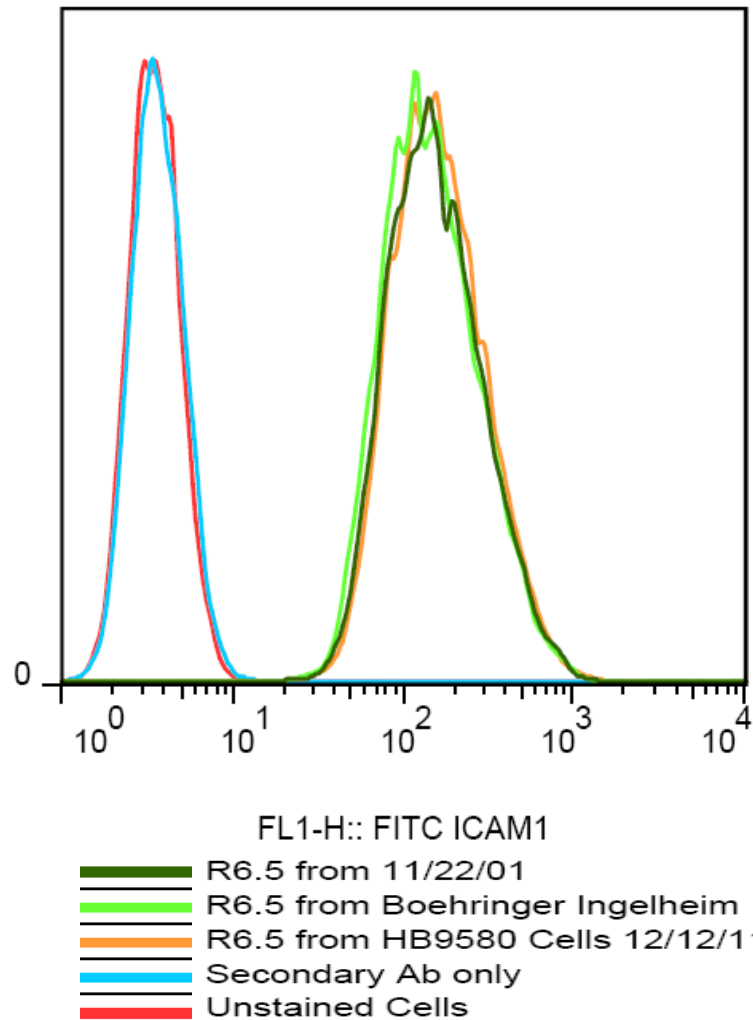


Figure A.2 ICAM-1 Staining using the R6.5 mAb isolated from the HB9580 Cell Line.

The mAb R6.5 isolated from the cell line HB9580 showed similar staining to ICAM-1 expressed on cultured Raji cells compared to other sources of R6.5. The FITC-labeled secondary antibody used detected Mouse IgG and was also used as a control.

Appendix C. Silver Staining of ICAM-1 Elution Fractions

Elution fractions collected using the R6.5 mAb in an immunoaffinity chromatography were analyzed for the presence of the human ICAM-1 (90-120 kD) using the silver staining methods described in Appendix A. Recombinant human monomeric ICAM-1 (rhICAM-1) was obtained from R&D Systems (Minneapolis, MN) and used as a positive control. Lysate samples from the ICAM-1 expressing Raji cell line and human tonsils that were not run through the immunoaffinity chromatography column were also run as positive controls. **Figure A.3** shows an image of the gel after silver staining.

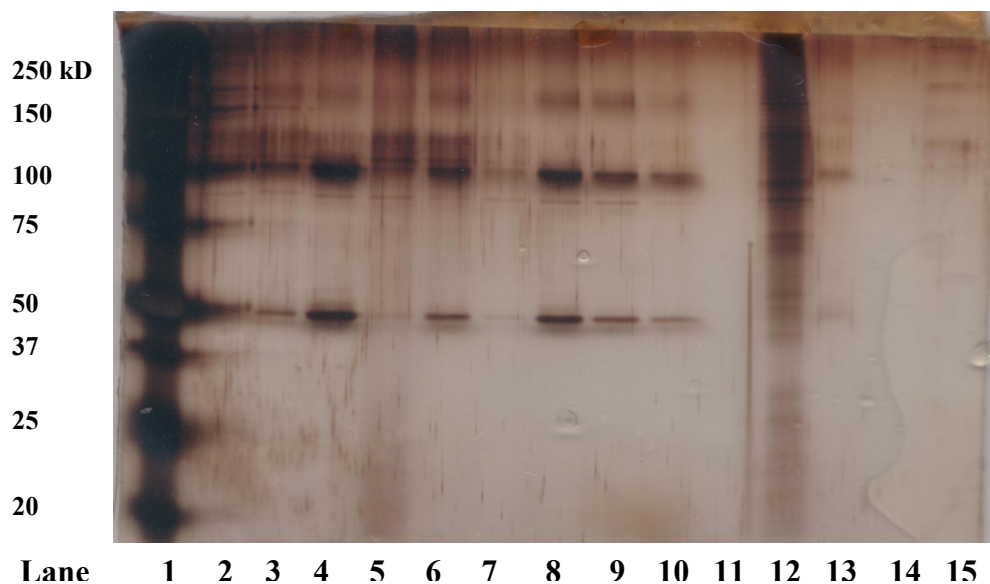


Figure A.3 Silver Staining of a gel run with ICAM-1 elution fractions.

Lane 1 is the protein marker. Lanes 2-10 contain ICAM-1 elution fractions isolated from human tonsils. Lane 12 is human tonsil lysate and lane 13 is lysate from the ICAM-1 expressing Raji cell line. Lane 15 is rhICAM-1.

Appendix D: Determination of Volumetric Flow Rate

The volumetric flow rate was determined using the Navier-Stokes Equation whose general form is¹⁹⁸:

$$\rho \frac{D\vec{v}}{Dt} = \rho\mathbf{g} - \nabla p + \mu\nabla^2\vec{v} \quad (1)$$

and the equation for shear stress, τ_{xz} , is

$$\tau_{xz} = -\mu \left(\frac{\partial v_x}{\partial z} + \frac{\partial v_z}{\partial x} \right) \quad (2)$$

where

ρ = fluid density
 μ = fluid viscosity
 \mathbf{g} = gravity
 t = time
 p = pressure

The x-component of equation (1) is:

$$\rho \left(\frac{\partial v_x}{\partial t} + v_x \frac{\partial v_x}{\partial x} + v_y \frac{\partial v_x}{\partial y} + v_z \frac{\partial v_x}{\partial z} \right) = \rho g_x - \frac{\partial p}{\partial x} + \mu \left(\frac{\partial^2 v_x}{\partial x^2} + \frac{\partial^2 v_x}{\partial y^2} + \frac{\partial^2 v_x}{\partial z^2} \right) \quad (3)$$

Assuming that:

1. The fluid flow is described by steady state motion ($\frac{\partial v_x}{\partial t} = 0$)
2. Gravity only acts in the z-direction ($g_{x=0}$)
3. There is no velocity in the y- or z-directions ($v_y = 0, v_z = 0$)
4. The fluid has a uniform density
5. There is no change in velocity in the x-direction ($\frac{\partial v_x}{\partial x} = 0$)
6. The pressure gradient is constant and varies linearly along the channel
7. The fluid is a Newtonian Fluid
8. The flow is laminar

Using assumptions 1-6 above and the coordinate system and flow chamber geometry shown in **Figure A.4** equation (2) and equation (3) simplify, respectively, to:

$$\tau_{xz} = -\mu \frac{\delta v_x}{\delta z} \quad (4)$$

$$\frac{1}{\mu} \frac{\delta p}{\delta x} = \frac{\delta^2 v_x}{\delta z^2} = \text{constant} \quad (5)$$

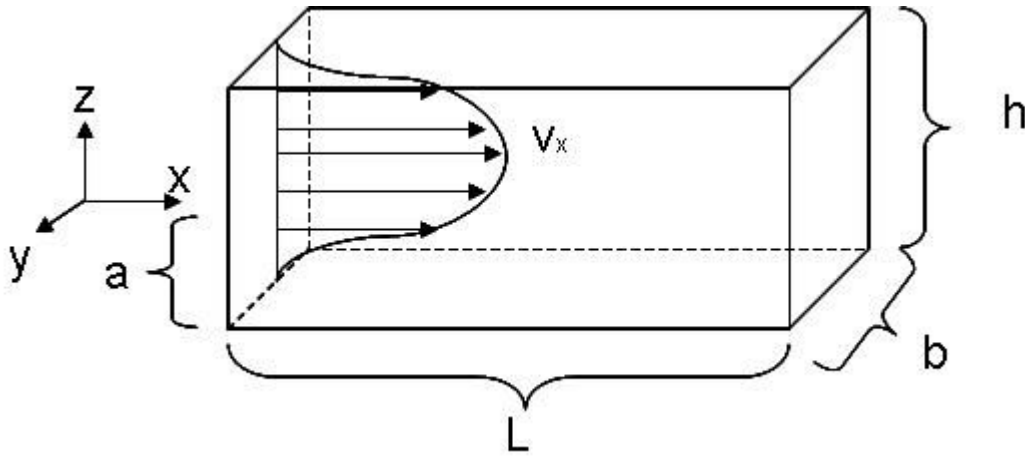


Figure A.4 Orientation of Fluid Flow Inside the Flow Chamber.

The coordinate axes are set up so that the origin is in the middle of the chamber such that $z=0$ is at the center and $z=\pm a$ at either wall. The chamber has dimensions width b , length L and a height $h=2a$ determined by the gasket dimension stated in section 3.2.5.

Our initial conditions are that

$$\frac{\delta v_x}{\delta z}(z=0) = 0 \quad (\text{IC 1})$$

$$v_x(z=a) = 0 \quad (\text{IC 2})$$

Integrating equation (5) once with respect to z we get:

$$\frac{\delta v_x}{\delta z} = \frac{1}{\mu} \frac{\delta p}{\delta x} z + c_1 \quad (6)$$

where c_1 is a constant of integration that we can solve for using initial condition 1 (IC 1):

$$c_1 = \frac{\delta v_x}{\delta z} = 0$$

Using the value found for c_1 and integrating equation (6) again with respect to z we get:

$$v_x = \frac{1}{2\mu} \frac{\delta p}{\delta x} z^2 + c_2 \quad (7)$$

where c_2 is a constant of integration that we can solve for using initial condition 2 (IC 2):

$$c_2 = \frac{-a^2}{2\mu} \frac{\delta p}{\delta x}$$

Plugging this value for c_2 into equation (7) we have:

$$v_x = \frac{1}{2\mu} \frac{\delta p}{\delta x} z^2 + \frac{-1}{2\mu} \frac{\delta p}{\delta x} a^2 = \frac{1}{2\mu} \frac{\delta p}{\delta x} (z^2 - a^2) = \frac{-a^2}{2\mu} \frac{\delta p}{\delta x} \left(1 - \left(\frac{z}{a}\right)^2\right) \quad (8)$$

Due to symmetry, the mean velocity in the flow chamber, U , is given by:

$$U = \frac{1}{a} \int_0^a v_x dz \quad (9)$$

Using equation (8) in equation (9) and integrating we have:

$$U = \frac{-a^2}{3\mu} \frac{\delta p}{\delta x} \quad (10)$$

We then recognize that

$$3U = \frac{-a^2}{\mu} \frac{\delta p}{\delta x}, \quad (11)$$

substituting into equation (8) we find:

$$v_z = \frac{3U}{2} \left(1 - \left(\frac{z}{a}\right)^2\right) \quad (12)$$

The volumetric flow rate, Q , is the product of the mean velocity of the fluid and the cross-sectional area (width×height). For a height, $h=2a$ and width, b , Q is given by:

$$Q = Ubh = 2ab \left[\frac{-a^2}{3\mu} \frac{dp}{dx} \right] = -\frac{2a^3b}{3\mu} \frac{dp}{dx} \quad (13)$$

Equation (13) allows us to solve for $\frac{dp}{dx}$ in terms of Q

$$\frac{dp}{dx} = -\frac{3\mu Q}{2a^3b} \quad (14)$$

Using equation (6) in equation (4) and evaluating at the height $z=a$ we can determine the wall shear stress

$$\tau_{xz}(z=a) = -\mu \frac{\delta v_x}{\delta z}(z=h) = -\mu \left[\frac{1}{\mu} \frac{dp}{dx} h \right] = -\frac{dp}{dx} h \quad (15)$$

If we substitute equation (14) into equation (15) we find:

$$\tau_{xz}(z=a) = \frac{3\mu Q}{2a^3b} a = \frac{3\mu Q}{2a^2b} = \frac{3\mu Q}{2\left(\frac{h}{2}\right)^2 b} = \frac{6\mu Q}{h^2b} \quad (16)$$

Solving for Q in terms of τ_{xz} we get:

$$Q = \frac{h^2b\tau_{xz}}{6\mu} \quad (17)$$

where

$$\mu = \text{fluid viscosity} = 0.01 \text{ P} = \frac{1 \text{ dyne} \cdot \text{s}}{\text{cm}^2} \text{ at } 20^\circ\text{C}$$

$$b = \text{channel width} = 0.5 \text{ cm}$$

$$h = \text{channel height} = \text{gasket thickness} = 0.0254 \text{ cm}$$

$$\tau_{xz} = \text{wall shear stress}$$

The volumetric flow rate in mL/minute is given by:

$$Q = \frac{h^2b\tau_{xz}}{6\mu} \cdot \frac{60\text{s}}{\text{min}}$$

Therefore, for a desired wall shear stress of $\frac{1 \text{ dyne}}{\text{cm}^2}$ for the values given above the flow rate of the pump should be set to 0.323 mL/min.

Bibliography

1. Levy JH. The human inflammatory response. *J Cardiovasc Pharmacol.* 1996;**27**:S31-7.
2. Goldman AS, Prabhakar BS. Immunology Overview. In: Baron S, editor. *Medical Microbiology*. 4th ed. Galveston (TX): The University of Texas Medical Branch at Galveston; 1996.
3. Steeber DA, Tedder TF. Adhesion molecule cascades direct lymphocyte recirculation and leukocyte migration during inflammation. *Immunol Res.* 2000;**22**:299-317.
4. Drickamer K. Two distinct classes of carbohydrate-recognition domains in animal lectins. *J.Biol.Chem.* 1988;**263**:9557-60.
5. Somers WS, Tang J, Shaw GD, Camphausen RT. Insights into the molecular basis of leukocyte tethering and rolling revealed by structures of P- and E-selectin bound to SLe(X) and PSGL-1. *Cell* 2000;**103**:467-79.
6. Freedman SJ, Sanford DG, Bachovchin WW, Furie BC, Baleja JD, Furie B. Structure and function of the epidermal growth factor domain of P-selectin. *Biochemistry* 1996;**35**:13733-44.
7. McEver RP, Cummings RD. Role of PSGL-1 binding to selectins in leukocyte recruitment. *J.Clin.Invest.* 1997;**100**:S97-103.
8. Lorant DE, Patel KD, McIntyre TM, McEver RP, Prescott SM, Zimmerman GA. Coexpression of GMP-140 and PAF by endothelium stimulated by histamine or thrombin: a juxtacrine system for adhesion and activation of neutrophils. *J.Cell Biol.* 1991;**115**:223-34.
9. Nermut MV, Green NM, Eason P, Yamada SS, Yamada KM. Electron microscopy and structural model of human fibronectin receptor. *EMBO J.* 1988;**7**:4093-9.
10. Faull RJ, Ginsberg MH. Inside-out signaling through integrins. *J.Am.Soc.Nephrol.* 1996;**7**:1091-7.
11. Hynes RO. Integrins: bidirectional, allosteric signaling machines. *Cell* 2002;**110**:673-87.
12. Anderson DC, Springer TA. Leukocyte adhesion deficiency: an inherited defect in the Mac-1, LFA-1, and p150,95 glycoproteins. *Annu.Rev.Med.* 1987;**38**:175-94.
13. Diamond MS, Staunton DE, Marlin SD, Springer TA. Binding of the integrin Mac-1 (CD11b/CD18) to the third immunoglobulin-like domain of ICAM-1 (CD54) and its regulation by glycosylation. *Cell* 1991;**65**:961-71.

14. Takagi J. Structural basis for ligand recognition by integrins. *Curr.Opin.Cell Biol.* 2007;**19**:557-64.
15. Zhang Y, Wang H. Integrin signalling and function in immune cells. *Immunology* 2012;**135**:268-75.
16. Elangbam CS, Qualls CW,Jr, Dahlgren RR. Cell adhesion molecules--update. *Vet.Pathol.* 1997;**34**:61-73.
17. Krieger M, Scott MP, Matsudaira PT, Lodish HF, Darnell JE, Zipursky L, et al. *Molecular cell biology* 5th ed. New York: W.H. Freeman and CO; 2004.
18. Hermann P, Armant M, Brown E, Rubio M, Ishihara H, Ulrich D, et al. The vitronectin receptor and its associated CD47 molecule mediates proinflammatory cytokine synthesis in human monocytes by interaction with soluble CD23. *J.Cell Biol.* 1999;**144**:767-75.
19. Nagae M, Re S, Mihara E, Nogi T, Sugita Y, Takagi J. Crystal structure of alpha5beta1 integrin ectodomain: Atomic details of the fibronectin receptor. *J.Cell Biol.* 2012;**197**:131-40.
20. Xie C, Zhu J, Chen X, Mi L, Nishida N, Springer TA. Structure of an integrin with an alphaI domain, complement receptor type 4. *EMBO J.* 2010;**29**:666-79.
21. Zhu J, Luo BH, Barth P, Schonbrun J, Baker D, Springer TA. The structure of a receptor with two associating transmembrane domains on the cell surface: integrin alphaIIbbeta3. *Mol.Cell* 2009;**34**:234-49.
22. Xiong JP, Stehle T, Diefenbach B, Zhang R, Dunker R, Scott DL, et al. Crystal structure of the extracellular segment of integrin alpha Vbeta3. *Science* 2001;**294**:339-45.
23. Lee JO, Rieu P, Arnaout MA, Liddington R. Crystal structure of the A domain from the alpha subunit of integrin CR3 (CD11b/CD18). *Cell* 1995;**80**:631-8.
24. Xie C, Shimaoka M, Xiao T, Schwab P, Klickstein LB, Springer TA. The integrin alpha-subunit leg extends at a Ca²⁺-dependent epitope in the thigh/genu interface upon activation. *Proc.Natl.Acad.Sci.U.S.A.* 2004;**101**:15422-7.
25. Takagi J, Petre BM, Walz T, Springer TA. Global conformational rearrangements in integrin extracellular domains in outside-in and inside-out signaling. *Cell* 2002;**110**:599-11.
26. Nishida N, Xie C, Shimaoka M, Cheng Y, Walz T, Springer TA. Activation of leukocyte beta2 integrins by conversion from bent to extended conformations. *Immunity* 2006;**25**:583-94.

27. Shimaoka M, Lu C, Palframan RT, von Andrian UH, McCormack A, Takagi J, et al. Reversibly locking a protein fold in an active conformation with a disulfide bond: integrin alphaL I domains with high affinity and antagonist activity in vivo. *Proc.Natl.Acad.Sci.U.S.A.* 2001;**98**:6009-14.
28. Shimaoka M, Shifman JM, Jing H, Takagi J, Mayo SL, Springer TA. Computational design of an integrin I domain stabilized in the open high affinity conformation. *Nat.Struct.Biol.* 2000;**7**:674-8.
29. Lu C, Shimaoka M, Zang Q, Takagi J, Springer TA. Locking in alternate conformations of the integrin alphaLbeta2 I domain with disulfide bonds reveals functional relationships among integrin domains. *Proc.Natl.Acad.Sci.U.S.A.* 2001;**98**:2393-8.
30. Beglova N, Blacklow SC, Takagi J, Springer TA. Cysteine-rich module structure reveals a fulcrum for integrin rearrangement upon activation. *Nat.Struct.Biol.* 2002;**9**:282-7.
31. Xiong JP, Stehle T, Zhang R, Joachimiak A, Frech M, Goodman SL, et al. Crystal structure of the extracellular segment of integrin alpha Vbeta3 in complex with an Arg-Gly-Asp ligand. *Science* 2002;**296**:151-5.
32. Takagi J, Springer TA. Integrin activation and structural rearrangement. *Immunol.Rev.* 2002;**186**:141-63.
33. Lu C, Takagi J, Springer TA. Association of the membrane proximal regions of the alpha and beta subunit cytoplasmic domains constrains an integrin in the inactive state. *J.Biol.Chem.* 2001;**276**:14642-8.
34. Lu C, Shimaoka M, Ferzly M, Oxvig C, Takagi J, Springer TA. An isolated, surface-expressed I domain of the integrin alphaLbeta2 is sufficient for strong adhesive function when locked in the open conformation with a disulfide bond. *Proc.Natl.Acad.Sci.U.S.A.* 2001;**98**:2387-92.
35. Raborn J, Luo BH. Mutagenesis studies of the beta I domain metal ion binding sites on integrin alphaVbeta3 ligand binding affinity. *J.Cell.Biochem.* 2011;.
36. Shimaoka M, Takagi J, Springer TA. Conformational regulation of integrin structure and function. *Annu.Rev.Biophys.Biomol.Struct.* 2002;**31**:485-516.
37. Emsley J, Knight CG, Fardale RW, Barnes MJ, Liddington RC. Structural basis of collagen recognition by integrin alpha2beta1. *Cell* 2000;**101**:47-56.
38. Lee JO, Bankston LA, Arnaout MA, Liddington RC. Two conformations of the integrin A-domain (I-domain): a pathway for activation? *Structure* 1995;**3**:1333-40.

39. Shimaoka M, Xiao T, Liu JH, Yang Y, Dong Y, Jun CD, et al. Structures of the alpha L I domain and its complex with ICAM-1 reveal a shape-shifting pathway for integrin regulation. *Cell* 2003;**112**:99-111.
40. Vorup-Jensen T, Ostermeier C, Shimaoka M, Hommel U, Springer TA. Structure and allosteric regulation of the alpha X beta 2 integrin I domain. *Proc.Natl.Acad.Sci.U.S.A.* 2003;**100**:1873-8.
41. Shimaoka M, Lu C, Salas A, Xiao T, Takagi J, Springer TA. Stabilizing the integrin alpha M inserted domain in alternative conformations with a range of engineered disulfide bonds. *Proc.Natl.Acad.Sci.U.S.A.* 2002;**99**:16737-41.
42. Xiong JP, Li R, Essafi M, Stehle T, Arnaout MA. An isoleucine-based allosteric switch controls affinity and shape shifting in integrin CD11b A-domain. *J.Biol.Chem.* 2000;**275**:38762-7.
43. Takagi J, Erickson HP, Springer TA. C-terminal opening mimics 'inside-out' activation of integrin alpha5beta1. *Nat.Struct.Biol.* 2001;**8**:412-6.
44. Abram CL, Lowell CA. Leukocyte adhesion deficiency syndrome: a controversy solved. *Immunol.Cell Biol.* 2009;**87**:440-2.
45. Fagerholm SC, Hilden TJ, Gahmberg CG. P marks the spot: site-specific integrin phosphorylation regulates molecular interactions. *Trends Biochem.Sci.* 2004;**29**:504-12.
46. Gahmberg CG, Fagerholm SC, Nurmi SM, Chavakis T, Marchesan S, Gronholm M. Regulation of integrin activity and signalling. *Biochim.Biophys.Acta* 2009;**1790**:431-44.
47. Liu S, Ginsberg MH. Paxillin binding to a conserved sequence motif in the alpha 4 integrin cytoplasmic domain. *J.Biol.Chem.* 2000;**275**:22736-42.
48. Liu S, Thomas SM, Woodside DG, Rose DM, Kiosses WB, Pfaff M, et al. Binding of paxillin to alpha4 integrins modifies integrin-dependent biological responses. *Nature* 1999;**402**:676-81.
49. Han J, Liu S, Rose DM, Schlaepfer DD, McDonald H, Ginsberg MH. Phosphorylation of the integrin alpha 4 cytoplasmic domain regulates paxillin binding. *J.Biol.Chem.* 2001;**276**:40903-9.
50. Carman CV, Springer TA. Integrin avidity regulation: are changes in affinity and conformation underemphasized? *Curr.Opin.Cell Biol.* 2003;**15**:547-56.
51. van Kooyk Y, Weder P, Hogervorst F, Verhoeven AJ, van Seventer G, te Velde AA, et al. Activation of LFA-1 through a Ca2(+)-dependent epitope stimulates lymphocyte adhesion. *J.Cell Biol.* 1991;**112**:345-54.

52. van Kooyk Y, van Vliet SJ, Figdor CG. The actin cytoskeleton regulates LFA-1 ligand binding through avidity rather than affinity changes. *J.Biol.Chem.* 1999;**274**:26869-77.
53. Leitinger B, Hogg N. The involvement of lipid rafts in the regulation of integrin function. *J.Cell.Sci.* 2002;**115**:963-72.
54. Krauss K, Altevogt P. Integrin leukocyte function-associated antigen-1-mediated cell binding can be activated by clustering of membrane rafts. *J.Biol.Chem.* 1999;**274**:36921-7.
55. Cabanas C, Hogg N. Ligand intercellular adhesion molecule 1 has a necessary role in activation of integrin lymphocyte function-associated molecule 1. *Proc.Natl.Acad.Sci.U.S.A.* 1993;**90**:5838-42.
56. Hynes RO, Zhao Q. The evolution of cell adhesion. *J.Cell Biol.* 2000;**150**:F89-96.
57. Burridge K, Mangeat P. An interaction between vinculin and talin. *Nature* 1984;**308**:744-6.
58. Burn P, Kupfer A, Singer SJ. Dynamic membrane-cytoskeletal interactions: specific association of integrin and talin arises in vivo after phorbol ester treatment of peripheral blood lymphocytes. *Proc.Natl.Acad.Sci.U.S.A.* 1988;**85**:497-501.
59. Goldmann WH, Ingber DE. Intact vinculin protein is required for control of cell shape, cell mechanics, and rac-dependent lamellipodia formation. *Biochem.Biophys.Res.Commun.* 2002;**290**:749-55.
60. Disatnik MH, Boutet SC, Lee CH, Mochly-Rosen D, Rando TA. Sequential activation of individual PKC isozymes in integrin-mediated muscle cell spreading: a role for MARCKS in an integrin signaling pathway. *J.Cell.Sci.* 2002;**115**:2151-63.
61. Miranti CK, Ohno S, Brugge JS. Protein kinase C regulates integrin-induced activation of the extracellular regulated kinase pathway upstream of Shc. *J.Biol.Chem.* 1999;**274**:10571-81.
62. Zhou X, Li J. Macrophage-enriched myristoylated alanine-rich C kinase substrate and its phosphorylation is required for the phorbol ester-stimulated diffusion of beta 2 integrin molecules. *J.Biol.Chem.* 2000;**275**:20217-22.
63. van Kooyk Y, Figdor CG. Avidity regulation of integrins: the driving force in leukocyte adhesion. *Curr.Opin.Cell Biol.* 2000;**12**:542-7.
64. Etienne-Manneville S, Hall A. Integrin-mediated activation of Cdc42 controls cell polarity in migrating astrocytes through PKCzeta. *Cell* 2001;**106**:489-98.

65. Guo W, Giancotti FG. Integrin signalling during tumour progression. *Nat.Rev.Mol.Cell Biol.* 2004;**5**:816-26.
66. Mullins RD, Heuser JA, Pollard TD. The interaction of Arp2/3 complex with actin: nucleation, high affinity pointed end capping, and formation of branching networks of filaments. *Proc.Natl.Acad.Sci.U.S.A.* 1998;**95**:6181-6.
67. Blanchoin L, Amann KJ, Higgs HN, Marchand JB, Kaiser DA, Pollard TD. Direct observation of dendritic actin filament networks nucleated by Arp2/3 complex and WASP/Scar proteins. *Nature* 2000;**404**:1007-11.
68. Alberts B, Johnson A, Lewis J, et al. *Molecular Biology of the Cell* . . 4th edition ed. New York: Garland Science; 2002.
69. Dominguez R, Holmes KC. Actin structure and function. *Annu.Rev.Biophys.* 2011;**40**:169-86.
70. Ridley AJ, Schwartz MA, Burridge K, Firtel RA, Ginsberg MH, Borisy G, et al. Cell migration: integrating signals from front to back. *Science* 2003;**302**:1704-9.
71. Vicente-Manzanares M, Webb DJ, Horwitz AR. Cell migration at a glance. *J.Cell.Sci.* 2005;**118**:4917-9.
72. Pertz O, Hodgson L, Klemke RL, Hahn KM. **Spatiotemporal dynamics of RhoA activity in migrating cells.** *Nature* 2006;**440**:1069-72.
73. Pillay J, den Braber I, Vrisekoop N, Kwast LM, de Boer RJ, Borghans JA, et al. In vivo labeling with ²H₂O reveals a human neutrophil lifespan of 5.4 days. *Blood* 2010;**116**:625-7.
74. Wheeler PR, Stevens A. *Wheeler's basic histopathology: a colour atlas and text.* : Churchill Livingstone; 2002.
75. Zhelev DV, Alteraifi A. Signaling in the motility responses of the human neutrophil. *Ann.Biomed.Eng.* 2002;**30**:356-70.
76. Tester AM, Cox JH, Connor AR, Starr AE, Dean RA, Puente XS, et al. LPS responsiveness and neutrophil chemotaxis in vivo require PMN MMP-8 activity. *PLoS One* 2007;**2**:e312.
77. Wagner JG, Roth RA. Neutrophil migration mechanisms, with an emphasis on the pulmonary vasculature. *Pharmacol.Rev.* 2000;**52**:349-74.
78. Davis HM, Carpenter DC, Stahl JM, Zhang W, Hynicka WP, Griswold DE. Human granulocyte CD11b expression as a pharmacodynamic biomarker of inflammation. *J.Immunol.Methods* 2000;**240**:125-32.

79. Zhu X, Tan Z, Chen J, Zhu M, Xu Y. Effects of ropivacaine on adhesion molecule CD11b expression and function in human neutrophils. *Int.Immunopharmacol.* 2010;**10**:662-7.
80. Contran RS, Kumar V, Collins T. *Robbins Pathologic Basis of Disease.* 6th ed. Philadelphia: W.B Saunders Company.
81. Tracey KJ, Cerami A. Tumor necrosis factor: an updated review of its biology. *Crit.Care Med.* 1993;**21**:S415-22.
82. Tracey KJ, Cerami A. Tumor necrosis factor: a pleiotropic cytokine and therapeutic target. *Annu.Rev.Med.* 1994;**45**:491-503.
83. Rollins BJ. Chemokines. *Blood* 1997;**90**:909-28.
84. Walz A, Burgener R, Car B, Baggiolini M, Kunkel SL, Strieter RM. Structure and neutrophil-activating properties of a novel inflammatory peptide (ENA-78) with homology to interleukin 8. *J.Exp.Med.* 1991;**174**:1355-62.
85. Moser B, Clark-Lewis I, Zwahlen R, Baggiolini M. Neutrophil-activating properties of the melanoma growth-stimulatory activity. *J.Exp.Med.* 1990;**171**:1797-802.
86. Moser B, Schumacher C, von Tscherner V, Clark-Lewis I, Baggiolini M. Neutrophil-activating peptide 2 and gro/melanoma growth-stimulatory activity interact with neutrophil-activating peptide 1/interleukin 8 receptors on human neutrophils. *J.Biol.Chem.* 1991;**266**:10666-71.
87. Nicholson GC, Tennant RC, Carpenter DC, Sarau HM, Kon OM, Barnes PJ, et al. A novel flow cytometric assay of human whole blood neutrophil and monocyte CD11b levels: upregulation by chemokines is related to receptor expression, comparison with neutrophil shape change, and effects of a chemokine receptor (CXCR2) antagonist. *Pulm.Pharmacol.Ther.* 2007;**20**:52-9.
88. Lasagni L, Francalanci M, Annunziato F, Lazzeri E, Giannini S, Cosmi L, et al. An alternatively spliced variant of CXCR3 mediates the inhibition of endothelial cell growth induced by IP-10, Mig, and I-TAC, and acts as functional receptor for platelet factor 4. *J.Exp.Med.* 2003;**197**:1537-49.
89. Walz A, Dewald B, von Tscherner V, Baggiolini M. Effects of the neutrophil-activating peptide NAP-2, platelet basic protein, connective tissue-activating peptide III and platelet factor 4 on human neutrophils. *J.Exp.Med.* 1989;**170**:1745-50.
90. Walz A, Schmutz P, Mueller C, Schnyder-Candrian S. Regulation and function of the CXC chemokine ENA-78 in monocytes and its role in disease. *J.Leukoc.Biol.* 1997;**62**:604-11.

91. Peveri P, Walz A, Dewald B, Baggiolini M. A novel neutrophil-activating factor produced by human mononuclear phagocytes. *J.Exp.Med.* 1988;**167**:1547-59.
92. Gijsbers K, Gouwy M, Struyf S, Wuyts A, Proost P, Opdenakker G, et al. GCP-2/CXCL6 synergizes with other endothelial cell-derived chemokines in neutrophil mobilization and is associated with angiogenesis in gastrointestinal tumors. *Exp.Cell Res.* 2005;**303**:331-42.
93. Wuyts A, Struyf S, Gijsbers K, Schutyser E, Put W, Conings R, et al. The CXC chemokine GCP-2/CXCL6 is predominantly induced in mesenchymal cells by interleukin-1beta and is down-regulated by interferon-gamma: comparison with interleukin-8/CXCL8. *Lab.Invest.* 2003;**83**:23-34.
94. Collin M, Linge HM, Bjartell A, Giwercman A, Malm J, Egesten A. Constitutive expression of the antibacterial CXC chemokine GCP-2/CXCL6 by epithelial cells of the male reproductive tract. *J.Reprod.Immunol.* 2008;**79**:37-43.
95. Utgaard JO, Jahnsen FL, Bakka A, Brandtzaeg P, Haraldsen G. Rapid secretion of prestored interleukin 8 from Weibel-Palade bodies of microvascular endothelial cells. *J.Exp.Med.* 1998;**188**:1751-6.
96. Wolff B, Burns AR, Middleton J, Rot A. Endothelial cell "memory" of inflammatory stimulation: human venular endothelial cells store interleukin 8 in Weibel-Palade bodies. *J.Exp.Med.* 1998;**188**:1757-62.
97. Cassatella MA, Bazzoni F, Ceska M, Ferro I, Baggiolini M, Berton G. IL-8 production by human polymorphonuclear leukocytes. The chemoattractant formyl-methionyl-leucyl-phenylalanine induces the gene expression and release of IL-8 through a pertussis toxin-sensitive pathway. *J.Immunol.* 1992;**148**:3216-20.
98. Orr Y, Taylor JM, Cartland S, Bannon PG, Geczy C, Kritharides L. Conformational activation of CD11b without shedding of L-selectin on circulating human neutrophils. *J.Leukoc.Biol.* 2007;**82**:1115-25.
99. Kahn J, Walcheck B, Migaki GI, Jutila MA, Kishimoto TK. Calmodulin regulates L-selectin adhesion molecule expression and function through a protease-dependent mechanism. *Cell* 1998;**92**:809-18.
100. Kahn J, Ingraham RH, Shirley F, Migaki GI, Kishimoto TK. Membrane proximal cleavage of L-selectin: identification of the cleavage site and a 6-kD transmembrane peptide fragment of L-selectin. *J.Cell Biol.* 1994;**125**:461-70.
101. Kishimoto TK, Jutila MA, Berg EL, Butcher EC. Neutrophil Mac-1 and MEL-14 adhesion proteins inversely regulated by chemotactic factors. *Science* 1989;**245**:1238-41.

102. Zhao L, Shey M, Farnsworth M, Dailey MO. Regulation of membrane metalloproteolytic cleavage of L-selectin (CD62L) by the epidermal growth factor domain. *J.Biol.Chem.* 2001;**276**:30631-40.
103. Soo A, Maher B, McCarthy J, Nolke L, Wood A, Watson RW. Pre-operative determination of an individual's neutrophil response: a potential predictor of early cardiac transplant cellular rejection. *J.Heart Lung Transplant.* 2009;**28**:1198-205.
104. Killock DJ, Ivetic A. The cytoplasmic domains of TNFalpha-converting enzyme (TACE/ADAM17) and L-selectin are regulated differently by p38 MAPK and PKC to promote ectodomain shedding. *Biochem.J.* 2010;**428**:293-304.
105. Kansas GS, Ley K, Munro JM, Tedder TF. Regulation of leukocyte rolling and adhesion to high endothelial venules through the cytoplasmic domain of L-selectin. *J.Exp.Med.* 1993;**177**:833-8.
106. Hafezi-Moghadam A, Thomas KL, Prorock AJ, Huo Y, Ley K. L-selectin shedding regulates leukocyte recruitment. *J.Exp.Med.* 2001;**193**:863-72.
107. Williams MA, Solomkin JS. Integrin-mediated signaling in human neutrophil functioning. *J.Leukoc.Biol.* 1999;**65**:725-36.
108. Vedder NB, Harlan JM. Increased surface expression of CD11b/CD18 (Mac-1) is not required for stimulated neutrophil adherence to cultured endothelium. *J.Clin.Invest.* 1988;**81**:676-82.
109. Merrill JT, Slade SG, Weissmann G, Winchester R, Buyon JP. Two pathways of CD11b/CD18-mediated neutrophil aggregation with different involvement of protein kinase C-dependent phosphorylation. *J.Immunol.* 1990;**145**:2608-15.
110. Lynn WA, Raetz CR, Qureshi N, Golenbock DT. Lipopolysaccharide-induced stimulation of CD11b/CD18 expression on neutrophils. Evidence of specific receptor-based response and inhibition by lipid A-based antagonists. *J.Immunol.* 1991;**147**:3072-9.
111. Buyon JP, Slade SG, Reibman J, Abramson SB, Philips MR, Weissmann G, et al. Constitutive and induced phosphorylation of the alpha- and beta-chains of the CD11/CD18 leukocyte integrin family. Relationship to adhesion-dependent functions. *J.Immunol.* 1990;**144**:191-7.
112. Yan SR, Sapru K, Issekutz AC. The CD11/CD18 (beta2) integrins modulate neutrophil caspase activation and survival following TNF-alpha or endotoxin induced transendothelial migration. *Immunol.Cell Biol.* 2004;**82**:435-46.
113. Anjem A, Varghese S, Imlay JA. Manganese import is a key element of the OxyR response to hydrogen peroxide in Escherichia coli. *Mol.Microbiol.* 2009;**72**:844-58.

114. Imlay JA. Chapter 5.4.4 Oxidative Stress. In: Böck, A., Curtiss, R., III, Kaper, J.B., Karp, P.D., Neidhardt, F.C., Nystrom, T., et al., editor. *EcoSal-Escherichia Coli and Salmonella: Cellular and Molecular Biology*: ASM Press; 2009.
115. Rada B, Leto TL. Oxidative innate immune defenses by Nox/Duox family NADPH oxidases. *Contrib.Microbiol.* 2008;**15**:164-87.
116. Segal BH, Leto TL, Gallin JI, Malech HL, Holland SM. Genetic, biochemical, and clinical features of chronic granulomatous disease. *Medicine (Baltimore)* 2000;**79**:170-200.
117. Nordenfelt P, Tapper H. Phagosome dynamics during phagocytosis by neutrophils. *J.Leukoc.Biol.* 2011;**90**:271-84.
118. Faurschou M, Borregaard N. Neutrophil granules and secretory vesicles in inflammation. *Microbes Infect.* 2003;**5**:1317-27.
119. Rice WG, Ganz T, Kinkade JM,Jr, Selsted ME, Lehrer RI, Parmley RT. Defensin-rich dense granules of human neutrophils. *Blood* 1987;**70**:757-65.
120. Naucler C, Grinstein S, Sundler R, Tapper H. Signaling to localized degranulation in neutrophils adherent to immune complexes. *J.Leukoc.Biol.* 2002;**71**:701-10.
121. Kjeldsen L, Bainton DF, Sengelov H, Borregaard N. Structural and functional heterogeneity among peroxidase-negative granules in human neutrophils: identification of a distinct gelatinase-containing granule subset by combined immunocytochemistry and subcellular fractionation. *Blood* 1993;**82**:3183-91.
122. Hasko G, Pacher P. A2A receptors in inflammation and injury: lessons learned from transgenic animals. *J.Leukoc.Biol.* 2008;**83**:447-55.
123. Kumar V, Sharma A. Adenosine: an endogenous modulator of innate immune system with therapeutic potential. *Eur.J.Pharmacol.* 2009;**616**:7-15.
124. Blackburn MR, Vance CO, Morschl E, Wilson CN. Adenosine receptors and inflammation. *Handb.Exp.Pharmacol.* 2009;**(193)**:215-69.
125. Fredholm BB, Arslan G, Halldner L, Kull B, Schulte G, Wasserman W. Structure and function of adenosine receptors and their genes. *Naunyn Schmiedebergs Arch.Pharmacol.* 2000;**362**:364-74.
126. Cronstein BN, Daguma L, Nichols D, Hutchison AJ, Williams M. The adenosine/neutrophil paradox resolved: human neutrophils possess both A1 and A2 receptors that promote chemotaxis and inhibit O₂ generation, respectively. *J.Clin.Invest.* 1990;**85**:1150-7.

127. Sullivan GW, Linden J, Buster BL, Scheld WM. Neutrophil A2A adenosine receptor inhibits inflammation in a rat model of meningitis: synergy with the type IV phosphodiesterase inhibitor, rolipram. *J.Infect.Dis.* 1999;**180**:1550-60.
128. Fortin A, Harbour D, Fernandes M, Borgeat P, Bourgoin S. Differential expression of adenosine receptors in human neutrophils: up-regulation by specific Th1 cytokines and lipopolysaccharide. *J.Leukoc.Biol.* 2006;**79**:574-85.
129. Gessi S, Varani K, Merighi S, Ongini E, Borea PA. A(2A) adenosine receptors in human peripheral blood cells. *Br.J.Pharmacol.* 2000;**129**:2-11.
130. Li J, Fenton RA, Wheeler HB, Powell CC, Peyton BD, Cutler BS, et al. Adenosine A2a receptors increase arterial endothelial cell nitric oxide. *J.Surg.Res.* 1998;**80**:357-64.
131. Desai A, Victor-Vega C, Gadangi S, Montesinos MC, Chu CC, Cronstein BN. Adenosine A2A receptor stimulation increases angiogenesis by down-regulating production of the antiangiogenic matrix protein thrombospondin 1. *Mol.Pharmacol.* 2005;**67**:1406-13.
132. Sitaraman SV, Merlin D, Wang L, Wong M, Gewirtz AT, Si-Tahar M, et al. Neutrophil-epithelial crosstalk at the intestinal luminal surface mediated by reciprocal secretion of adenosine and IL-6. *J.Clin.Invest.* 2001;**107**:861-9.
133. Zhong H, Wu Y, Belardinelli L, Zeng D. A2B adenosine receptors induce IL-19 from bronchial epithelial cells, resulting in TNF-alpha increase. *Am.J.Respir.Cell Mol.Biol.* 2006;**35**:587-92.
134. Koshiba M, Rosin DL, Hayashi N, Linden J, Sitkovsky MV. Patterns of A2A extracellular adenosine receptor expression in different functional subsets of human peripheral T cells. Flow cytometry studies with anti-A2A receptor monoclonal antibodies. *Mol.Pharmacol.* 1999;**55**:614-24.
135. Apasov S, Chen JF, Smith P, Sitkovsky M. A(2A) receptor dependent and A(2A) receptor independent effects of extracellular adenosine on murine thymocytes in conditions of adenosine deaminase deficiency. *Blood* 2000;**95**:3859-67.
136. Chen Y, Corriden R, Inoue Y, Yip L, Hashiguchi N, Zinkernagel A, et al. ATP release guides neutrophil chemotaxis via P2Y2 and A3 receptors. *Science* 2006;**314**:1792-5.
137. Save S, Mohlin C, Vumma R, Persson K. Activation of adenosine A2A receptors inhibits neutrophil transuroepithelial migration. *Infect.Immun.* 2011;**79**:3431-7.
138. Alexander WS, Hilton DJ. The role of suppressors of cytokine signaling (SOCS) proteins in regulation of the immune response. *Annu.Rev.Immunol.* 2004;**22**:503-29.

139. Schulte G, Fredholm BB. Signalling from adenosine receptors to mitogen-activated protein kinases. *Cell.Signal.* 2003;**15**:813-27.
140. Charalambous C, Gsandtner I, Keuerleber S, Milan-Lobo L, Kudlacek O, Freissmuth M, et al. Restricted collision coupling of the A2A receptor revisited: evidence for physical separation of two signaling cascades. *J.Biol.Chem.* 2008;**283**:9276-88.
141. Lin MC, Almus-Jacobs F, Chen HH, Parry GC, Mackman N, Shyy JY, et al. Shear stress induction of the tissue factor gene. *J.Clin.Invest.* 1997;**99**:737-44.
142. Lukashev D, Ohta A, Apasov S, Chen JF, Sitkovsky M. Cutting edge: Physiologic attenuation of proinflammatory transcription by the Gs protein-coupled A2A adenosine receptor in vivo. *J.Immunol.* 2004;**173**:21-4.
143. Bshesh K, Zhao B, Spight D, Biaggioni I, Feokistov I, Denenberg A, et al. The A2A receptor mediates an endogenous regulatory pathway of cytokine expression in THP-1 cells. *J.Leukoc.Biol.* 2002;**72**:1027-36.
144. Kamei Y, Xu L, Heinzl T, Torchia J, Kurokawa R, Gloss B, et al. A CBP integrator complex mediates transcriptional activation and AP-1 inhibition by nuclear receptors. *Cell* 1996;**85**:403-14.
145. Cavalcante IC, Castro MV, Barreto AR, Sullivan GW, Vale M, Almeida PR, et al. Effect of novel A2A adenosine receptor agonist ATL 313 on *Clostridium difficile* toxin A-induced murine ileal enteritis. *Infect.Immun.* 2006;**74**:2606-12.
146. Koizumi S, Odashima M, Otaka M, Jin M, Linden J, Watanabe S, et al. Attenuation of gastric mucosal inflammation induced by indomethacin through activation of the A2A adenosine receptor in rats. *J.Gastroenterol.* 2009;**44**:419-25.
147. Naganuma M, Wiznerowicz EB, Lappas CM, Linden J, Worthington MT, Ernst PB. Cutting edge: Critical role for A2A adenosine receptors in the T cell-mediated regulation of colitis. *J.Immunol.* 2006;**177**:2765-9.
148. Odashima M, Bamias G, Rivera-Nieves J, Linden J, Nast CC, Moskaluk CA, et al. Activation of A2A adenosine receptor attenuates intestinal inflammation in animal models of inflammatory bowel disease. *Gastroenterology* 2005;**129**:26-33.
149. Mazzon E, Esposito E, Impellizzeri D, DI Paola R, Melani A, Bramanti P, et al. CGS 21680, an agonist of the adenosine (A2A) receptor, reduces progression of murine type II collagen-induced arthritis. *J.Rheumatol.* 2011;**38**:2119-29.
150. Varani K, Massara A, Vincenzi F, Tosi A, Padovan M, Trotta F, et al. Normalization of A2A and A3 adenosine receptor up-regulation in rheumatoid arthritis patients by treatment with anti-tumor necrosis factor alpha but not methotrexate. *Arthritis Rheum.* 2009;**60**:2880-91.

151. Varani K, Padovan M, Vincenzi F, Targa M, Trotta F, Govoni M, et al. A2A and A3 adenosine receptor expression in rheumatoid arthritis: upregulation, inverse correlation with disease activity score and suppression of inflammatory cytokine and metalloproteinase release. *Arthritis Res. Ther.* 2011;**13**:R197.
152. Hasko G, Linden J, Cronstein B, Pacher P. Adenosine receptors: therapeutic aspects for inflammatory and immune diseases. *Nat.Rev.Drug Discov.* 2008;**7**:759-70.
153. Moore CC, Martin EN, Lee GH, Obrig T, Linden J, Scheld WM. An A2A adenosine receptor agonist, ATL313, reduces inflammation and improves survival in murine sepsis models. *BMC Infect.Dis.* 2008;**8**:141.
154. Sharma AK, Linden J, Kron IL, Laubach VE. Protection from pulmonary ischemia-reperfusion injury by adenosine A2A receptor activation. *Respir.Res.* 2009;**10**:58.
155. Sharma AK, Laubach VE, Ramos SI, Zhao Y, Stukenborg G, Linden J, et al. Adenosine A2A receptor activation on CD4+ T lymphocytes and neutrophils attenuates lung ischemia-reperfusion injury. *J.Thorac.Cardiovasc.Surg.* 2010;**139**:474-82.
156. Jordan JE, Zhao ZQ, Sato H, Taft S, Vinten-Johansen J. Adenosine A2 receptor activation attenuates reperfusion injury by inhibiting neutrophil accumulation, superoxide generation and coronary endothelial adherence. *J.Pharmacol.Exp.Ther.* 1997;**280**:301-9.
157. Maddock HL, Broadley KJ, Bril A, Khandoudi N. Role of endothelium in ischaemia-induced myocardial dysfunction of isolated working hearts: cardioprotection by activation of adenosine A(2A) receptors. *J.Auton.Pharmacol.* 2001;**21**:263-71.
158. Lasley RD, Jahania MS, Mentzer RM, Jr. Beneficial effects of adenosine A(2a) agonist CGS-21680 in infarcted and stunned porcine myocardium. *Am.J.Physiol.Heart Circ.Physiol.* 2001;**280**:H1660-6.
159. Glover DK, Ruiz M, Takehana K, Petruzella FD, Rieger JM, Macdonald TL, et al. Cardioprotection by adenosine A2A agonists in a canine model of myocardial stunning produced by multiple episodes of transient ischemia. *Am.J.Physiol.Heart Circ.Physiol.* 2007;**292**:H3164-71.
160. Sullivan GW, Rieger JM, Scheld WM, Macdonald TL, Linden J. Cyclic AMP-dependent inhibition of human neutrophil oxidative activity by substituted 2-propynylcyclohexyl adenosine A(2A) receptor agonists. *Br.J.Pharmacol.* 2001;**132**:1017-26.
161. Fredholm BB, Zhang Y, van der Ploeg I. Adenosine A2A receptors mediate the inhibitory effect of adenosine on formyl-Met-Leu-Phe-stimulated respiratory burst in neutrophil leucocytes. *Naunyn Schmiedebergs Arch.Pharmacol.* 1996;**354**:262-7.

162. Cronstein BN, Rosenstein ED, Kramer SB, Weissmann G, Hirschhorn R. Adenosine; a physiologic modulator of superoxide anion generation by human neutrophils. Adenosine acts via an A2 receptor on human neutrophils. *J.Immunol.* 1985;**135**:1366-71.
163. Cronstein BN. Adenosine, an endogenous anti-inflammatory agent. *J.Appl.Physiol.* 1994;**76**:5-13.
164. Day YJ, Li Y, Rieger JM, Ramos SI, Okusa MD, Linden J. A2A adenosine receptors on bone marrow-derived cells protect liver from ischemia-reperfusion injury. *J.Immunol.* 2005;**174**:5040-6.
165. Sevigny CP, Li L, Awad AS, Huang L, McDuffie M, Linden J, et al. Activation of adenosine 2A receptors attenuates allograft rejection and alloantigen recognition. *J.Immunol.* 2007;**178**:4240-9.
166. Lappas CM, Rieger JM, Linden J. A2A adenosine receptor induction inhibits IFN-gamma production in murine CD4+ T cells. *J.Immunol.* 2005;**174**:1073-80.
167. Alam MS, Kurtz CC, Wilson JM, Burnette BR, Wiznerowicz EB, Ross WG, et al. A2A adenosine receptor (AR) activation inhibits pro-inflammatory cytokine production by human CD4+ helper T cells and regulates Helicobacter-induced gastritis and bacterial persistence. *Mucosal Immunol.* 2009;**2**:232-42.
168. Health News. Santen Files IND for Clinical Data's ATL313 for primary open angle glaucoma and ocular hypertension. 2010; Available at: <http://www.news-medical.net/news/20101223/Santen-files-IND-for-Clinical-Datas-ATL313-for-primary-open-angle-glaucoma-and-ocular-hypertension.aspx>. Accessed April, 2012.
169. Sylvester E, Vizi AL. *Handbook of Neurochemistry and Molecular Neurobiology: Neurotransmitter Systems*. Volume 11 ed. : Springer; 2008.
170. Abraham E. Neutrophils and acute lung injury. *Crit.Care Med.* 2003;**31**:S195-9.
171. Taqueti VR, Mitchell RN, Lichtman AH. Protecting the pump: controlling myocardial inflammatory responses. *Annu.Rev.Physiol.* 2006;**68**:67-95.
172. Brown KA, Brain SD, Pearson JD, Edgeworth JD, Lewis SM, Treacher DF. Neutrophils in development of multiple organ failure in sepsis. *Lancet* 2006;**368**:157-69.
173. Nemeth T, Mocsai A. The role of neutrophils in autoimmune diseases. *Immunol.Lett.* 2012;**143**:9-19.
174. DiVietro JA, Brown DC, Sklar LA, Larson RS, Lawrence MB. Immobilized stromal cell-derived factor-1alpha triggers rapid VLA-4 affinity increases to stabilize lymphocyte

- tethers on VCAM-1 and subsequently initiate firm adhesion. *J.Immunol.* 2007;**178**:3903-11.
175. Nauseef WM. Isolation of human neutrophils from venous blood. *Methods Mol.Biol.* 2007;**412**:15-20.
176. Böyum A. Isolation of mononuclear cells and granulocytes from human blood. Isolation of monuclear cells by one centrifugation, and of granulocytes by combining centrifugation and sedimentation at 1 g. *Scand J Clin Lab Invest Suppl.* 1968;**97**:77-89.
177. Egger G, Burda A, Glasner A. A simple method for measuring the F-actin content of human polymorphonuclear leukocytes in whole blood. *Virchows Arch.* 2001;**438**:394-7.
178. Cronstein BN, Levin RI, Belanoff J, Weissmann G, Hirschhorn R. Adenosine: an endogenous inhibitor of neutrophil-mediated injury to endothelial cells. *J.Clin.Invest.* 1986;**78**:760-70.
179. Bouma MG, Jeunhomme TM, Boyle DL, Dentener MA, Voitenok NN, van den Wildenberg FA, et al. Adenosine inhibits neutrophil degranulation in activated human whole blood: involvement of adenosine A2 and A3 receptors. *J.Immunol.* 1997;**158**:5400-8.
180. Liu L, Schwartz BR, Lin N, Winn RK, Harlan JM. Requirement for RhoA kinase activation in leukocyte de-adhesion. *J.Immunol.* 2002;**169**:2330-6.
181. Goldfinger LE, Han J, Kiosses WB, Howe AK, Ginsberg MH. Spatial restriction of alpha4 integrin phosphorylation regulates lamellipodial stability and alpha4beta1-dependent cell migration. *J.Cell Biol.* 2003;**162**:731-41.
182. Lim CJ, Kain KH, Tkachenko E, Goldfinger LE, Gutierrez E, Allen MD, et al. Integrin-mediated protein kinase A activation at the leading edge of migrating cells. *Mol.Biol.Cell* 2008;**19**:4930-41.
183. Konstandin MH, Sester U, Klemke M, Weschenfelder T, Wabnitz GH, Samstag Y. A novel flow-cytometry-based assay for quantification of affinity and avidity changes of integrins. *J.Immunol.Methods* 2006;**310**:67-77.
184. Andrew SM, Titus JA. Purification and Fragmentation of Antibodies . *Current Protocols in Immunology* 1997;.
185. Wayne M. Yokoyama. Production of Monoclonal Antibody Supernatant and Ascites Fluid. *Current Protocols in Molecular Biology* 2008;.
186. Laudanna C. Analysis of integrin-dependent rapid adhesion under laminar-flow conditions. *Methods Mol.Biol.* 2004;**239**:17-26.

187. Streeter PR, Berg EL, Rouse BT, Bargatze RF, Butcher EC. A tissue-specific endothelial cell molecule involved in lymphocyte homing. *Nature* 1988;**331**:41-6.
188. Bonifacino JS, Dell'Angelica EC, Springer TA. Immunoprecipitation. *Curr.Protoc.Immunol.* 2001;**Chapter 8**:Unit 8.3.
189. Springer TA. Immunoaffinity chromatography. *Curr.Protoc.Immunol.* 2001;**Chapter 8**:Unit 8.2.
190. Howe AK, Baldor LC, Hogan BP. Spatial regulation of the cAMP-dependent protein kinase during chemotactic cell migration. *Proc.Natl.Acad.Sci.U.S.A.* 2005;**102**:14320-5.
191. Lim CJ, Han J, Yousefi N, Ma Y, Amieux PS, McKnight GS, et al. Alpha4 integrins are type I cAMP-dependent protein kinase-anchoring proteins. *Nat.Cell Biol.* 2007;**9**:415-21.
192. Stephens P, Romer JT, Spitali M, Shock A, Ortlepp S, Figdor CG, et al. KIM127, an antibody that promotes adhesion, maps to a region of CD18 that includes cysteine-rich repeats. *Cell Adhes.Commun.* 1995;**3**:375-84.
193. Yi L, Chandrasekaran P, Venkatesan S. TLR signaling paralyzes monocyte chemotaxis through synergized effects of p38 MAPK and global Rap-1 activation. *PLoS One* 2012;**7**:e30404.
194. Vararattanavech A, Lin X, Torres J, Tan SM. Disruption of the integrin alphaLbeta2 transmembrane domain interface by beta2 Thr-686 mutation activates alphaLbeta2 and promotes micro-clustering of the alphaL subunits. *J.Biol.Chem.* 2009;**284**:3239-49.
195. Yauch RL, Felsenfeld DP, Kraeft SK, Chen LB, Sheetz MP, Hemler ME. Mutational evidence for control of cell adhesion through integrin diffusion/clustering, independent of ligand binding. *J.Exp.Med.* 1997;**186**:1347-55.
196. Petruzzelli L, Maduzia L, Springer TA. Activation of lymphocyte function-associated molecule-1 (CD11a/CD18) and Mac-1 (CD11b/CD18) mimicked by an antibody directed against CD18. *J.Immunol.* 1995;**155**:854-66.
197. Shao JY, Xu J. A modified micropipette aspiration technique and its application to tether formation from human neutrophils. *J.Biomech.Eng.* 2002;**124**:388-96.
198. Kundu PK, Cohen IM. *Fluid Mechanics*. 3rd edition ed. : Elsevier Academic Press; 2004.